SYNTHESIS OF GELATIN-CELLULOSE HYDROGEL MEMBRANE FOR COPPER AND COBALT REMOVAL FROM SYNTHETIC WASTEWATER

This dissertation is submitted in fulfillment of the requirement for the Master of Engineering: Chemical

TRÉSOR LUKUSA KABEYA

218251912

Vaal University of Technology

Private Bag X021, Vanderbijlpark 1900, South Africa

Supervisor: Dr John Kabuba Tshilenge

Co-supervisor: Dr Lay Shoko

APRIL, 2021

DECLARATION

I **TRÉSOR LUKUSA KABEYA**, declare that, to best of my knowledge, this dissertation is the results of my own work except where otherwise stated. It has not been submitted before for any degree or examination to any other university or institution. Due references in literature were indicated and acknowledged wherever other sources were involved according to the standard referencing practices.

……

Trésor Lukusa Kabeya

……day of……

……	……
Dr John Kabuba Tshilenge	Dr Lay Shoko
Supervisor	Co-supervisor
……day of……	……day of……

ABSTRACT

Heavy metal ions are one of the most toxic materials in the environment. Adsorption is the most used process for the removal of heavy metals from wastewater. Much research has been conducted into processes to remove heavy metals using different adsorbents. Various adsorbents have been used to remove heavy metal ions from wastewater especially those that are harmful to mankind. Zeolite, clay, activated carbon and biopolymers are the most common adsorbents used.

In this research, gelatin, and cellulose nanocrystals (CNCs) were used to synthesize a hydrogel membrane to remove Cu(II) and Co(II) metal ions from mining processes wastewater. The synthetic wastewater was prepared in the laboratory to conduct the experiments. Batch experiments were conducted to obtain the optimum conditions for the Cu(II) and Co(II) metal ions. The effect of parameters such as pH, ratio, contact time, and temperature were also determined.

The optimum conditions obtained were 120 min contact time for both metal ions at the temperature of 30^{o}C, pH 5 for copper and pH 7 for cobalt. The high removal of both metals ions was obtained using the ratio 3:1 (75% Gelatin and 25% CNCs) at the temperature of 303K. The maximum adsorption capacity of Cu(II) and Co(II) was 7.6923 mg/g and 10.988 mg/g, respectively. The high percentage removal of Cu(II) and Co(II) metal ions obtained was found to be 70.5% for Cu(II) at pH 5 and 74.5% for Co(II) at pH 7. The experimental data fit well to Pseudo-first-order kinetic and Freundlich isotherm models (K_F= 1.89x10^3 mg/g for copper and 3.7x10^2 mg/g for cobalt) for both metal ions. The values of energy (E) from D-R model have shown that the adsorption of both metal ions was of physical nature (E<8kJ/mol) then confirmed by the thermodynamic results ($\Delta H°$). The kinetic diffusion models have shown that the experimental data fit well with the film diffusion (R^2= 0.977 and 0.989) for both metal ions at pH 5. Negative values of $\Delta G°$obtained for both metal ions indicate that the adsorption process was spontaneous. The positive values of $\Delta H°$ obtained showed a physical adsorption process and also indicate that the adsorption process of both metal ions was endothermic. The positive values of $\Delta S°$ indicate an increase in randomness at the solid/solution interface during adsorption.

Keywords: Adsorption, Cellulose nanocrystals, Copper and Cobalt removal, Gelatin-Cellulose Hydrogel Membrane.

DEDICATION

In Memoriam of my father

ROGER KABEYA LUVUNGULA

ACKNOWLEDGMENTS

I thank JHW for his unconditional love and protection. I thank Him for taking care of me.

I wish to express my sincere gratitude to my guide Dr John Kabuba Tshilenge, for his supervision, precious suggestions, and advice that enabled me to prepare this thesis.

Likewise, I would like to offer my thanks to my Co-supervisor Dr Lay Shoko for his guidance and help to make this thesis.

I am thankful to the Department of Chemical Engineering at the Vaal University of Technology for providing equipment and other laboratory services essential for completion of the test work and all the staff members of Chemical Engineering who directly or indirectly helped me during my research work.

The financial support from the Vaal University of Technology with the postgraduate award is greatly appreciated.

I am thankful to my mentor Professors from the University of Lubumbashi (DRC): Emery Kalonda, Jean Mulamba, Marsi Mbayo, Jean-Baptiste Lumbu, Albert Kanangila and Michael Monga for their advice.

Many thanks to my fellow postgraduate colleagues and to my friends: Jean-Claude Banza, Welling Tshibwabwa, Nzungu Ndu, Bongani M., Franklin Mwambu, John Mutonkole, Eddy Mbuyu, Raphäel Tshana, Abel Teuluila, Guelorg Kabwika, Aubin Mulomba, Mylene Kat, Valentin Irung, Raissa Ilunga, Zephyrin Kasungu, Guelord Sompo, Mike Tumba, and Gilbert Kasonga for their advises.

An exceptional thanks to my friend Arnaud Stevens Marcel for his extraordinary help that I can qualify for “Activation’s Energy” necessary to achieve my Master’s Degree. I cannot fully express my gratitude to you.

To you, my cousin Cedrick Kapongo, I am thankful for your help and good moment spent in Nelson Mandela’s Country.

Thank you so much to you, Chance Nkulu, for your love, support, and patience.

I would like to thank everybody who played a significant role in the completion of this work, as well as expressing my apology that I could not mention all the names individually.

Finally, I want to dedicate my work to the best Mother Ever, my Mom Christine-Eugenie Mbelu, and my sisters: Madeleine Mbombo, Florence Ndomba, Yvette Mpwekela, Pélagie Mbelu, Viviane Kalanga, Deogratias Kalambayi, Blandine Nsumpi, and Vivian Kaleka. Without their endless encouragement, love, and support, completing this thesis would have been impossible. I am deeply grateful to them for each day of my life and my expression of thanks is not enough.

LIST OF RELATED PUBLICATION

Lukusa K., Kabuba J. & Shoko L.: Synthesis of Gelatin-CNCs hydrogel Membrane for removal of Cu(II) and Co(II) from synthetic wastewater, *Arabian Journal for Science and Engineering*, Under review,(2020), AJSE-S-20-03824.

TABLE OF CONTENTS

LIST OF FIGURES

LIST OF TABLES

LIST OF ABBREVIATIONS AND SYMBOLS

2D	Two dimensional
3D	Three dimensional
AAS	Atomic Absorption Spectroscopy
ANOVA	Analysis of variance
b_T	Temkin constant
CCD	Central Composite Design
C_e	Concentration at equilibrium
CNCs	Cellulose Nanocrystals
DNA	Deoxyribonucleic Acid
D-R	Dublinin-Radushkevich
DRC	Democratic Republic of Congo
E	Energy (kJ/mol)
EDTA	Ethylene diamine tetra-acetic acid
FTIR	Fourier Transform Infrared Spectroscopy
GCHM	Gelatin Cellulose Hydrogel Membrane
HMs	Heavy Metals
k_1	Pseudo-first-order kinetic model (min^{-1})
k_2	Pseudo-second-order kinetic model (min^{-1})
K_D	Distribution constant
K_F	Freundlich constant
K_L	Langmuir constant
LEM	Liquid Emulsion Membrane
PIM	Polymer Inclusion Membrane
q_e	Amount of adsorbed metal ions
q_m	Maximum capacity of adsorption at equilibrium
RSM	Response Surface Methodology
SEM	Scanning Electron Microscopy
WHO	World Health Organization
ΔG^o	Gibbs free energy (kJ/mol)
ΔH^o	Change in enthalpy (kJ/mol)
ΔS^o	Change in entropy (kJ/K.mol)
E	Polanyi potential

CHAPTER 1: INTRODUCTION

1.1 Background

In countries with mining potential such as DR Congo and Zambia nearly all metallurgical plants dump their tailings in rivers or handle solid waste near rivers. This solid waste undergoes leaching by rainwater, which entrains all metals in surface or underground rivers. This situation contaminates the sources of drinking water used by humans, livestock, and sometimes used for watering the fields. The pollution of aquatic ecosystems can also cause contamination of fish with toxic substances, which poses a significant public health risk (Muhune *et al*., 2020; Pourret & Faucon, 2016).

Industrial activities are one of the main sources of water pollution. Cobalt (Co), Nickel (Ni), Lead (Pb), Chromium (Cr), Copper (Cu), Iron (Fe); Cadmium (Cd), and Mercury (Hg) are heavy metals (HMs) often found in industrial effluents.

Nevertheless, Co(II) and Cu(II) ions are toxic and not biodegradable, therefore, they must be removed from wastewater. The high concentration of these cations (copper and cobalt) in drinking water leads to necrotic changes in liver and kidney, bone defects, low blood pressure, paralysis, mucosal irritation, depression, gastrointestinal irritation, lung cancer, and Deoxyribonucleic Acid (DNA) damage (Sheikh, 2016; Al-Shahrani, 2014; Qiu *et al*., 2009). According to World Health Organization (WHO), the limited concentration of Co(II) and Cu(II) ions in drinking water should not exceed 0.002mg/ℓand 2mg/ℓ, respectively (Wogu & Okaka, 2011; Uaury *et al*., 1998).

Several physical and chemical methods can be used for the removal of heavy metals from wastewater. Conventional methods such as precipitation, coagulation, flotation, membrane filtration, solvent extraction, adsorption, reverse osmosis, electrochemical treatment, bioremediation, electrodialysis, supercritical fluids extraction, and ion exchange have all been developed to remove Cu(II) and Co(II) ions from wastewater (García-Díaz *et al*., 2018). In general, these removal methods require high operating costs (Eloussaief *et al*., 2009; Jiang *et al*., 2004). Adsorption is the most frequently used method due to its low cost and possible insensitivity to toxic pollutants and does not result in the formation of harmful substances. Adsorption is a method that is easy to use

and design. The advantage of this method is the possibility to regenerate the adsorbent by desorption, being therefore a reversible technique, so it is considered a technology that is not aggressive with the environment. Different types of adsorbents were developed. Cellulose and gelatin were found to be the most frequently used materials in adsorption processes (Akpomie *et al*., 2015; Silva Filho *et al*., 2013).

Cellulose is a widely available and renewable biopolymer in nature. It can be used for the preparation of various functional materials due to the high specific surface areas, and OH group. Excellent adsorption performance and relatively high adsorption capacity for the removal of HMs ions from aqueous solutions may be obtained after modification of cellulose with functional groups such as NH_2, SO_3, and COOH groups (Yu *et al*., 2013). Gelatin is a water-soluble biopolymer that is obtained as a degradation product of water-insoluble protein collagen, andcan remove HMs ions from drinking water. Lone *et al*., (2019) and Hayeeye *et al*., (2018), found that gelatin and cellulose polymers show an increased number of binding sites for metals ions.

The hydrogel membranes or hydrogel films are the unconventional membranes often used for pharmaceutical, medicine, drug delivery, soft tissuesuch as anti-adhesive applications because of their promising properties such as swelling. Hydrogel membranes can also be used in water treatment as filtration membrane where the solution goes through the hydrogel membrane film as described for gel membrane permeation (Yao *et al*., 2019; Marks *et al*., 2019; Tran *et al*., 2018; Fujiyabu *et al.*, 2017; Getachew *et al*., 2017; Moreau *et al*., 2016; Ahmed, 2015; Jing *et al*., 2013; Kenavy *et al*., 2013; Mateescu *et al*., 2012). Due to the abundance of ion-coordinating sites and their aptitude to adsorb a large amount of water, hydrogel films have been found recently in another application in water treatment to remove metal ions using adsorption (Zhang *et al*., 2019; Perumal *et al*., 2019; Qi *et al*., 2019; Alizadehgiashi *et al*., 2018; El-Halah & López-Carrrasquero, 2018).

In the literature, many optimization studies are available for the removal of heavy metals ions from wastewater using different adsorbents. Response Surface Methodology (RSM) has been used to optimize the removal of lead (Adetokun *et al*., 2019; Hasan & Setiabudi, 2019; Javanbakht & Ghoreishi, 2017; Amini *et al*., 2008), cobalt (Musapatika

et al., 2012), copper (Li *et al.*, 2009), chromium (Bayuo *et al*., 2020; Adetokun *et al*., 2019), cadmium (Adetokun *et al*., 2019; Saini *et al.*, 2019), zinc (Alman-Abad *et al*., 2020; Biswas *et al.*, 2019), etc.

The optimization conditions for adsorption of copper and cobalt ions onto Gelatin-Cellulose Hydrogel Membrane (GCHM) using Central Composite Design (CCD) based on RSM have been evaluated.

This study has identified the high potential of modified cellulose-gelatin using ethylene diamine-tetra-acetic acid (EDTA) as a cross-linking agent in the adsorption of Cu(II) and Co(II) ions from hydrometallurgical processes' wastewater.

1.2 Problem statement

Nowadays, the widespread existence of metals ions such as Cu(II) and Co(II) in water are potentially threatening to the ecosystem and public health since these metal ions are toxic and non-biodegradable (Zhang *et al*., 2019). Therefore, the removal of Cu(II) and Co(II) ions from wastewater before release in the environment is necessary and very important. Synthesized cellulose and gelatin hydrogel membrane have been selected as the adsorbent materials because they are easy to operate, non-toxic and renewable.

1.3 Objectives

1.3.1 Main objective

The main objective of this study is to synthesize an adsorbent membrane using cellulose nanocrystals (CNCs) and gelatin at different ratios and modified with EDTA as a cross-linking agent to remove Cu(II) and Co(II) ions from aqueous solutions through batch adsorption.

1.3.2 Specific objectives

(a) To characterize the synthesized membrane using Infrared spectroscopy (FTIR) and the Scanning Electron Microscope (SEM).

(b) To determine the effect of the pH, temperature, contact time, ratio of CNCs and gelatin, on the removal of Cu(II) and Co(II) ions.

(c) To investigate the thermodynamic feasibility of the adsorption process.

(d) To study the equilibrium isotherm and kinetic models.

1.4 Research questions

(a) What are the characteristics of synthesizing membrane cellulose-gelatin using Infrared spectroscopy (FTIR) and scanning electron microscope (SEM)?

(b) What are the effects of the temperature, contact time, ratio of CNCs and gelatin, on the removal of Cu(II) and Co(II)?

(c) What is the thermodynamic feasibility of the process?

(d) What is the suitable isotherm and kinetic models describing the process?

1.5 Outline of the Dissertation

Chapter 1 provides an introduction to the study, as well as the motivation and reasoning behind the study. The problem statement, linked to the motivation, was also discussed, as were the aims and objectives that were pursued to the successful completion of the study.

Chapter 2 presents the literature relevant to this study will be discussed. This will include information on removal techniques of copper and cobalt metals ions from wastewater.

Chapter 3 covers the methodology on synthesis of gelatin-cellulose hydrogel membrane, adsorption process studies and analyzing technique for the characterization of GCHM.

Chapter 4 presents the results and discussions on the adsorption of copper, and cobalt metals ions onto GCHM.

Chapter 5 deals with the conclusion of the research project and recommendations for future works.

1.6 References

Adetokun A.A., Uba S. & Garba Z.N.: Optimization of adsorption of metal ions from a ternary aqueous solution with activated carbon from Acacia Senegal (L.) Willd pods using Central Composite Design, *Journal of King Saud University-Science* 31 (2019), 1452-1462.

Ahmed E.M.: Hydrogel: Preparation, characterization, and applications: A review, *Journal of Advanced Research* 6 (2015), 105-121.

Akpomie K.G., Dawodu F.A. & Adebowale K.O.: Mechanism on the sorption of heavy metals from binary-solution by a low cost montmorillonite and its desorption potential, *Alexandria Engineering Journal* 54 (2015), 757-767.

Alizadehgiashi M., Khuu N., Khabibullin A., Henry A. & Tebbe M.: Nanocolloidal hydrogel from heavy metal scavenging, *American Chemical Society Nano* 12 (2018), 8160-8168.

Alman-Abad Z.S., Pirkharrati H. &Asadzadeh F.: Application of response surface methodology for optimization of zinc elimination from a polluted soil using tartaric acid, *Adsorption Science and Technology* 38, *3-4* (2020), 79-93.

Al-Shahrani S.S: Treatment of wastewater contaminated with cobalt using Saudi activated bentonite, *Alexandria Engineering Journal* 53 (2014), 205-211.

Amini M., Younesi H., Bahramifar N., Lorestani A.A.Z., Ghorbani F., Daneshi A. & Sharifzadeh M. : Application of response surface methodology for optimization of lead biosorption in an aqueous solution by Aspergillus niger, *Journal of Hazardous Materials* 154 (2008), 694-702.

Bayuo J., Abukari M.A. & Pelig-Ba K.B.: Optimization using central composite design (CCD) of response surface methodology (RSM) for biosorption of hexavalent chromium from aqueous media, *Applied Water Science* 10, *135* (2020), 1-12.

Biswas S., Bal M., Brhera S.K., Sen T.K & Meikap B.C.: Process optimization study of Zn^{2+} adsorption on biochar-alginate composite adsorbent by response surface methodology (RSM), *Water* 11, *325* (2019), 1-15.

El-Halah A. & López-Carrrasquero F.: Applications of Hydrogels in the adsorption of metallic ions, *Ciencia e Ingenieria* 1, *39* (2018), 1-28.

Eloussaief M., Jarraya I. & Benzina M.: Adsorption of copper ions on two clays from Tunisia: pH and temperature effects, *Applied Clay Science* 46 (2009), 409-413.

Fujiyabu T., Li X., Shibayama M., Chung U. & Sakai T.: Permeation of water through Hydrogels with controlled network structure, *Macromolecules* 50 (2017), 9411-9416.

García-Díaz I., López FA. & Alguacil F J.: Carbon Nanofibers: A New Adsorbent for Copper Removal from Wastewater, *Metals* 8 (2018), 914-927.

Getachew B.A., Kim S-R & Kim J-H.: Self-healing Hydrogel pore-filled water filtration Membranes, *American Chemical Society Environmental Science & Technology* 51 (2017), 905-913.

Ghrab S., Benzima M. & Lambert S.D.: Copper Adsorption from wastewater using Bone Charcoal, *Advances in Materials Physics and Chemistry* 7 (2017), 139-147.

Hasan R. & Setiabudi H.D.: Removal of Pb(II) from aqueous solution using KCC-!: optimization by response surface methodology (RSM), *Journal of King Saud University-Science* 31 (2019), 1182-1188.

Hayeeye F., Yu Q.J., Sattar M., Chinpa W. & Sirichote O.: Adsorption of Pb^{2+} ions from aqueous solutions by gelatin/activated carbon composite bead form, *Adsorption Science & Technology* 36, *1-2* (2018), 355-371.

Javanbakht V. & Ghoreishi S.M.: Application of response surface methodology for optimization of lead removal from an aqueous solution by a novel

superparamagnetic nanocomposite, *Adsorption Science and Technology* 35, *1-2* (2017), 241-260.

Jiang L.Y., Yang X.E & He Z.L.: Growth response and phytoextraction of copper at different levels in soils by Elsholtziasplendes, *Chemosphere* 55 (2004), 1179-1187.

Jing G., Wang L., Yu H., Amer W.A. & Zhang L.: Recent progress on study of hybrid Hydrogels for water treatment, *Colloids and surface A: Physicochemical and Engineering Aspects* 416 (2013), 86-94.

Kamaruzaman S., Aris N.I.F., Yahaya N., Hong L.S. & Razak M.R.: Removal of Cu(II) and Cd(II) ions from Environmental Water Samples by using Cellulose Acetate Membrane, *Journal of Environment Analytical Chemistry* 4, *4* (2017), 1-8.

Kenavy E.-R., Kamoun E.A., MohyEldin M.S. & El-Meligy M.A.: Physically crosslinked poly-(vinyl alcohol)-hydroxyethyl starch blend Hydrogel Membranes: Synthesis and characterization for biomedical applications, *Arabian Journal of Chemistry*, (2013).

Khulbe K.C. & Matsuura T.: Removal of heavy metals and pollutants by membrane adsorption techniques, *Applied Water Science* 8, 9 (2018), 1-30.

Li J., Hu J., Sheng G., Zhao G. & Huang Q.: Effect of pH, ionic strength, foreign ions and temperature on the adsorption of Cu (II) from aqueous solution to GMZ bentonite, *Colloids and Surface A: Physicochemical and Engineering Aspects* 349 (2009), 195-201.

Lone S., Yoon H.D., Lee H & Cheong I.W.: Gelatin-chitosan hydrogel particles for efficient removal of Hg(II) from wastewater, *Environmental Science Water Research & Technology* (2019), 83-90.

Marks R., Seaman J., Peresz-Calleja P., Kim J., Nerenberg R. & Doudrick K.: Catalytic Hydrogel Membrane reactor for aqueous contaminants, *Environmental Science & Technology* 53 (2019), 6492-6500.

Mateescu A., Wang Y., Doslalek J. & Jonas U.: Thin Hydrogel Films for optical biosensor Applications, *Membrane* 2 (2012), 40-69.

Mobasherpour I., Salahi E. & Ebrahimi M.: Thermodymics and kinetics of adsorption of Cu(II) from aqueous solutions onto multi-walled carbon nanotubes, *Journal of Saudi Chemical Society* 18 (2014), 792-801.

Moreau D., Chauvet C., Etienne F., Rannou F.P & Corté L.: Hydrogels films and coatings by swelling-induced gelation, *PNAS* (2016), 1-6.

Muhune K.S., Mbayo K.M., Tshisand T.P., Muyumba N.W., Kayembe K.O., Kaya M.D., Banza I.B., Misenga T.A., Lukusa T., Tshibanda K.D., Kalonda M.E. & Lumbu S. J-B.: Evaluation of soil contamination by metallic trace elements to the roadside on Lubumbashi-Kipushi section (DRC), *International Journal of Advanced Research*, 8, *9* (2020), 1187-1195.

Musapatika E.T., Singh R., Moodley K., Nzila C., Onyango M.S. & Ochieng A.: Cobalt removal from wastewater using pine sawdust, *African Journal of Biotechnology* 11, 39 (2012) 9407-9415.

Perumal S., Atchudan R., Yoon D.H., Joo J. & Cheong I.W.: Spherical chitosan-gelatin hydrogel particles for removal of multiple heavy metal ions from wastewater, *Industrial & Engineering Chemical Research* 58 (2019), 9900-9907.

Pourret O. & Faucon M-P. : Cobalt : A Comprehensive Reference source on the chemistry of the Earth, *Encyclopedia of Geochemistry* (2016), White, M.W. (Ed.), Springer.

Qi X., Lin L., Shen L., Li Z., Qin T., Qian Y., Wu X., Wei X., Gong Q & Shen J. :Effecient Decontamination of lead ions from wastewater by salecan polysaccharide-

based Hydrogels, *American Chemical Society Substainable Chemistry& Engineering* 7 (2019), 11014-11023.

Qiu W. & Zheng Y.: Removal of lead, copper, nickel, cobalt, and zinc from water by cancrinite-type zeolite synthesized from fly ash, *Chemical Engineering Journal* 145 (2009), 483-488.

Saini S., Chawla J., Kumar R. & Kaur I.: Response surface methodology (RSM) for optimization of cadmium ions adsorption using $C_{16\text{-}6\text{-}16}$ incorporated mesoporous MCM-41, *SN Applied Sciences* 1, *894* (2019), 1-10.

Sheikh I.: Cobalt Poisoning, A comprehensive Review of the Literature, *Journal of Medical Toxicology and Clinical Forensic Medicine* 2, *6* (2016), 1-6.

Silva Filho E.C., Santos Júnior L.S., Fernandes Silva M.M., Fonseca M.G., Abreu Santana S.A. & Airoldi C.: Surface cellulose Modification with 2-Aminomethylpyridine for Copper, Cobalt, Nickel and Zinc Removal from Aqueous solution, *Materials Research* 16, *1* (2013), 79-87.

Tran V.V., Park D. & Lee Y-C.: Hydrogel applications for adsorption of contaminants in water and wastewater treatment, *Environmental Science and Pollution Research* 25 (2018), 24569-24599.

Uaury R., Olivares M. & Gonzalez M.: Essentiality of copper in humans, *American Journal of Clinical Nutrition* 67 (1998), 952S-9S.

Wang X. & Liu P.: Adsorption of Pb(II) by a polyvinylidene bearing chelating poly-(amino phosphonic acid) and poly(amino carboxylic acid) groups, *Adsorption Science & Technology* 36, *9-10* (2018), 1571-1594.

Wogu M.D. & Okaka C.E.: Pollution studies on Nigerian rivers: heavy metals in surface water of warri river, Delta State, *Journal of Biodiversity and Environmental Sciences* 1, *3* (2011), 7-12.

Worch E.: Adsorption Technology in Water Treatment, De Gruyter, Germany, (2012).

Yao Y., Wang H., Wang R., Chai Y & Ji W.: Fabrication and performance characterization of the membrane from self-dispersed gelatin-coupled cellulose microgels, *Cellulose* 26 (2019), 3255-3269.

Yu X., Tong S., Ge M., Wu L., Zuo J., Coa C. & Song W.: Adsorption of heavy metal ions from aqueous solution by carboxylated cellulose nanocrystals, *Journal of Environmental Sciences* 25, *5* (2013), 933-943.

Zhang C., Li H., Yu Q., Jia L. & Wan L.Y.: Poly(aspartic acid) Electrospun nanofiber Hydrogel Membrane-based reusable colorimetric sensor for Cu(II) and Fe(II) detection, *American Chemical Society Omega* 4 (2019), 14633-14639.

CHAPTER 2: LITERATURE REVIEW

2.1 Introduction

This chapter highlights the literature reports on the removal techniques of Cu(II) and Co(II) ions using cellulose and gelatin as adsorbent materials. The advantages and disadvantages associated with the use of conventional methods in the metal removal of Cu(II) and Co(II) ions from aqueous solutions are elaborated. An overview of the adsorption process, properties of cellulose and gelatin, and possible modification techniques are given. Isotherm, kinetic models, and thermodynamic studies are discussed. Characterization techniques such as SEM and FTIR are explained. The optimization technique using RSM is also discussed.

2.2 Removal techniques of copper and cobalt from wastewater

Several physical and chemical techniques such as Ion exchange, chemical precipitation, liquid-liquid separation, Membrane adsorption, Liquid emulsion membrane (LEM), Polymer inclusion membrane (PIM), Hydrogel Membrane, and Adsorption Membrane, have been developed for heavy metals' removal from wastewater.

2.2.1 Liquid-Liquid Separation

The liquid-liquid separation or solvent extraction is a technique of separation based on the constant of distribution (K_D) of one or many metals into two solvents that are non-mixable (organic phase and aqueous phase). It is shown that the liquid-liquid extraction is a good technique to separate heavy metals from industrial wastewater and in the development of the separation process (Fetouhi *et al*., 2016; Fillipi *et al*., 1998). The solvent extraction process is represented by equation (2.1):

$$M_{aq}^{2+} + 2RH \rightarrow 2RM + 2H^{+} \qquad (2.1)$$

where, $M^{2+}{}_{aq}$ is the metallic solute in the aqueous solution, and *RH,* the extracting ligand in the organic phase.

Shengo *et al*., 2019 have reported the liquid-liquid extraction of Cu (II) and Co (II) ions from DRC's ores.

2.2.2 Chemical precipitation

Chemical precipitation is widely used for heavy metal removal from inorganic effluent. This technique depends on the pH of metal removal. After pH adjustment, the dissolved metal ions are converted into an insoluble solid phase via a chemical reaction with a precipitating agent such as lime. Typically, the precipitated metal from the solution is in hydroxide form (Barakat, 2011; Kurniawan *et al*., 2006). The conceptual mechanism of heavy metal removal by chemical precipitation is represented by the equation (2.2):

$$M^{2+} + (HO)^{-} \leftrightarrow M(OH)_{2\downarrow} \qquad (2.2)$$

where, M^{2+} and HO^{-} are the dissolvent metal ions and precipitant respectively, while $M(OH)_2$ is the insoluble metal hydroxide.

The chemical agents most used for the precipitation of Cu(II)ions are $Mg(OH)_2$; $Ca(OH)_2$ and $Fe(OH)_3$ (Tünay & Kabdasli, 1994). Many agents were used for cobalt precipitation in literature. It has been shown that the EDTA and nitrilotriacetic acid (NTA) may be used as ligand-sharing agents for the precipitation of cobalt (Fu *et al*., 2011).

2.2.3 Ion-exchange

The ion-exchange process is one of the most frequently used in wastewater laden with heavy metals. In this process, there is a reversible interchange of ions between the solid and liquid phases that occur, where an insoluble substance (resin) removes ions from an electrolytic solution and releases other ions in a chemically equivalent amount without any structural change of the resin. Ion-exchange can also be used to recover valuable heavy metals from inorganic effluent. After separating, from loaded resin; the metal is recovered with a higher concentration by elution with suitable reagents (Fu *et al*., 2011; Kurniawan *et al*., 2006). Since the acidic functional group of resin consists of sulfonic acid, it is assumed that the physicochemical interactions that may occur during metal removal can be expressed as follows:

$$n\ R\text{-}SO_3H + M^{n+} \leftrightarrow (R\text{-}SO_3^{-})_n M^{n+} + n\ H^{+} \qquad (2.3)$$

$$n\ R\text{-}COOH + M^{n+} \leftrightarrow (R\text{-}COO^{-})_n M^{n+} + n\ H^{+} \qquad (2.4)$$

where,$(R\text{-}SO_3^-)$ and M^{n+} represent the anionic group attached to the ion exchange resin and the metal cation, respectively, while *n* is the coefficient of the reaction component, depending on the oxidation state of metal ions.

Several studies were made to remove heavy metals from wastewater using ions exchange. It is shown by Al-Shahrani (2014) that adsorption of cobalt ions on Saudi activated bentonite was fast. The equilibrium was reached after 30 minutes with a maximum adsorption of 99% at pH 8.

2.2.4 Polymer Inclusion Membrane (PIM)

The PIM is a new type of membrane which has long-term stability. It is useful for industrial applicationsthat in the past where its utilization was considered hypothetical. This kind of membrane has been used by Kebiche-Senhadji *et al.* (2008) to facilitate Cd(II) transport cellulose tri-acetate polymer inclusion membrane using anion Aliquat 336 and cation Di-(2-ethylhexyl)phosphoric acid (D2EPHA) metal carriers. In this study, the maximal Cd(II) obtained in 8 hours was 97.8% and 91.8% with (D2EPHA) and Aliquat 336, respectively. Many researchers have used it to remove Cu(II) and Co(II) ions using PIM (Blitz-Raizh *et al*., 2007; Kozlowski *et al*., 2006; Wang *et al*., 2000; Paugam & Buff, 1998).

2.2.5 Liquid Emulsion Membrane (LEM)

The LEM is another type of membrane used in wastewater treatment for the removal of heavy metals. It was used by Mohamed *et al*. (2013) for the removal of cobalt from wastewater. That LEM was containing Cyanex 301 as a carrier and Span 80 as a surfactant for the extraction of Co(II). This kind of membrane is interesting because of high efficiency, where both extraction and stripping steps are combined. From this study, it was shown that maximum extraction was 96.86% after 5 minutes for 10 ml of LEM that can extract 1 g/L of Co(II) from nitric acid solution as optimum conditions.

2.2.6 Membrane adsorption

Membrane adsorbent was increasingly used recently for the treatment of inorganic effluents due to its convenient operation. Membranes used for this purpose have the

dual functions of membrane filtration and adsorption to be very effective to remove trace amounts of pollutants such as cationic heavy metals (Khulbe & Matsuura, 2018; Tian *et al*., 2011; O'Connell *et al*., 2010). A membrane adsorbent is made by connecting functional groups, the surface and pore wall of polymer membranes, the target pollutants are selectively adsorbed to the functional group (see Figure 1).

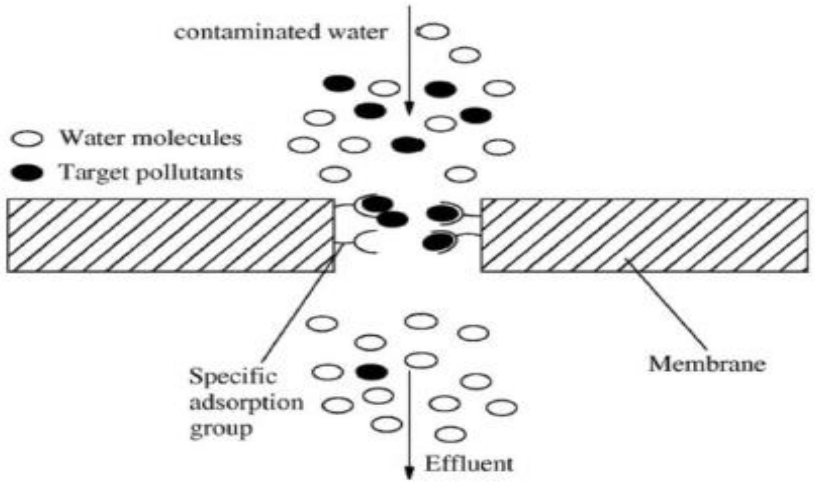

Figure 1: Principle of membrane adsorbent (Khulbe *et al.*, 2018)

This kind of membrane has been used by Kamaruzaman *et al*. (2017) for the removal of Cu(II) and Cd(II) from wastewater. Hayeeye *et al*. (2017) had used gelatin and activated carbon composite bead form for adsorption of Pb(II) ions from aqueous solutions. From this study, it is shown that the equilibrium isotherms were well described by the Langmuir isotherm model and the highest maximum adsorption capacity was found to be 370 mg/g at pH 5. The highest adsorption efficiency observed was 90%.

2.2.7 Membrane Hydrogels

Hydrogels are three-dimensional (3D) hydrophilic networks that can absorb large quantities of water yet remain insoluble in aqueous solution (Palantöken *et al*., 2019; Lin *et al*, 2016). Membrane hydrogels were recently used in wastewater treatment for the removal of heavy metals. The metal ions such as copper, mercury, nickel, and silver were made the object of adsorption using nano-colloidal hydrogel as adsorbent. Due to the high surface area and abundance of ion-coordinating sites on the surface of nano-

particle building blocks, the microgels had exhibited a high ion-sequestration capacity (Alizadehgiashi *et al*., 2018). Perumal *et al*., (2019) had used Chitosan-Gelatin hydrogel for removal of Hg^{2+}, Pb^{2+}, Cd^{2+}, and Cr^{3+} metal ions. The high removal was 98% for Hg^{2+} ions in a single metal. This result was affected by the composition of hydrogels rather than the pore size or the degree of swelling. The hydrogel was also used for adsorption of Cu(II) and Co(II) ions in wastewater by Zhang *et al*. (2019) and Reshetnyak *et al*. (2012).

2.2.8 Adsorption Process

Adsorption is a mass transfer process by which a substance is transferred from the liquid phase to the surface of a solid as presented in Figure 2 and is bound by physical and/or chemical interactions. Recently, the adsorption was found to be one of the alternative treatment techniques for wastewater laden with heavy metals (Barakat, 2011; Kurniawan *et al*., 2006).

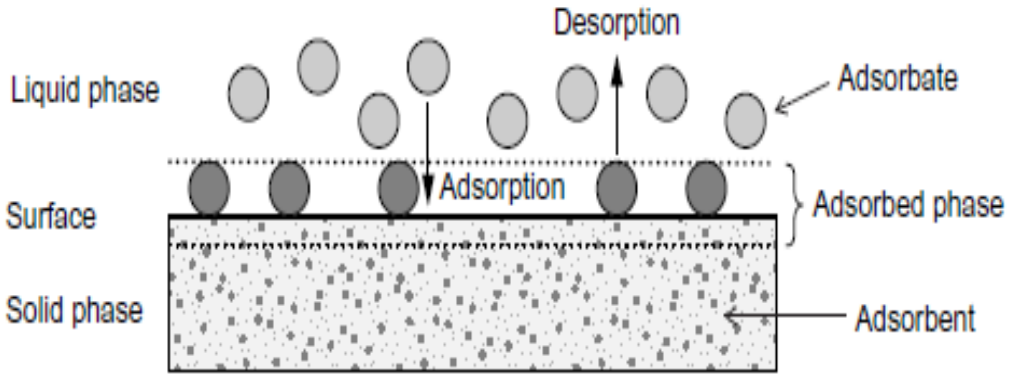

Figure 2: The basic term of Adsorption (Worch, 2012)

The bond of metal ions laden from wastewater at the surface of adsorbent (solid) involves physical adsorption by Van Der Wall's interaction between the adsorbate and the substrate. It also due to the chemical adsorption where the molecules or atoms stick to the surface by forming chemical covalent bonds and tend to find sites that maximize their coordination number with the substrate (Worch, 2012; Atkins & Julio, 2006).

The high adsorption capacity and surface reactivity, adsorption using natural materials or modified biopolymers have been recently developed and applied for the removal of

Cu(II) and Co(II) ion laden in wastewater (Negm *et al*., 2014; El-Sheikh *et al*., 2012; Sarkar & Majumdar, 2011; Stafiej *et al*., 2007; Coşkun *et al*., 2006).

2.3 Adsorption Materials

Many adsorbent materials were used in wastewater treatment to remove heavy metals. These materials can be organic or inorganic such as cellulose acetate, chitosan, starch, gelatin, bentonite, kaolinite, clay, zeolite, activated carbon, and sepiolite.

2.3.1 Cellulose

The polysaccharide is among the polymers most frequently found on earth. Most of this carbohydrate is derived from various sources andis often used in water treatment. Cellulose is a natural polymeric carbohydrate the most found in the nature (see Figure 3). It is non-toxic, biodegradable, and soluble in most organic solvents. The carbohydrate as the cellulose may be a product from the substrates such as wood and cotton and it is used as an energy source, and for textile industries. It consists of *β*-D-glucopyranose repeat units which are covalently linked by acetal functionalities between the equatorial OH group on the carbon atom C4 and C1, hence the name *β*-1, 4-glucan (Mudasir *et al*., 2015).

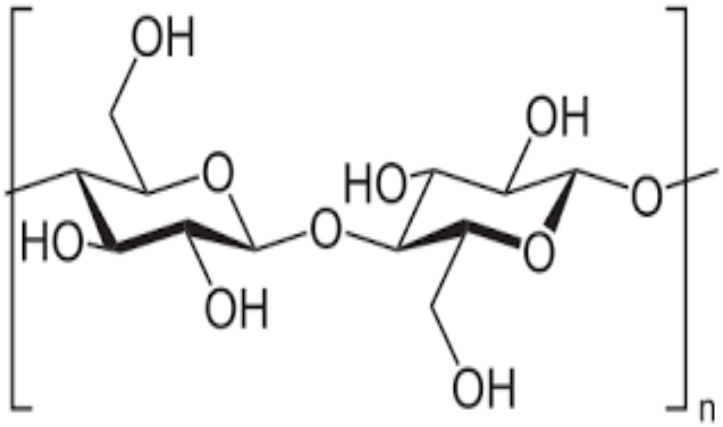

Figure 3: Chemical structure of Cellulose (Silva Filho *et al.*, 2013)

Cellulose acetate has been used by Kamaruzaman *et al*. (2017), as membrane modified with *N, N-dimethyl-formamide* (DMF) for the removal of Cu(II) and Cd(II) ions from environmental water samples. The determination of the adsorption capacity of Cellulose Acetate Membrane (CAM) was carried out in batch adsorption. In this study, it has been

shown that the maximum adsorption capacity of Cu(II) and Cd(II) ions were about 14.22 mg/g at pH 8 and 11.20 mg/g at pH 10, respectively.

2.3.2 Gelatin

Gelatin (see Figure 4) is a polypeptide with high molecular weight. It may be obtained from the connective tissue, skin and bone of animals and also obtained from fish and insects by thermal degradation of the fibrous insoluble protein-collagen. Gelatin is a biopolymer, soluble in water and widely used in food as an ingredient. Gelatin is also mostly used in the preparation of membrane for the removal of heavy metals in the wastewater treatment (Jiaolong *et al*., 2016; Abdalbasit & Hariod, 2013; Bdalbasit *et al*., 2013; Kandge *et al*., 2002).

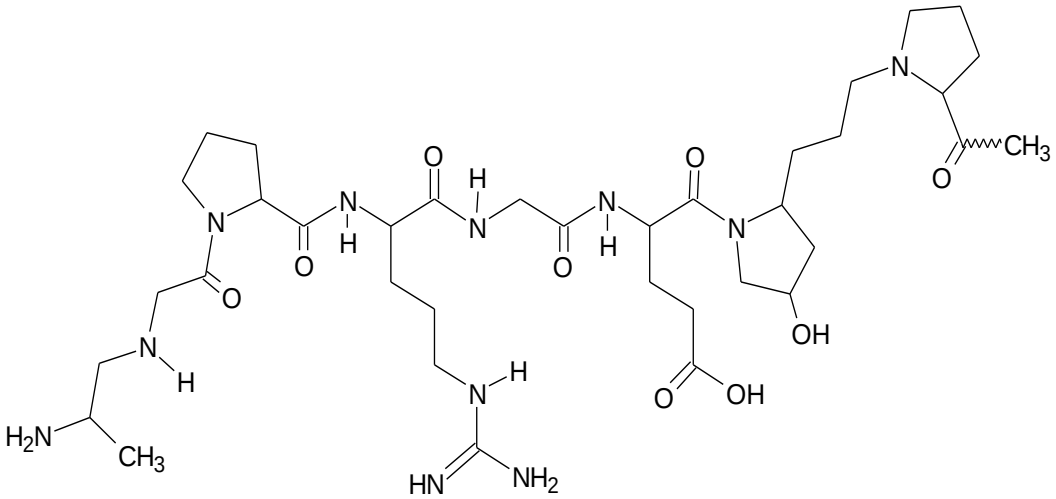

Figure 4: Chemical structure of gelatin (Hayeeye *et al*., 2018)

It is shown that the chemical modification of carbohydrates may increase its adsorption capacity for heavy metals in wastewater from mining processes (O'Connell *et al*., 2008). This chemical modification consists of the modification of cellulose chemical structure with the introduction of chelating or metal-binding functionalities or by grafting of selected monomers to the cellulose either directly by introduction of metal-binding capacity or with the subsequent fictionalization of these grafted polymer chains with known chelating moieties (Mudasir *et al*., 2015).

To improve the removal efficiency of heavy metal from wastewater, many adsorbent membranes were synthesized by several researchers. Tian *et al*., (2011), prepared a cellulose acetate nonwoven membrane for heavy metal ion adsorption using

electrospinning and surface modification with poly (methacrylic acid). This membrane was used for removing heavy metals ions such as Cu^{2+}, Hg^{2+}, and Cd^{2+}.

2.4 Factors affecting the adsorption process

The adsorption process involves several parameters for the removal of copper and cobalt from wastewater. The main factors currently used are initial pH, temperature, contact time, and initial concentration in metal(s) (Moussout *et al*., 2018).

2.4.1 Effect of pH

pH has a strong influence on the adsorption process, as it can increase or decrease the yield of adsorption removal. A study made by Badawi *et al*. (2017) has proved that the variation of the medium's pH, affects the adsorption process by the mobility of metallic ions. The metallic ions (M^{2+}) such as Cu(II) and Co(II) can be present in solution in the form of M^{2+} and $M(OH)_2$ for different values of pH. It is shown that in the alkaline medium, the efficiency of metallic ions M^{2+} removal increased from pH 7 to 9 and low efficiency of biosorbents at pH 7; it could be due to the increase in competition for the adsorption sites by H^+ and M^{2+}. As pH increased, more negatively charged surface sites became available thus facilitating greater M^{2+} ions adsorption (El-Sheikh *et al*., 2012).

2.4.2 Effect of temperature

Temperature is very important and plays a great role in the adsorption process. It can increase or decrease the efficiency of metallic ions M^{2+} removal and that it depends also on the nature of the adsorbent. Eloussaief *et al*. (2009) have shown that the adsorption of Cu^{2+} on clays decreases with the decrease of temperature. However, Li *et al*. (2009), proved that the adsorption of Cu^{2+} on *Na-bentonite* increases with the rise of temperature. The adsorption efficiency of Co^{2+} ions on apricot stone activated carbon increases with the temperature over the range of 25-30^{o}C as it has also been determined by Abbas *et al*. (2014).

2.4.3 Effect of contact time

Contact time represents the time of interaction between the biosorbent and the metal ions in the solution. Many studies have shown that the yield of adsorption of metal ions

increases when the immersion time between the biosorbent, and the metal ions increases (Badawi *et al*., 2017). In using botanic biosorbents (rice husk, palm leaf and water hyacinth) for the adsorption of Cu(II) and Co(II) ions, Sadeek *et al*. (2015), reported that the adsorption efficiencies were increased by increasing the immersion time. The maximum adsorption efficiencies were recorded for Cu^{2+} ions at 96.8% and 92.6% using the tree biosorbents at pH 7. A similar observation has been made by El-Sheikh *et al*. (2012) that the adsorption efficiencies of Cu^{2+} and Co^{2+} ions were increased with the immersion time using the modified chitosan. Thus, the yield of adsorption is a function of contact time (Liu *et al*., 2015).

2.4.4 Effect of initial concentration

Initial ion concentration plays an important role in the adsorption yield and amount of metal ions adsorbed from the medium. Sadeek *et al*. (2015) have shown that the adsorption efficiency of metal increases with the lower initial concentration and decreases with a higher initial concentration of metal ions. At lower concentrations, the biosorbents surfaces do not reach the saturation concentration. Parab *et al*., (2006) had also proved that the adsorption yield of Co^{2+} ions decreases with increasing of concentration in metal ions; higher efficiency removal was 85.4% for an initial concentration of 20mg/ℓ.

2.5 Response Surface Methodology

RSM is essentially a particular set of mathematical and statistical methods for designing experiments, building models, evaluating the effects of variables and searching optimum conditions of variables to predict targeted responses (Lingamdinne *et al*., 2018). The main advantages of RSM are the reduced numbers of experimental trials needed to evaluate multiple parameters and their interactions, making this technique useful for developing, improving, and optimizing the process. By careful design of experiments, the objective is to optimize a response (output variable) which is influenced by several independent variables (input variables) (Ayed *et al*., 2010; Kiran *et al*., 2007). The second-order polynomial design, central composite design (CCD), is the most widely used approach of RSM, and may be employed to understand the interactive effects of

the operational variables on metal adsorption. The beauty of CCD for the sequential experimentation is that it requires only a few design points and provides a reasonable guideline for data fit. A second order polynomial regression model equation (see Equation 2.5) is assessed here to predict metal adsorption efficiency under a certain condition of process variables.

$$Y(\%) = b_0 + \sum b_i X_i + \sum b_{ii} X_i^2 + \sum b_{ij} X_i X_j \qquad (2.5)$$

where, Y is the response of the system, b_0 is the constant coefficient, b_i,b_{ii}, and b_{ij} are the regression coefficients and X_i,X_j indicate the independent variables. The statistical calculation is based on the relationship between the coded (X_i) and the real values (P_i).

The chi-square that is a test of statistical analysis is applied. It is a non-linear technique used to compare experimental and predicted data as given in Equation (2.6).

$$X^2 = \frac{[q_{e(exp)} - q_{e(pred)}]^2}{q_{e(pred)}} \qquad (2.6)$$

where, $q_{e(exp)}$ and $q_{e(pred)}$ are experimental andpredicted, respectively. If data from the model is similar to the experimental data, X^2 will be a smaller number and if they are different, X^2 will be a bigger number.

The RSM was used to optimize the adsorption of many metal ions (Davarnejad *et al*., 2018; Shojaeimehr *et al*., 2014; Esfandiar *et al*., 2014; Ja*et al*., 2011).

2.6 Adsorption isotherms

The equilibrium between the adsorbent and the adsorbate describes the adsorption isotherms. The isotherms also describe the performance of adsorbents to remove the metallic ions at a time, pH, and temperature given by Equation 2.7. The Langmuir, Freundlich, Tempkin, and Dublinin-Radushkevich (D-R) models are often used to analyze the experimental data (Dastkhoon *et al*., 2015).

2.6.1 Langmuir isotherm

Langmuir adsorption isotherm describes the adsorption of metal ions on the adsorbents as a monolayer, and that adsorption takes place at specific homogeneous sites. The energy of adsorption of all sites is the same and independent of other metal ions adsorbed already in the proximate sites (Shrestha, 2015; Blahovec *et al*., 2009; Vieira *et al*., 2007). It is given by Equation (2.7).

$$\frac{C_e}{q_e} = \frac{1}{q_{mK_L}} + \frac{C_e}{q_m} \qquad (2.7)$$

Linearizing Equation (2.7) results in the linear form of the Langmuir model, Equation (2.8):

$$\frac{1}{q_m} + \left(\frac{1}{q_m} K_L\right) \frac{1}{C_e} \qquad (2.8)$$

where, C_e is the concentration at equilibrium *(mg/ℓ)*; q_e is the amount of adsorbed M^{2+}ions per unit mass at equilibrium *(mg/g)*; q_m is maximum capacity of adsorption at equilibrium *(mg/g)* and K_L is the Langmuir constant related to the free adsorption of thermodynamic equilibrium of adsorption. The constants q_m and K_L are calculated by the plot of C_e/q_e versus C_e with slope $1/q_m$ and intercept $1/(q_mK_L)$.

$$R_L = \frac{1}{1+K_L C_o} \qquad (2.9)$$

where, R_L is a dimensional constant separation, C_o (mg/ℓ) is the maximum initial concentration.

The separation factor R_L shows that the adsorption process is favourable if the R_L value is $0<R_L<1$, unfavourable when $R_L>1$, linear when $R_L=1$ and irreversible at value of $R_L=0$.

The Langmuir isotherm of cobalt ion (R^2= 0.75) has been evaluated by Igberase *et al*., (2017); Osińska (2016); Al-Shahrani (2014).

2.6.2 Freundlich isotherm

The Freundlich isotherm model can be suitable for all situations to describe the adsorption process. This isotherm is often used in prediction models for multisolute

adsorption (Shrestha, 2015; Blahovec *et al*., 2009; Vieira *et al*., 2007). The Freundlich isotherm is given by Equation (2.10).

$$q_e = K_F C_e^{1/n} \quad (2.10)$$

Linearizing Equation (2.10) gives the linear form for the Freundlich Equation.

$$\ln q_e = lnK_F + \frac{1}{n} \ln C_e \quad (2.11)$$

where, C_e is the concentration at equilibrium (mg/ℓ); q_e: the amount of adsorbed M^{2+} ions per unit mass at equilibrium *(mg/g)*; *1/n*: Freundlich constant describes the affinity of M^{2+} for the adsorbent. K_F and n_1 can be calculated from a linear plot of *ln* q_e against *ln* C_e.

The cobalt's Freundlich isotherm (R^2= 0.936) was investigated by Igberase *et al*. (2017); Osińska (2016); Al-Shahrani (2014).

2.6.3 Temkin isotherm

The Temkin isotherm takes into account the interactions between adsorbents and metal ions to be adsorbed and is based on the assumption that the free energy of sorption is a function of the surface coverage. The linear form of the isotherm is given by Equation (2.12).

$$q_e = B\ ln\ A + B\ ln\ C_e \quad (2.12)$$

where, *A (L/g)* is the equilibrium binding constant and $B = RT/b_T$ is related to the heat adsorption, *R* is the gas constant (8.314 J/mol K), *T (K)* is the absolute temperature and b_T is the Temkin constant. The constant *A* and *B* are obtained from the linear plot of q_e versus *ln* C_e (Akpomie *et al*., 2015).

2.6.4 Dubinin-Radushkevich (D-R) isotherm

The D-R isotherm does not assume a homogenous surface or a constant adsorption potential as the Langmuir isotherm was applied.

$$\ln q_e = \ln q_m - \beta\varepsilon^2 \quad (2.13)$$

where,$\beta(mol^2/J^2)$ is a coefficient related to the mean free energy of adsorption, $q_m(mg/g)$ is the maximum adsorption capacity and ε is the Polanyi potential which is expressed as

$$\varepsilon = RT\ ln\ (1+1/C_e) \quad (2.14)$$

$$E = \frac{1}{\sqrt{2\beta}} \quad (2.15)$$

where, E (kJ/mol) is the energy and R is the universal gas constant (8.314J/kmol).

The D-R constants are calculated from the linear plot of $ln\ q_e$ versus ε^2 (Akpomie *et al*., 2015; Al-Shahrani, 2014; El Nemr *et al*., 2010).The Dubinin-Radushkevich isotherm (R^2= 0.75) of cobalt metal ion was also investigated by Al-Shahrani (2014). Garcia-Diaz *et al.,* (2018) calculated E (7.34 <8 kJ/mol) and found that the mechanism of adsorption has a physical nature.

2.7 Kinetic studies

The kinetic study is very important for the adsorption process because it describes the mechanism of adsorption and for the determination of the rate-controlling steps for the adsorption process includes the diffusion control, chemical reactions, and particle diffusion. Various models have been used to describe the adsorption process but the most known is the kinetic model proposed by Lagergren for the pseudo-first-order and pseudo-second-order (Dastkhoon *et al*., 2015; Abbas *et al*., 2014, Zhao *et al*., 2013).

2.7.1 Pseudo-first-order kinetic model

With the Pseudo-first-order kinetic model, it is supposed that the efficiency of adsorption is proportional to the number of adsorption active sites of the adsorbent (Badawi *et al*., 2017; Ajmal *et al*., 2005). The Pseudo-first-order kinetic is given in Equation (2.16).

$$\log(q_e - q_t) = \log q_e - (\frac{k_1 t}{2.303}) \quad (2.16)$$

where, q_e and q_t are the concentration of the M^{2+} ions adsorbed at equilibrium and at a *t* time *(mg/g)*; respectively: k_1 is the rate constant of the reaction (min^{-1}). The rate constant can be calculated as the plot of $ln\ (q_e\text{-}q_t)$ against *t*, gives a straight line with the slope $-k_1$ and intercept $ln\ q_e$ (Badawi *et al*., 2017; Dastkhoon *et al*., 2015; Alyuz & Veli, 2009;

Rengaraj *et al*., 2007).Pseudo-first-order order of cobalt ion was evaluated (Igberase *et al*., 2017; Abbas *et al*., 2014).

2.7.2 Pseudo-second-order kinetic model

The pseudo-second-order kinetic predicts the rate-determining step of the adsorption process and the bonds nature between the adsorbents and the metal ions (Bajpai *et al*., 2010; Ajmal*et al*., 2005). It is given in Equation (2.17):

$$\frac{dq}{dt} = k_2(q_e - q_t)^2 \qquad (2.17)$$

By integration the Equation (2.13) with the boundary condition $t = 0,\ q = 0$, and $t = t,\ q = q_t$ gives the linear form of the second-order kinetic model as shown in Equation (2.18):

$$\frac{1}{q_t} = \left(\frac{1}{k_2 q_e^2}\right) t + \left(\frac{1}{q_e}\right) \qquad (2.18)$$

where q_e and q_t are the concentration of the M^{2+} ions *(mg/g)* adsorbed at equilibrium and at time t (min). The values of k_2 and q_e for different initial concentrations are calculated from the slope and intercept of the linear plot of t/q_t versus t (Badawi *et al*., 2017; Dastkhoon *et al*., 2015; Alyuz *et al*., 2009; Rengaraj *et al*., 2007). The pseudo second order of copper and cobalt ions were investigated by Ghrab *et al*. (2017) and Al-Shahrani (2014).

2.7.3 Elovich model

In reactions involving chemical adsorption of gases on a solid surface without desorption of the products, the rate decreases with time due to an increase in surface coverage. The Elovich model is one of the most useful models to describe such activated chemical adsorption, which is given by Equation (2.19). The Elovich equation is also used successfully to describe the kinetic second-order assuming that the actual solid surfaces are energetically heterogeneous, but the equation does not propose any definite mechanism for adsorbate–adsorbent (Rudzinski and Panczyk, 2000).

$$q_t = \frac{1}{\beta}\ln \alpha.\beta + \frac{1}{\beta}\ln t \qquad (2.19)$$

where, q_e and q_t are the concentration of the M^{2+} ions (mg/g) adsorbed at equilibrium and at time t (min). α is the initial adsorption rate (mg/min) at contact time t = 0, and β is the extent of surface coverage and activated energy (g/mg).

2.7.4 Kinetic diffusion models

Three adsorption mechanisms were considered to evaluate the adsorption of copper and cobalt from the aqueous solution (Qiu *et al*., 2009).

(a) Film diffusion-controlled process: The metal species diffused from the aqueous solution to the solid surface

$$ln\left(1-\frac{q_t}{q_e}\right)=-Kt \qquad (2.20)$$

(b) Particle diffusion-controlled process: The ion diffused inside the solid material

$$ln\left(1-\left(\frac{q_t}{q_e}\right)^2\right)=-Kt \qquad (2.21)$$

(c) Moving boundary process

$$3-3\left(1-\frac{q_t}{q_e}\right)^{\frac{2}{3}}-2\frac{q_t}{q_e}=K \qquad (2.22)$$

where K (min^{-1}) is the rate constant model, q_e and q_t (mg/g) are the sorption capacities at equilibrium and contact time, respectively, and t is time (min).

The results obtained by Garcia-Diaz *et al*. (2018) on the kinetic diffusion models showed that the Cu^{2+} adsorption onto carbon nanofibers could be better explained by the particle diffusion model, where K= 0.0525 min^{-1}.

2.8 Thermodynamic studies

The thermodynamic study is very important to evaluate the feasibility of the adsorption process. The thermodynamic parameters such as Gibbs free energy change *(ΔG°)*, enthalpy change *(ΔH°)*, and entropy *(ΔS°)* are usually used to describe the nature of the

process (Arshadi *et al*, 2014; Hino *et al.*, 2010; Singh *et al*., 2010). The Gibbs free energy can be calculated from the Equation (2.23).

$$\Delta G^\circ = -RT \ln K_D \qquad (2.23)$$

where, ΔG° is the Gibbs free energy change *(kJ mol^{-1})*, R is the universal gas constant *(8.314 J mol^{-1} K^{-1})*, K_D is the distribution coefficient or equilibrium constant which is dependent on temperature, and T is the temperature *(K)*. The K_D value can also determine from the Equation (2.24) and (2.25) (Bajpai *et al*., 2010).

$$K_D = q_e/C_e \qquad (2.24)$$

$$K_D = e^{-\Delta G^\circ/RT} \qquad (2.25)$$

where, C_e is the concentration at equilibrium *(mg/ℓ)*, q_e is the amount of adsorbed M^{2+} per unit mass at equilibrium *(mg/g)*.

Other parameters such as the enthalpy change (ΔH°) and the entropy change (ΔS°) are very important and can be determined from the Equation (2.26) (Hino et al., 2010; Singh *et al*., 2010):

$$\Delta G^\circ = \Delta H^\circ - T\Delta S^\circ \qquad (2.26)$$

where, ΔH° is the enthalpy change *(kJ mol^{-1})* and ΔS° is the entropy change *(J mol^{-1}K^{-1})*.

Substituting Equation (2.23) into Equation (2.26) gives Equation (2.27) which can be used to determine the values of the enthalpy change and the entropy change through the Van't Hoff plot *(ln K_D against 1/T)* (Hashemian *et al*., 2016; Hino *et al*., 2010).

$$-\ln K_D = \left(\frac{\Delta H^0}{R}\right).\frac{1}{T} - \frac{\Delta S^0}{R} \qquad (2.27)$$

Thermodynamic parameters of adsorption of copper and cobalt onto new carboxylated sugarcane aredetermined by Pedrosa Xavier *et al*. (2018).

Garcia-Diaz *et al.* (2018) studied a new adsorbent for copper removal from wastewater at temperature (293, 313 and 333K), and found that the ΔH° is lower than $T\Delta S^\circ$, so the sorption process was dominated by entropic rather than enthalpic changes.

2.9 References

Abbas M., Kaddour S. & Trari M.: Kinetic and equilibrium studies of cobalt adsorption on apricot stone active carbon, *Journal of Industrial and Engineering Chemistry* 20 (2014), 745 – 751.

Abdalbasit A.M. & Hariod F.A.: Review: Gelatin, Source, Extraction and Industrial Applications, *Acta Scientarium Polonorum, Technology Alimentary*, 12, *2* (2013), 135 – 147.

Ajmal M, Rao R.A.K & Khan M.A.: Adsorption of copper from solution on *Brassica cumpestris* (mustard oil cake), *Journal of Hazardous Materials B* 122 (2005), 177-183.

Akpomie K.G., Dawodu F.A. & Adebowale K.O.: Mechanism on the sorption of heavy metals from binary-solution by a low cost montmorillonite and its desorption potential, *Alexandria Engineering Journal* 54 (2015), 757-767.

Alizadehgiashi M., Khuu N., Khabibullin A., Henry A. & Tebbe M.: Nanocolloidal hydrogel from heavy metal scavenging, *American Chemical Society Nano* 12 (2018), 8160-8168.

Al-Shahrani S.S.: Treatment of wastewater contaminated with cobalt using Saudi activated bentonite, *Alexandria Engineering Journal* 53 (2014), 205-211.

Alves Dias P., Blagoeva D., Pavel C. & Arvantidis N.: Cobalt: Demand-supply balances in the transition to electric mobility, EUR 29381 EN, *Publications office of the European Union*, Luxembourg, 2018.

Alyuz B. & Veli S.: Kinetic and equilibrium studies for the removal of nickel and zinc from aqueous solutions by ion exchange resins, *Journal of Hazardous Materials* 167 (2009), 482-488.

Arshadi M., Amiri M.J. & Mousavi S.: Kinetic, equilibrium and thermodynamic investigations of Ni (II), Cd (II), Cu (II) and Co (II) adsorption on barley staw ash, *Water Resources and Industry* 6 (2014), 1-17.

Atkins Peter & Julio De Paula: Physical Chemistry, 8th Edition, W. H Freeman and Company, New York, (2006).

Ayed L., Khelifi E., Jannet H.B., Miladi H., Cheref A., Achour S. & Bakhrouf A.: Response surface methodology for decolorization of azo dye Methyl Orange by bacterial consortium: Produced enzymes and metabolites characterization, *Chemical Engineering Journal* 165 (2010), 200-208.

Badawi M.A., Negm N.A., Abou Kana M.T.H., Hefni H.H. & Abdel Moneem M.M., Adsorption of aluminum and lead from wastewater by chitosan-tannic acid modified biopolymers: Isotherms, kinetics, thermodynamics and process mechanism, *International Journal of Biological Macromolecules* 99 (2017), 465-476.

Bajpai S.K. & Jain A.: Removal of copper (II) from aqueous solutions using spent tea leaves (STL) as a potential sorbent, *Water SA* 36 (2010), 221-228.

Barakat M.A.: New trends in removing heavy metals from industrial wastewater. *Arabian Journal of Chemistry* 4 (2011), 361-377.

Bdalbasit A.M. & Hariod F.A. Review: Gelatin, Source, Extraction and Industrial Applications*, Acta ScientariumPolonorum Technology Alimentary* 12, *2*, (2013), 135-147.

Blahovec J. & Yanniotis S.: Modified classification of sorption isotherms, *Journal of Food Engineering* 91 (2009), 72-77.

Blitz-Raizh A.H., Paimin R., Cattrall R.W. & Kolev S.D.: Separation of cobalt (II) from nickel (II) by solid phase extraction into Aliquat 336 chloride immobilized in poly(vinylchloride), *Talanta* 71 (2007), 419.

Coşkun R., Soykan C. & Saçak M.: Adsorption of copper (II), nickel (II) and cobalt (II) ions from aqueous solution by methacrylic acid/ acrylamide monomer mixture grafted poly(ethylene terephthalate) fiber, *Separation and Purification Technology* 49 (2006), 107-114.

Dastkhoon M., Ghaedi M., Asfaram A., Goudarzi A., Langroodi S.M., Tyagi I., Agarwal S. & Gupta V.K.: Ultrasound assisted adsorption of malachite green dye onto ZnS, Cu-NP-AC: Equilibrium isotherms and kinetic studies-Response surface optimization, *Separation and Purification Technology* 156 (2015), 780-788.

Davarnejad R., Moraveji M.K. & Havaie M.: Integral technique for evaluation and optimization of Ni (II) ions adsorption onto regenerated cellulose using surface methodology, *Arabian Journal of Chemistry* 11 (2018), 370-379.

El-Nemr A., El-Sikaily & Khaled A.: Modeling of adsorption isotherms of methylene blue onto rice hush activated carbon, Egyptian Journal of Aquatic Research 36, 1 (2010), 403-425.

Eloussaief M., Jarraya I. & Benzina M., Adsorption of copper ions on two clays from Tunisia: pH and temperature effects, *Applied Clay Science* 46 (2009), 409-413.

El-Sheikh R., Hefni H.H., El-Farargy A.F., Bekhit M. & Negm N.A.: Adsorption Efficiency of Chemically modified Chitosan towards copper and cobalt Ions from Industrial Waste Water, *Egyptian Journal of Chemistry* 55, *3* (2012), 291-305.

Esfandiar N., Nasernejad B. & Ebadi T.: Removal of Mn (II) from groundwater by sugarcane bagasse and activated carbon (a comparative study): Application of response surface methodology (RSM), *Journal of Industrial and Engineering Chemistry* 20 (2014), 3726-3736.

Fetouhi B., Belarbi H., Benabdellah A., Kasmi-Mir S. & Kirsch G.: Extraction of the heavy metals from the aqueous phase in ionic liquid 1-butyl-3-methylimidazolium hexafluorophosphate by N-salicylideneaniline, *Journal of Material Environment Science* 7, *3* (2016), 746-754.

Fillipi B.R., Scamehorn J.F., Christian S.D. & Taylor R.W.: A comparative economic analysis of copper removal from waste by ligand-modified micellar-enhanced

ultrafiltration and by conventional solvent extraction, *Journal of Membrane Science* 145 (1998), 27- 44.

Fu F. & Wang Q.: Removal metal ions from wastewaters: Review, *Journal of Environmental Management* 92 (2011), 407-418.

Garcia-Diaz I., Lopez F.A. & Alguacil F.J.: Carbon Nanofibers: A New Adsorbent for Copper Removal from Wastewater, *Metals* 8, *914*(2018), 1 – 13.

Ghrab S., Benzina M. & Lambert S.D.: Copper adsorption from wastewater using bone charcoal, *Advances in Materials Physics and Chemistry* 7 (2017) 139 – 147.

Hashemian S., Saffari H. & Ragabion S.: Adsorption of Cobalt (II) from Aqueous Solution by Fe_3O_4/Bentonite nanocomposite, *Water Air Soil Pollution* (2015).

Hayeeye F., Yu Q.J., Sattar M., Chinpa W. & Sirichote O.: Adsorption of Pb^{2+} ion aqueous solutions by gelatin/activated composite bead form, *Adsorption Science and Technology* 36, 1-2 (2018), 355-371.

Hino S., Ichikawa T. & Kojima Y.: Thermodynamic properties of metal amides determined by ammonia pressure-composition isotherms, *Journal of Chemical Thermodynamics* 42 (2010), 140-143.

Igberase E., Osifo P. & Ofomaja A.: The adsorption of Pb, Zn, Cu, Ni and Cd by modified ligand in a single component aqueous solution: Equilibrium, Kinetic, Thermodynamic and adsorption studies, *International Journal of Analytical Chemistry* (2017).

Ja R-D., Mao Z-Z., Chang Y-Q. & Zhao L-P.: Soft-sensor copper extraction process in cobalt hydrometallurgy based on adaptive hybrid model, *Chemical Engineering Research and Design* 89 (2011), 722-728.

Ji F., Li C., Tang B., Xu J., Lu G. & Liu P.: Preparation of cellulose acetate/zeolite composite fiber and its adsorption behavior for heavy metal in aqueous solution, *Chemical Engineering Journal* 209 (2012), 325-333.

Jiaolong W., Lina W., Ziyu Z., Hanjian L., Pan X., Lan L. & Junchao W.: Biodegradable Polymer Membranes Applied in Guided Bine / Tissue Regeneration: A Review, *Polymers* 8, *115*, (2016), 1-20.

Kamaruzaman S., Aris N.I.F., Yahaya N., Hong L.S. & Razak M.R.: Removal of Cu(II) and Cd (II) ions from Environmental Water Samples by using Cellulose Acetate Membrane, *Journal of Environment Analytical Chemistry* 4, *4* (2017), 1-8.

Kandge Y., Jinshu M., Yuji Y., Wenguang L., Yuanlu C., Kaiyong C. & Feng Z.: Chitosan/Gelatin network based biomaterials in tissue engineering, *Biomedical Engineering-Applications, Basis and communications,* 14, *3*, (2002), 115-121

Kara M., Yuzer H., Sabah E. & Celik M.S.: Adsorption of cobalt from aqueous solutions onto sepiolite, *Water Research* 37 (2003), 224-232.

Kebiche-Senhadji O., Mansouri L., Tingry S., Seta P. & Benamor M.: Facilitated Cd (II) transport across CTA polymer inclusion membrane using anion (Aliquat 336) and cation (D2EHPA) metal carriers, *Journal of Membrane Science* 310 (2008), 438-445.

Khulbe K.C. & Matsuura T.: Removal of heavy metals and pollutants by membrane adsorption techniques, *Applied Water Science* 8, 9 (2018), 1-30.

Kiran B., Kaushik A. & Kaushik C.P.: Response surface methodological approach for optimizing removal of Cr (VI) from aqueous solution using immobilized cyanobacterium, *Chemical Engineering Journal* 126 (2007), 147-153.

Kozlowski C.A.: Facilitated transport of metal ions through composite and polymer inclusion membranes, *Desalination* 198 (2006), 132 – 140

Kurniawan T.A., Chan G.Y.S., Lo W.H. & Babel S.: Physico-chemical treatment techniques for wastewater laden with heavy metals, *Chemical Engineering Journal* 118 (2006), 83-98.

Li J., Hu J., Sheng G., Zhao G. & Huang Q.: Effect of pH, ionic strength, foreign ions and temperature on the adsorption of Cu(II) from aqueous solution to GMZ bentonite, *Colloids and Surface A: Physicochemical and Engineering Aspects* 349 (2009), 195-201.

Lin N., Gèze A., Wouessidjewe D., Huang J. & Dufresne A.: Biocompatible double-membrane hydrogels from cationic cellulose nanocrystals and anionic alginate as complexing drugs code livery, *American Chemical Society Applied Materials & Interfaces* 8 (2016), 6880-6889.

Lingamdinne L.P., Koduru J.R., Chang Y-Y. & Karri R.R.: Process optimization and adsorption of Pb(II) on nickel ferrite-reduced graphene oxide nano-composite, *Journal of Molecular Liquids* 250 (2018), 202-211.

Liu C. & Bai R.: Adsorption removal of copper ions with highly porous chitosan/ cellulose acetate blend hollow fiber membranes, *Journal of Membrane Science* 284 (2006), 313-322.

Liu P., Borrell P.F., Božič M., Kokol V. & Oksman K.: Nanocelluloses and their phosphorylated derivatives for selective adsorption of Ag^{+}, Cu^{2+} and Fe^{3+} from industrial effluents, *Journal of Hazardous Materials* 294 (2015), 177-185.

Mobasherpoor I., Salahi E. & Ebrahimi M.: Thermodynamics and kinetics of adsorption of Cu (II) from aqueous solutions onto multi-walled carbon nanotubes, *Journal of Saudi Chemical Society* 18 (2014), 792-801.

Mohamed Y.T., Hussin L.M.S., Gad H.M.H., Daifullah & Abo-El-Enein S.A.: Membrane stability and removal of cobalt from waste solution using Liquid Emulsion Membrane, *Journal of Membrane and Separation Technology* 2 (2013), 102-108.

Moussout H., Ahlafi H., Aazza M. & Maghat H.: Critical of linear and nonlinear equations of Pseudo-first-order and Pseudo-second-order kinetic models, *Karbala International Journal of Modern Science* 4 (2018), 244-254.

Mudasir A., Shakeel A., Babu L.S & Saiqa I.: Adsorption of heavy metal ions, Role of chitosan and cellulose for water treatment, *International Journal of Pharmacognosy* 2, *6*, (2015), 280-289.

Negm N.A., El-Sheikh R., El-Farargy A.F., Hefni H.H.H. & Bekhit M.: Treatment of industrial wastewater containing copper and cobalt ions using modified chitosan, *Journal of Industrial and Engineering Chemistry* (2014).

O'Connell D.W., Birkinshaw C. & O'Dwyer T.F.: Heavy metal adsorbents prepared from the modification of cellulose: A review, *Bioresource Technology* 99 (2008), 6707-6724.

Olgun A. & Atar N.: Removal of copper and cobalt from aqueous solution onto waste containing, *Chemical Engineering Journal* 176 (2011), 140-147.

Osińska M.: Removal of lead (II), copper (II), cobalt (II) and nickel (II) ions from aqueous solutions using carbon gels, *Journal of Sol-Gel Science and Technology* (2016), 1 – 16.

Özer A., Gürbüz G., Çalimli A. & Körbahti B.K.: Biosorption of copper (II) ions on *Entreromorphaprolifera*: Application of response surface methodology (RSM), *Chemical Engineering Journal* 146 (2009), 377-387.

Palantöken S., Bethke K., Zivanovic V., Kalinka G., Kneipp J. & Rademann K.: Cellulose hydrogels physically crosslinked by glycine: Synthesis characterization, thermal and mechanical properties, *Journal of Applied Polymer Science* (2019), 1-11.

Parab H., Joshi S., Shenoy N., Lali A., Sarma U.S. & Sudersanan M.: Determination of kinetic and equilibrium parameters of the batch adsorption of Co(II), Cr(III) and Ni(II) onto coir pith, *Process Biochemistry* 41 (2006), 609-615.

Paugam M.-F. & Buff J.: Comparison of carrier-facilitated copper (II) ion transport mechanism in supported liquid membrane and in plasticized cellulose triacetate membrane, *Journal of Membrane Science* 147 (1988), 207.

Pedrosa Xavier A.L., Adarme Herrera O.F., Furtado L.M., Dias Ferreira G.M., Mendes da Silva L.H., Gil L.F & Alves Gurgel L.V.: Modeling adsorption of copper (II), cobalt (II) and nickel (II) metal ions from aqueous solution onto a new carboxylated sugarcane bagasse. Part II: Optimization of monocomponent fixed-bed column adsorption, *Journal of Colloid and Interface Science* 516 (2018), 431 – 445.

Perumal S., Atchudan R., Yoon D.H., Joo J. & Cheong I.W.: Spherical chitosan-gelatin hydrogel particles for removal of multiple heavy metal ions from wastewater, *Industrial & Engineering Chemical Research* 58 (2019), 9900-9907.

Qiu H., Lv L., Pan B., Zhang Q., Zhang W. & Zhang Q.: Critical review in adsorption kinetic models, *Journal of Zhejiang University SCIENCE A* 10 (2009) 716-724.

Qiu W. & Zheng Y.: Removal lead, copper, nickel, cobalt, and zinc from water by a cancrinite-type zeolite synthesized from fly ash, *Chemical Engineering Journal* 145 (2009), 483-488.

Rengaraj S., Yeon J-W., Kim Y., Jung Y., Ha Y-K. & Kim W-H.: Adsorption characteristics of Cu (II) onto ion exchange resins 252H and 1500H: Kinetics, isotherms and error analysis, *Journal of Hazardous Materials* 143 (2007), 469-477.

Reshetnyak E.A., Ivchenko N.V. & Nikitina N.A.: Photometric determination of aqueous cobalt (II), nickel (II), copper (II) and iron (III) with 1-nitroso-2-naphthol-3,6-disulfonic acid disodium salt in gelatin films, *Central European Journal of Chemistry* 10, *5* (2012), 1617 – 1623.

Rudzinski W. & Panczyk T.: Kinetics of Isothermal Adsorption on Energetically Heterogeneous Solid Surfaces: A New Theoretical Description Based on the Statistical Rate Theory of Interfacial Transport. *Journal of Physical Chemistry B.* 104 (2000), 9149-9162.

Sadeek S.A., Negm N.A., Hefni H.H.H. & Abdel Wahab M.M.: Metal adsorption by agriculture biosorbents: Adsorption isotherm, Kinetic and biosorbents chemical structures, *International Journal of Biological Macromolecules* 81 (2015), 400-409.

Sarkar M. & Majumdar P.: Application of response surface methodology for optimization of heavy metal biosorption using surfactant modified chitosan bead, *Chemical Engineering Journal*, 175 (2011), 376-387.

Shengo M.L., Kime M.-B., Mambwe M.P. & Nyembo T.K.: A review of the beneficiation of copper-cobalt-bearing minerals in the Democratic Republic of Congo, *Journal of Sustainable Mining* 18 (2019), 226 – 246.

Shojaeimehr T., Rahimpour F., Ali Khadivi M. & Sadeghi M.: A modeling study by response surface methodology (RSM) and artificial neural network (ANN) on Cu^{2+} adsorption optimization using light expendend clay aggregate (LECA), *Journal of Industrial and Engineering Chemistry* 20 (2014), 870-880.

Shrestha R.M.: Removal of Cd (II) ions from Aqueous Solution by Adsorption on Activated carbon Prepared from Lapsi (*Choerospondiasaxillaris*) Seed Stone, *Journal of the Institute of Engineering* 11, *1* (2015), 140-150.

Silva Filho E.C., Santos Júnior L.S., Fernandes Silva M.M., Fonseca M.G., Abreu Santana S.A. & Airoldi C.: Surface Cellulose Modified with 2-Aminomethylpyridine for Copper, Cobalt, Nickel and Zinc Removal from Aqueous Solution, *Materials Research* 16, *1* (2013), 79-87.

Singh R., Chadetrik R., Kumar R., Bishnoi K., Bhatia D., Kumar A., Bishnoi N.R. & Singh N.: Biosorption optimization of lead (II), cadmium (II) and copper (II) using response surface methodology and applicability in isotherms and thermodynamics modeling, *Journal of Hazardous Materials* 174 (2010), 623-634.

Stafiej A. & Pyrzynska K.: Adsorption of heavy metal ions with carbon nanotubes, *Separation and Purification Technology* 58 (2007), 49-52.

Tian Y., Wu M., Liu R., Li Y., Wang D. & Tan J.: Electrospun membrane of cellulose acetate for heavy metal ion adsorption in water treatment, *Carbohydrate Polymers* 83 (2011), 743-748.

Tünay O. & Kabdasli N.I.: Hydroxyde precipitation of complexed metals, *Water Resource* 28, *10* (1994), 2117-2124.

Valenta R.K., Kemp D., Owen J.R., Corder G.D. & Lèbre É.: Re-thinking complex ore bodies: Consequences for the future word supply of copper, *Journal of Cleaner Production* 220 (2019), 816-826.

Vieira R.S., Guibal E., Silva E.A. & Beppu M.M.: Adsorption and desorption of binary mixtures of copper and mercury ions on natural and crosslinked chitosan membranes, *Adsorption* 13 (2007), 603-611.

Wang L., Paimin R., Cattrall R.W., Shen W. & Kolev S.D.: The extraction of cadmium (II) and copper (II) from hydrochloric acid solutions using am Aliquat 336/PVC membrane, *Journal of Membrane Science* 176 (2000), 105-111.

Worch E.: Adsorption Technology in Water Treatment, De Gruyter, Germany, (2012).

Zhang W., Hu L. & Liu Y.: Optimized synthesis of novel hydrogel for the adsorption of copper and cobalt ions in wastewater, *RSC Advances* 9 (2019), 16058-16068.

Zhao H., Xu J., Lan W., Wang T. & Luo G.: Microfluidic production of porous chitosan/silica hybrid microspheres and its Cu (II) adsorption performance, *Chemical Engineering Journal* 229 (2013), 82-89.

CHAPTER 3: METHODOLOGY

The chapter gives a detailed account of the experimental procedures followed to attain the objectives of this research regarding the adsorption process.

3.1 Chemical reagents and materials

All the chemicals used in this research for the adsorption processes and membrane preparation, including sodium hydroxide sodium, hydrochloric acid, Cellulose nanocrystals (CNCs) gelatin, Cupric sulfate ($CuSO_4.5H_2O$) and Cobalt chloride ($CoCl_2.6H_2O$) were of analytical reagent grade (98-99.5%) and were obtained from Sigma Aldrich and LabChem.

3.2 Preparation of GCHM and synthetic solution

3.2.1 Preparation of gelatin-CNCs hydrogel membrane

Adequate quantities of CNCs were dispersed in 50mL of water (see Table 1). The CNCs' suspension was then homogenized using a homogenizer (Model: SH-II-7C) to ensure the CNCs were suspended uniformly. A certain amount of gelatin (see Table 1) was then added into the CNCs' suspension. The mixture was then stirred at 55°C until one phase was obtained.

Table 1: Composition of GCHM Hydrogel

	Ratio 1:3 (%) A (g)	Ratio 1:1 (%) B (g)	Ratio 3:1 (%) C (g)	Water (mL)
Gelatin	2.5	5.0	7.5	50
CNCs	7.5	5.0	2.5	

The cross-linking agent (EDTA 1%) was then added dropwise. After 4 hours, the mixture was poured into a Petri dish and placed in the oven at 45°C until the mixture was dried. Hydrogels as films were removed from the Petri dish and washed with distilled water to remove unreacted chemicals. The EDTA and water traces were then extracted from films using acetone (Yao *et al*., 2019; Yin & Amin, 2014).

3.2.2 Preparation of synthetic water

The synthetic water of Cu(II) and Co(II) solutions (A) of concentration of 250 mg/ℓ which correspond to 1.965 g and 2.002 g, respectively were prepared by dissolving $CuSO_4.5H_2O$ and $CoCl_2.6H_2O$ salts in deionized water in 2000 mL volumetric flasks. 1200 mL of demineralized water was added to 800mL of solution (A) to prepare a solution (B) of 100 mg/ℓ. Solution of concentration 100mg/ℓ of Cu(II) and Co(II) ions was prepared for the adsorption studies.

Solutions of 1 ppm, 5 ppm, and 10 ppm of Cu^{2+} and Co^{2+} synthetic water were prepared to standardize the Atomic Absorption Spectrophotometer (AAS) before analysis of samples.

3.3 Adsorption studies

The adsorbed quantity and the percentage removal of binary metal ions were calculated using the following equations, respectively:

$$q_e = V(C_o - C_e)/m \quad (3.1)$$

$$\% \text{ Adsorbed} = 100[(C_o - C_e)/C_o] \quad (3.2)$$

where, q_e*(mg/g)* is the quantity of metal ions adsorbed per unit mass of adsorbent, C_o *(mg/ℓ)* is the initial metal ion concentration, C_e *(mg/ℓ)* is the equilibrium metal ion concentration in solution, *V (L)* is the volume of solution used and *m (g)* is the mass of the adsorbent.

The final concentrations were compared with the initial concentration. The adsorption did take place because the final concentrations were lower than the initial concentration (Kabuba & Banza, 2020).

3.4 Experimental procedure

The experiments were carried out in 250 mL of the plastic container, at a constant agitation speed (250 rpm) with a 100 mL solution. An amount of 0.25 g of adsorbent (GCHM) was added into 100 mL of binary metal ions solution and the mixtures were

placed in a rotary shaker between 15 and 120 minutes. The effect of various operating temperatures ranging between 30^{o}C and 75^{o}C was investigated using a thermo-shaker.

For studying the effect of pH, the solution of binary metal ions was adjusted to a value between 3 and 9 by using 1M of HCl and NaOH solutions.

The adsorption of Cu(II) and Co(II) ions by GCHM was tested in batch experiments. A shaker was used for mixing the solution. To establish the optimum conditions that are suitable for the removal of Cu(II) and Co(II), several operational parameters were optimized, and they include effects of contact time, pH, temperature, contact time andthe ratio of CNCs and Gelatin. To ensure the validity of the results and reputability, all experiments were performed in triplicate and the data was reported as average values.

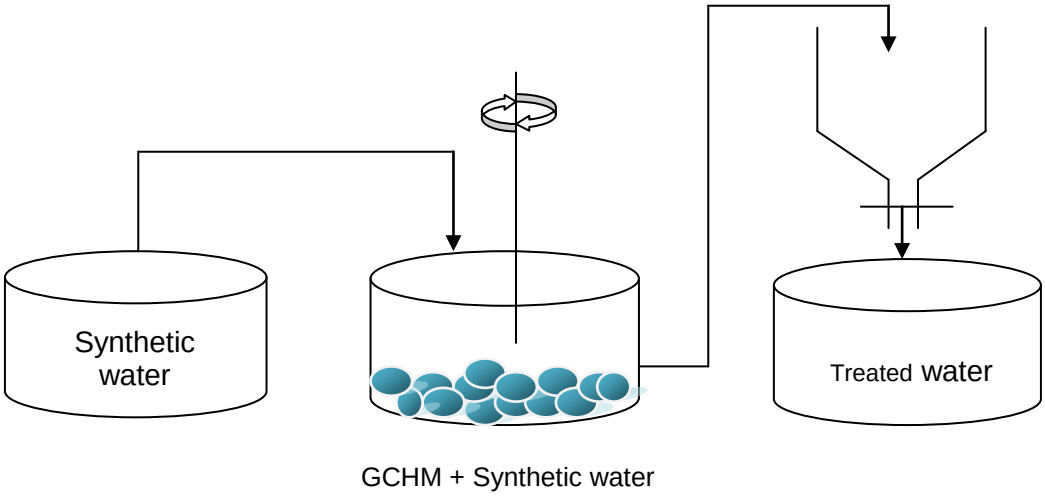

Figure 5: Schematic representation of the experimental setup

A batch experiment was conducted to determine the effect of pH, operating temperature, contact time, and GCHM-ratio on the adsorption process of GCHM. The percentage of ions removed using GCHM was considered as a measure of the uptake percentage. The uptake efficiency (%) was calculated according to Equation (3.2) (Kabuba, 2016).

3.5. Analyzing techniques

3.5.1 Atomic absorption spectroscopy analysis (AAS)

Atomic absorption spectroscopy (AAS) was used to determine the concentration of Cu(II) and Co(II) in solution. This was to determine the performance of the Gelatin-CNCs in recovering the targeted metals. The Atomic Absorption Spectrophotometer (a Varian Spectra (20/20)) was used with instrument parameters set at wavelengths for the two metals at Cu (324.7 nm) and Co (240.7 nm) and a spectral band of 0.2 nm for both metals for all AAS analyses. The flame type used was air-acetylene. Standards of 1000 mg/ℓ, 2000 mg/ℓ and 3000 mg/ℓ were then prepared and a calibration curve was drawn using these standards. A hollow cathode tube is containing the same element then discharges monochromatic light of similar wavelength as the element being analyzed, and was passed through the vaporized sample. The element absorbs the radiant light from the hollow cathode tube and the degree of absorption expresses the amount of the element present in the sample (Muhammad, 2012; Skoog *et al*., 2004). Dilution was applied stoichiometrically where the concentrations of the unknown solutions of copper and cobalt exceeded the concentration range of the standards.

3.5.2 Scan Electron Microscope-Energy Dispersive Spectroscopy (SEM-EDS)

The scanning electron microscopy joined together with the energy dispersive x-ray spectroscopy (SEM-EDS) was used to study the surfaces of solids to give information about topological and morphological presentations. Analytical tool may assist researchers to provide viable explanations about the behaviour of solids.

The SEM is based on energetic electrons that hit the sample, thus producing signals that are responsible for the scanning process. Primary electrons released from the source provide energy to the atomic electrons of the specimen which can then release as the secondary electrons and an image can be formed by collecting these secondary electrons from each point of the specimen; the basic requirement for SEM to operate is under a vacuum to avoid interactions of electrons with gas molecules in order to obtain a high resolution. Besides, the primary electrons produced and emitted from the electron

gun are accelerated by heating or applying high energy in the range of 1−40 keV (Akhtar *et al*., 2018).

The SEM was following some steps. A portion of the sample was milled and mounted together with non-processed samples. The mounted samples were coated with carbon and finally scanned with the SEM-EDS.

The SEM-EDS was conducted to describe the morphology and the chemistry of raw samples using an SEM JEOL JSM-840 instrument. The granular slag sample was crushed, screened to obtain different particle sizes of +300, +212, +150, +106, +75, +53, +38 mm was then mounted and coated with carbon together with non-processed samples to make the surface more conducive and to ameliorate the visibility. The mounted samples were then inserted in the instrument and subjected to an electron beam under a vacuum to obtain micrographs of the sand stones.

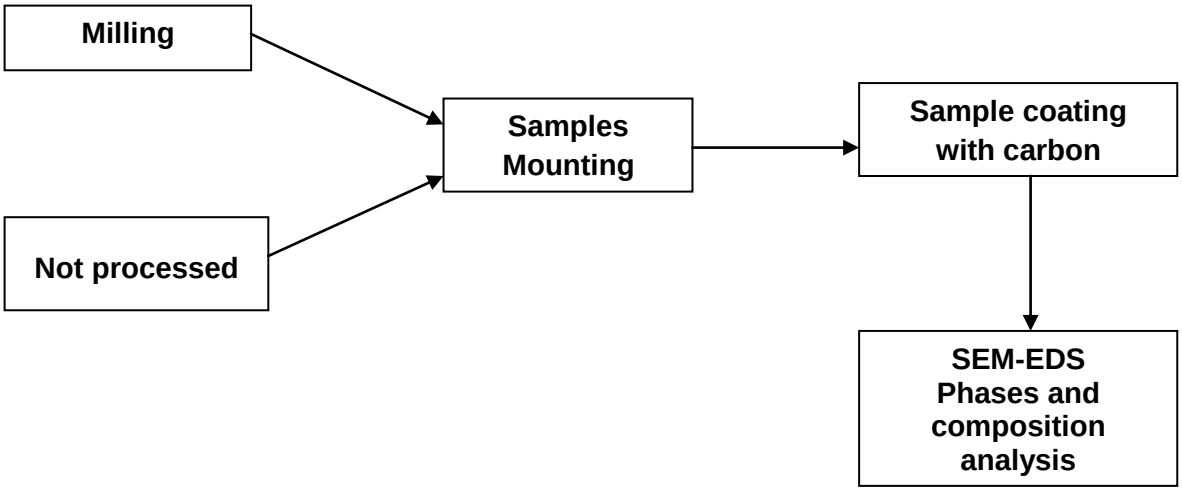

Figure 6: Samples preparation and SEM-EDS

The SEM instrument used was coupled with EDS with an automated image investigation system using a back scattered electron beam (BSE). The X-ray detector of the EDS calculates the number of emitted X-rays in opposition to their energy. The energy of the X-ray is characteristic of the element from which the X-ray was emitted. A spectrum of the energy in opposition to relative counts of the detected X-rays is found and assessed for qualitative and quantitative identification of existing chemical elements. The chemical

composition analysis of some spotted contrasts on the mounted and coated sample was then determined using EDS.

3.5.3 Fourier Transform Infrared (FTIR)

The FTIR analysis was utilized to determine the functional groups on the structure of GCHM (approx. 75µm) with a bromide binder in a ratio of 1:10 of sample to binder (0.05 g GCHM: 0.5 g binder) and mixing using a pestle and mortar until homogeneity of the mixture was achieved. The pellet was analyzed for its peaks. Results of IR spectra were obtained using a Midac FTIR 5000 Spectrophotometer on CaF_2 plates. The IR data are listed with their individual characteristic peaks in wavenumber (cm^{-1}). The results are reported in the form of graphs in Chapter 4.

The vibrational frequencies of a given chemical group are expected in specific regions which depend on the type of atoms involved and the type of chemical bonds. The tables of the main functional groups (carboxyl, amine, alcohol, amino acid…) are available. Within these vibration ranges, the frequencies of the functional groups are modulated by the specific environment of the group (Berthomieu & Hienerwadel, 2009).

The principle of this method of analysis is based on the electromagnetic radiation that interacts with a substance that can be absorbed, transmitted, reflected, scattered, or have photoluminescence, which provides significant information on the molecular structure and the energy level transition of that substance. The detector measures the intensity of the radiation transmitting through a sample. Its outputs as a function of time are converted into a plot of absorption against wavenumber by a computer using a Fourier transform method (Munajad *et al*., 2018).

Infra-red radiation may be absorbed by covalent bonds present in a sample resulting in the vibration of the bond at a specific amplitude unique to that type of a covalent bond due to the absorbed frequency. The absorbed frequency largely depends (among other factors) on the geometry and the weights of the atoms present in the vibrating covalent bond (Skoog *et al*., 2004).

3.6 RSM-CCD procedure

The RSM by using CCD is used to design the experiments, evaluate the effect of the process parameters, identify the optimum conditions, and build a regressive model. In this study, the independents process factors (ratio, contact time, pH and temperature) and their interactive effects on the percentage of Cu(II) and Co(II) removal, were investigated. An optimization procedure is needed to design the experimental and verify their interactive effects (Lingamdinne *et al*., 2018).

The experimental range and coded levels of the selected process variables along with their units are shown in Table 6. The experimental runs were designed for the process parameters in the range of the pH (3-9); the ratio of gelatin (25-75%); contact time (15-120 min) and temperature (30-75°C).

The interactions between the various independent process variables and their resultant impact on the output (response) variable were studied systematically using surface contour plots. CCD with a full factorial was developed using Design-Expert software. Each factor was varied over three levels: the high level (+1), the low level (-1) and the center points (coded level 0) (Li *et al*., 2013). The processing factors and levels involved in the study are shown in Table 7.

Based on the RSM-CCD framework, an experimental design matrix with 21 experiments as shown in Table 8, was obtained. To predict the removal efficiency, and develop a polynomial regression model, the ANOVA approach was used. To estimate the best optimal values of process variables that give maximum removal efficiency, the quadratic model fitted by RSM along with the desirability index is used (Dehghani *et al*., 2020).

3.7 References

Akhtar K., Khan S.A., Khan S.B. & Asiri A.M.: Scanning Electron Microscopy: Principle and Applications in Nanomaterials characterization, *Springer International Publishing AG, part of Springs Nature* (2018), 113-145.

Berthomieu C. & Hiererwadel R.: Fourier Transform Infrared (FTIR) spectroscopy, *Photosynthesis Research* (2009), 157-170.

Dehghani M.H., Karri R.R, Yeganeh Z.T., Mahvi A.H., Nourmoradi H., Salari M., Zarei A. & Sillanpää M.: Statistical modelling of endocrine discrupting compounds adsorption onto activated carbon prepared from wood using CCD-RSM and D.E hybrid evolutionary optimization framework: comparaison of linear Vs non-linear isotherm and kinetic parameters, *Journal of Molecular Liquids* 302 (2020), 112526.

Kabuba J. &Banza M.: Modification of clinoptilolite with dialkylphosphinic acid for the selective removal of cobalt (II) and nickel (II) from hydrometallurgical effluent, *The Canadian Journal of Chemical Engineering*, Accepted, (2020).

Kabuba J.T.: Application of neural network techniques to the ion-exchange process and prediction of abrasiveness characteristics of thermal coal, D.Tech (Metallurgy), Unpublished, University of Johannesburg (2016).

Li J., Peng J., Guo S. & Zhang L.: Application of response surface methodology (RSM) for optimization of sintering process for the preparation of magnesia partially stabilized zirconia (Mg-PSZ) using natural baddeleyite as starting material, *Ceramics International* 39 (2013), 197-202.

Lingamdinne L.P., Koduru J.R., Chang Y-Y. & Karri R.R.: Process optimization and adsorption of Pb(II) on nickel ferrite-reduced graphene oxide nano-composite, *Journal of Molecular Liquids* 250 (2018), 202-211.

Muhammad A.F.: Atomic Absorption Spectroscopy, InTech, Croatia (2012).

Munajad A., Subroto C. & Suwarno: Fourier Transform Infrared (FTIR) Spectroscopy Analysis of Transformer Paper in Mineral Oil-Paper Composite Insulation under Accelerated Thermal Aging, *Energies* 364, 11 (2018), 1-2.

Perumal S., Atchudan R., Yoon D.H., Joo J. & Cheong I.W.: Spherical chitosan-gelatin hydrogel particles for removal of multiple heavy metal ions from wastewater, *Industrial & Engineering Chemical Research* 58 (2019), 9900-9907.

Skoog D.A., West D.M., Holler F.J. & Crouch S.R.: Fundamentals of Analytical Chemistry, 8th Edition, Brooks/Cole, USA (2004).

Yao Y., Wang H., Wang R., Chai Y & Ji W.: Fabrication and performance characterization of the membrane from self-dispersed gelatin-coupled cellulose microgels, *Cellulose* 26 (2019), 3255-3269.

Yin O.S & Amin M.C.I.M.: Synthesis of chemical cross-linked gelatin hydrogel reinforced with cellulose nanocrystals (CNC), *AIP Conference Proceedings* 1614 (2014), 375-380.

CHAPTER 4: RESULTS AND DISCUSSION

4.1 Characterization of GCHM

4.1.1 FTIR analysis

The samples of cellulose pure, gelatin pure and their mixtures have been prepared on the disc of CaF_2 and analyzed using Midac FTIR 5000 Spectrophotometer. The absorption FTIR spectra obtained are represented in the Figures 7a-7d.

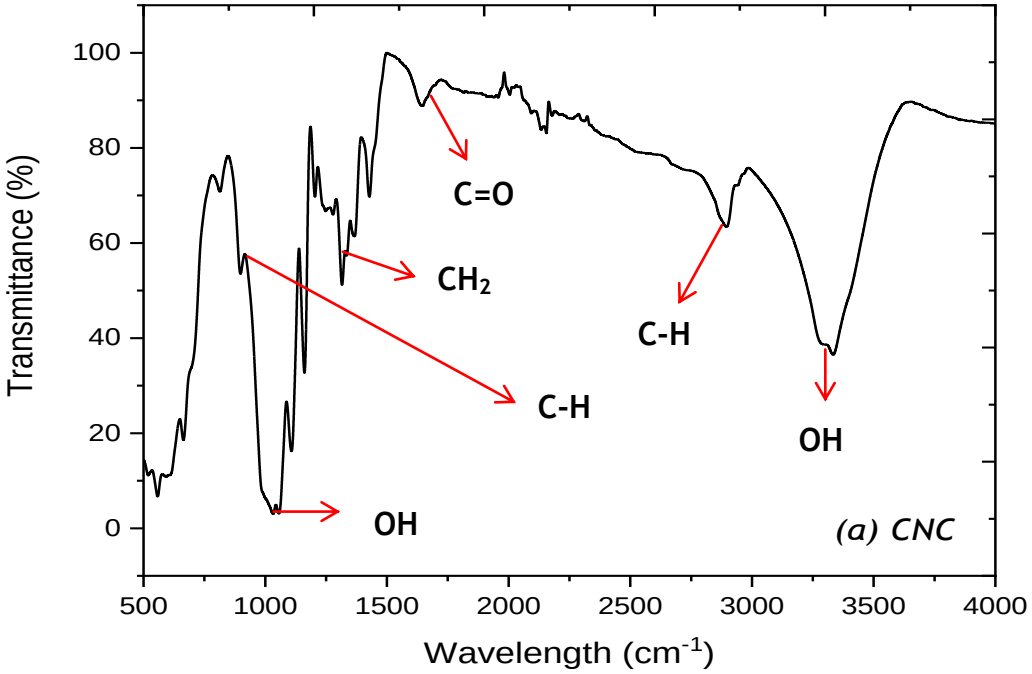

Figure 7a: Spectra FTIR of CNC

The CNCs have shown the characteristic bands around 3000 and 3650 cm^{-1} that represents the strong elongation vibration band of the OH function. At 2950 cm^{-1}, an elongation vibration band for bound C-H that is confirmed by the deformation band around 1500 cm^{-1} is observed. The band around 1450 cm^{-1} is the vibration shear of CH_2 (Alemdar & Sain, 2008; Sain & Panthapulakkal, 2006). The peak at 1700 cm^{-1} is characteristic of the elongation vibration band of the carboxyl (C=O) confirmed by the characteristic band around 890 cm^{-1} that corresponds to the C-H of aldehyde group (Munster *et al*., 2017). The peak around 1000 $cm^{-1}$is attributed to OH function (Yao *et al*., 2019).

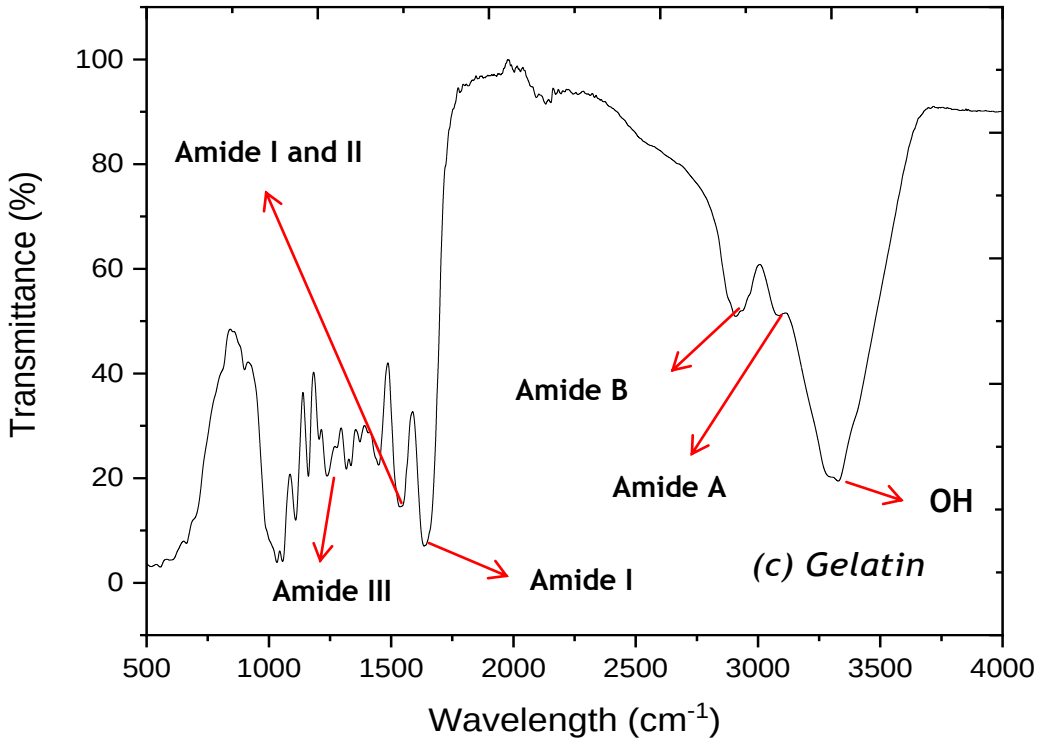

Figure 7b: Spectra FTIR of gelatin

The FTIR spectra of gelatin has presented the characteristic peaks around of 2955 cm^{-1} for the vibration band of the amide A, of 2700 cm^{-1} for the vibration band of the amide B, of 1600 cm^{-1} for the vibration band of the amide (I), of 1500 cm^{-1} for the vibration band of the amide (I), of 1500 cm^{-1} for the vibration band of the amide (II) and of 1200 cm^{-1} for the vibration band of the amide (III). The amide (III) is represented by the combination of the elongation vibration peaks of C-N and the deformation vibration peaks of N-H. Moreover, the amide (I) is characterized by the elongation vibration of C=O to which is added a contributive band of elongation vibration of C-N, of deformation out-of-plan of C-C-N. Finally, the amide (II) is characterized by the elongation vibration band of C-N and that of out-of-plane deformation of N-H out-of-plan (Merina Paul Das *et al*., 2017; Fernandes de Almeida *et al*., 2012; Al-Saidi *et al*., 2012).The peaks below 1000 cm^{-1} are characteristic of low molecular weight amides (Fernandes de Almeida *et al*., 2012).

After analyzing the FTIR spectra of gelatin and CNCs, the spectra of the mixtures of gelatin and CNC in proportions A, B, and C were analyzed (Fig. 7d).

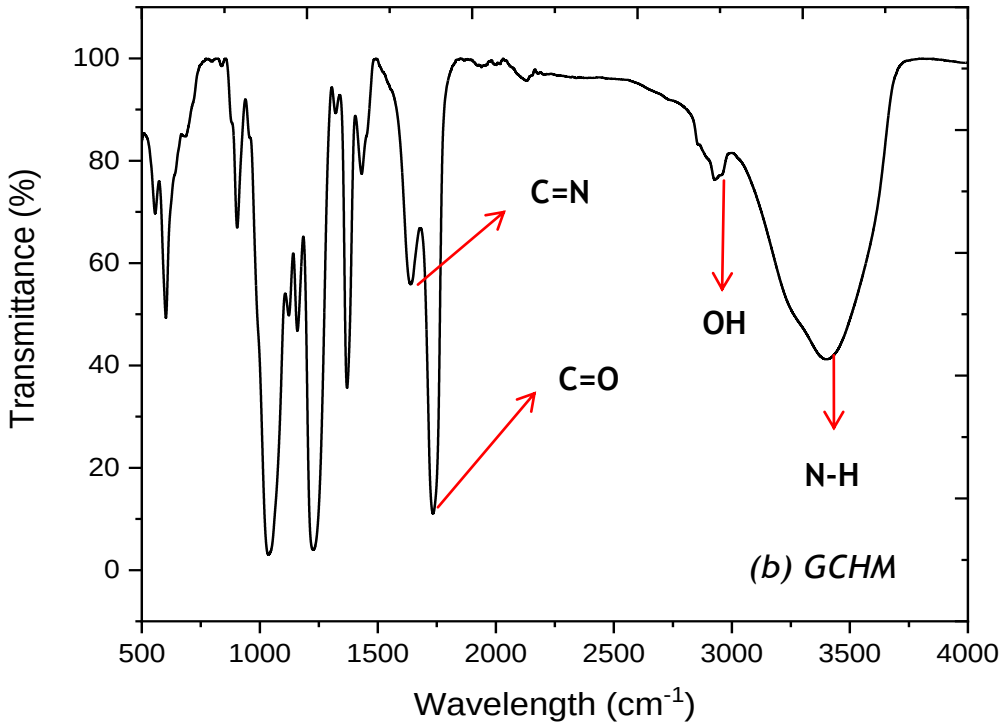

Figure 7c: Spectra of CNC-Gelatin Hydrogel Membrane at a ratio of 25÷75%

The FTIR spectra of the mixture of GCHM (A, B, and C) (see Figure 1c) show the characteristic band between 3240-3634 cm^{-1} of the elongation vibration of N-H, between 2894-2942 cm^{-1} of O-H which is confirmed by the deformation band between 1403-1451 cm^{-1}, at 1700 cm^{-1} of the elongation vibration of C=O confirmed by the C-O band 1149 and 1240 cm^{-1} and a less elongation band of C=N at 1640 cm^{-1}.

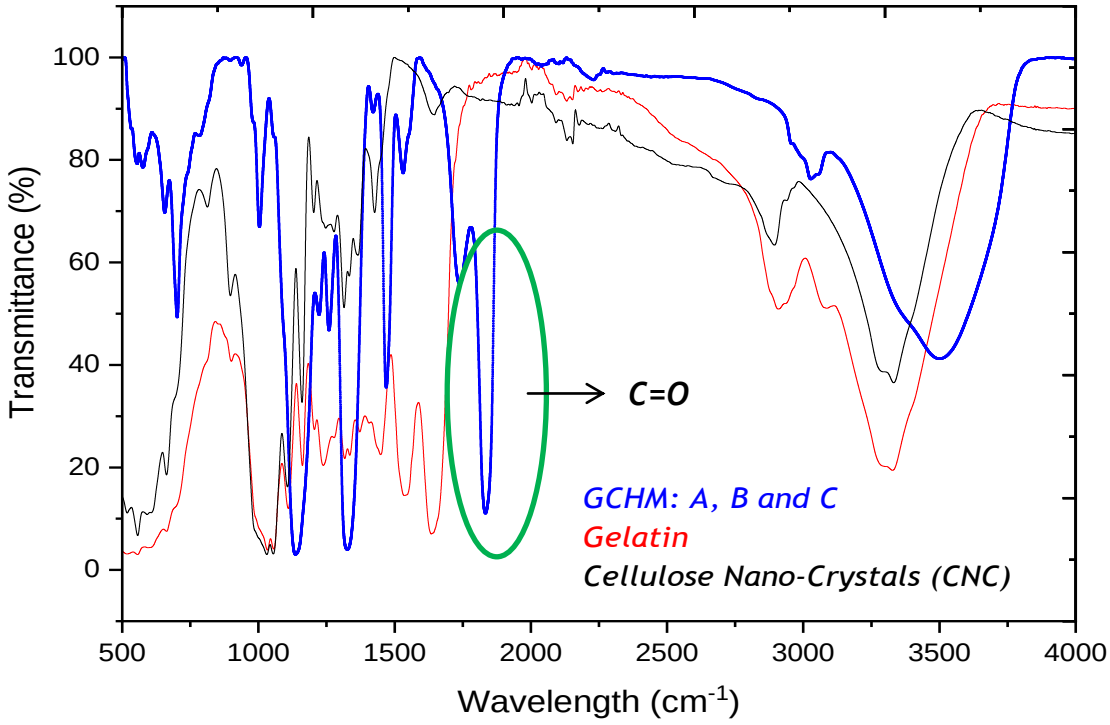

Figure 7d: Spectra of CNCs, Gelatinand, GCHM

A comparison of the values of different bands shows a bathochromic effect coupled with a decrease in the intensity of certain bands (Silvestein *et al*., 2007; Feinsten, 1995). The bands are appearing between 2400 and 3600 cm^{-1} (N-H and O-H) for mix A which moves to 3000 and 3600 cm^{-1} for mix B up to 3240-3634 cm^{-1} for the mix C. The same phenomenon is observed with the C=N band which moves from 1490 cm^{-1}, at 1550 cm^{-1} to 1650 cm^{-1} when moving from ratio A, B, and C, respectively, for the gelatin-cellulose mixture. In addition, they were observed as a slight constancy of the carboxyl band at 1700 cm^{-1} except for the intensity of the band which increased slightly when going from ratio A to B.

The bathochromic effect observed with increasing gelatin content is evidence that new bonds are formed and therefore new functions are formed. This is why there was disappearance of certain bands and the decrease in the intensity of others. The optimum ratio appears to be that of the gelatin-cellulose of 75%:25%. Indeed, increasing the gelatin content could improve the quality and behaviour of the membrane.

4.1.2 SEM analysis

The SEM was used to observe the change in the morphological structure of the GCHM; the SEM image of GCHM modified with EDTA is presented in Figures 8A, 8B, and 8C. The images were taken by applying 4 kV voltage with different magnification times for the clarification of the surface. The SEM images of GCHM powder before adsorption were studied in Figure 8.

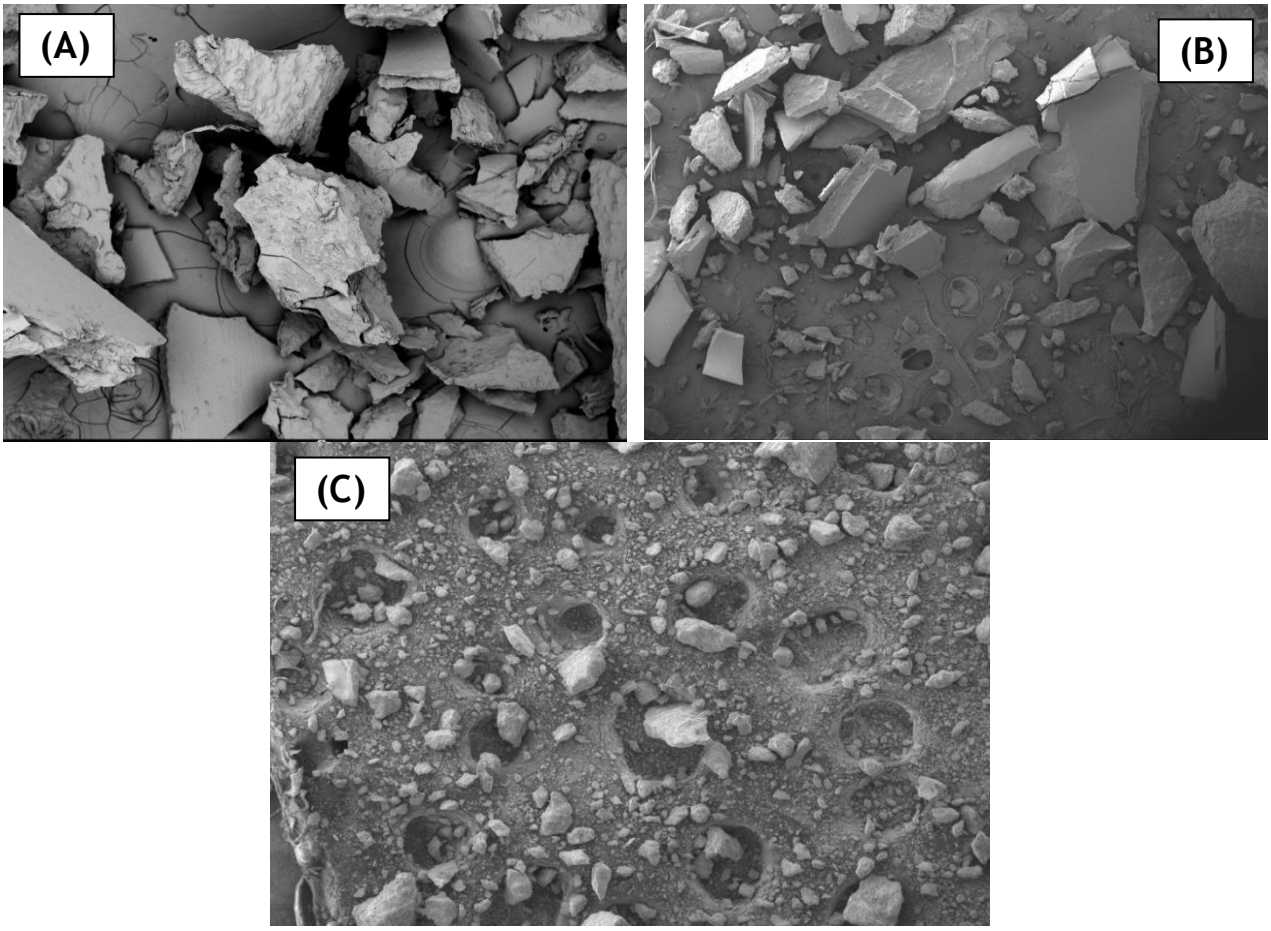

Figure 8: The SEM images of GCHM A (25:75%), B (50:50%), and C (75:25%)

Porosity characterization is based on the presence of open pores, which are related to properties such as permeability and surface area of the porous structure. The SEM image indicates the presence of bigger particles with irregular shapes (Figures 8A and 8B). Figure 8C shows the cavities of different shapes and sizes, and larger pores

between the particles could be observed, which will be helpful for the solution permeating through the GCHM (Wang *et al.*, 2018).

The high porosity provides a favourable adsorption of copper and cobalt ions (Hassan *et al.*, 2014). The presence of such granules increases the surface area of the composite, which is suitable for effective adsorption of metal ions. A visible change in surface morphology can be observed following adsorption. Small openings and holes on the surface increase the contact of the adsorption and therefore lead to pore diffusion during the adsorption process (Kabuba & Banza, 2020; Fasso-Kankeu, 2018). A morphology that changes as the gelatin concentration increases (Figure 8C>Figure 8B> Figure 8A) and consequently, several pores have been observed. Figure 8C reveals well-developed shapes and small particles and larger pores, with an external surface full of cavities, which indicated the new material (Figure 8C) was able to absorb a large amount of Cu(II) and Co(II) ions.

4.2 Adsorption study

4.2.1 Effect of solution pH

The solution pH affects the surface charge of the adsorption sorbent and the degree of ionization and specification of the adsorbate. Figure 9 shows the effect of pH on the percentage of Cu(II) and Co(II) ions adsorbed by GCHM. The result indicated that the removal of both metals ions from solution is strongly affected by the pH of the medium. The adsorption was low in acidic medium but increased with increases in the pH of the solution.

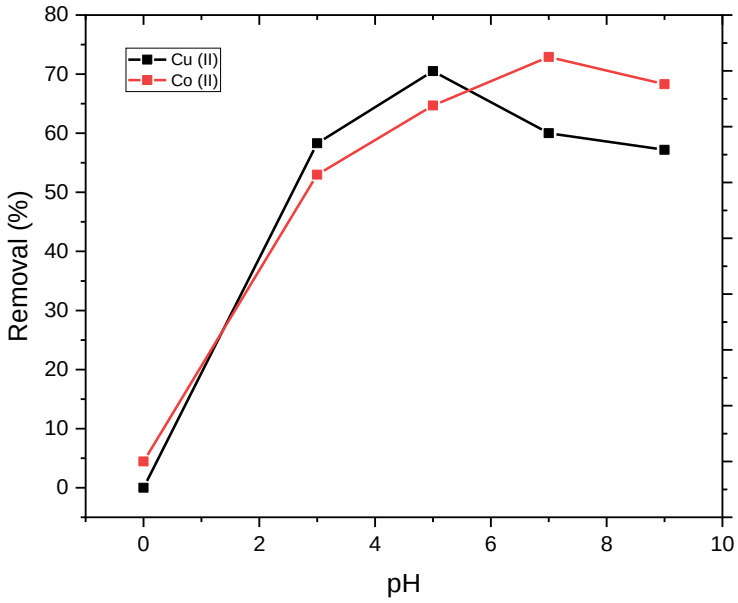

Figure 9: Effect of pH on the removal of Cu(II) and Co(II), Ratio 3:1 at 30^{o}C

The highest removals were 70.5 % and 72.5% for Cu(II) and Co(II) at pH 5 and pH 7, respectively. It has been reported by Kumaruzaman *et al. (*2017), Akpomie *et al*., (2015), Al-Shahrani, (2014) and El-Sheikh *et al*., (2012) that at low pH from 3 to 5 values, the adsorption of both metal ions was low because large quantities of protons (H^{+}) compete with the removal cations for the functional groups sites on GCHM, and also the electrostatic repulsion between Cu(II) and Co(II). As the pH of the solution increases, the number of positively charged available sites decreased and the number of the negatively charged active sites increased. The adsorption of copper and cobalt ions was mainly influenced by the pH of the solution. As the high percentage removal of Cu(II) and Co(II) was obtained at pH 5 and 7 for Cu(II) and Co(II) ions, respectively. Therefore, pH 5 and 7 were chosen in this study for all subsequent experiments since high removal was achieved.

4.2.2 Effect of Gelatin-CNCs Ratios

The effect of gelatin and CNCs ratios was investigated in this study. The ratios of both chemicals have played a big role in the percentage removal of both ion metals at different values of pH. Figure 10 shows the effect of gelatin and cellulose nanocrystals (CNCs) ratio on the removal of Cu(II) and Co(II).The pH and temperature were kept

constants for this experiment at pH 5 and 7 for all of three investigated adsorbents (three ratios).

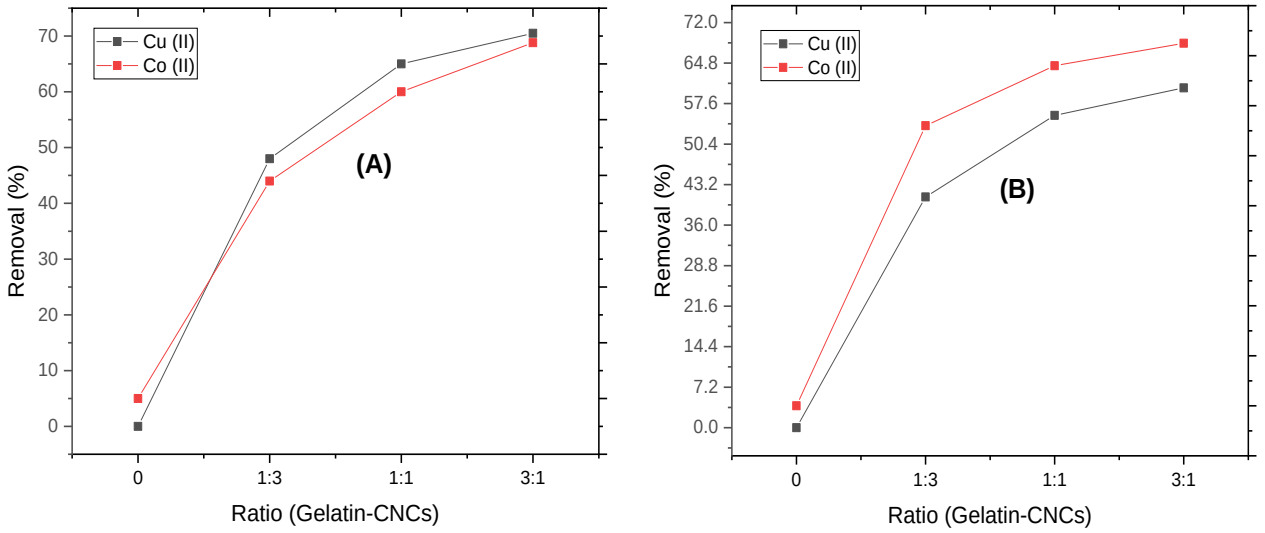

Figure 10: Effect of ratio on percentage removal of Cu(II) and Co(II), pH 5 (A) and pH 7 (B), 120 min at 30^{o}C

The results in Figure 10 shows that the percentage removal of both ion metals increases with an increased gelatin amount. The high percentage removal was 70.5 and 72.5% for Cu(II) and Co(II) at pH 5 and 7, respectively. It is shown that for pH ≥ 7, there is an increase in swelling ratio with increasing counter ions in the GCHM (Yin *et al.*, 2014; Reshetnyak *et al*., 2012). This situation is due to the presence of lone pairs from the amino acid of gelatin. According to Yin *et al*., (2014), the isoelectric point (pI) of gelatin is 4.9 and at this point, the numbers of negative charges are equal to positive charges, and therefore the net charge of the network is zero. The electrical attractions between opposite charges lead to the collapse of the network. Above the isoelectric point, the network is negatively charged forming anionic gel. At pH 5, which pH≈pI, the hydrogel hardly swells. This situation can explain why the percentage removal of copper and cobalt metal ions are low and almost closer to pH5 (Figure 10A).

4.2.3 Effect of time on removal

The effect of contact time on the percentage removal of Cu(II) and Co(II) ions into GCHM for different values of pH can be seen in Figure 11, in order to investigate the outcomes of the research done by Liu *et al*. (2015) that state that the percentage removal was a function of contact time. The effect of shaking time on Cu(II) and Co(II) ions adsorption was investigated by varying the contact time between the adsorbate and adsorbent in the range 15 – 120 minutes. The initial concentration of Cu(II) and Co(II) ions was 100 mg/ℓ, while the dose of GCHM was 0.25g/100mL of Cu(II) and Co(II) ions solution. The pH of the solution was kept constant at pH 5 and 7 for Cu(II) and Co(II), respectively.

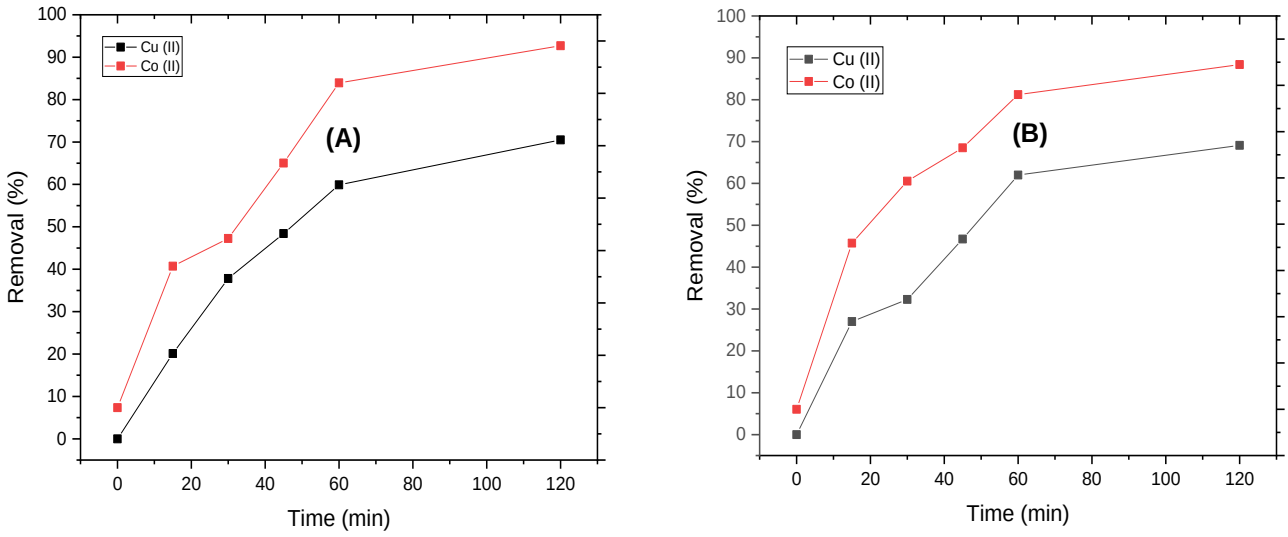

Figure 11: Effect of Time on removal of Cu(II) and Co(II), Ratio 3:1,; pH 5 (A) and pH 7 (B) at 30^{o}C

Two regions can be observed in the adsorption behaviour as seen in Figure 11, the rapid and slow removals. The rapid adsorption is favoured by the abundant availability of the active sites on the adsorbent. This can be ascribed to the fact that, initially all adsorbent sites are vacant. As discussed previously, the highest removal of Cu(II) and Co(II) are achieved at pH of 5 and 7, respectively. Therefore, the removal rate of Cu(II) and Co(II) are initially delayed at pH 5 and 7, respectively due to the effect of pH. From 60 minutes, the removal became too slow (equilibrium), which is due to the non-availability of vacant active sites on the adsorbent surface (Kumaruzaman *et al*., 2017).

The adsorption rate of Cu(II) and Co(II) compared with researches using different adsorbents, Cellulose Acetate Membrane (Kumaruzaman *et al*., 2017) and activated bentonite (Al-Shahrani, 2014) was delayed, and the sorption equilibration was not reached quickly. The time needed for adsorption to reach equilibrium can be attributed to the low adsorption capacity of GCHM and also to the high initial concentration of Cu(II) and Co(II) metal ions (the mass adsorbent was 0.25g per 100mL of solution).

4.2.4 Effect of temperature

The variation in the amount of Cu(II) and Co(II) adsorbed unto GCHM as a function of solution temperature is shown in Figure 12. It was observed that the temperature showed a negative effect on adsorption of Cu(II) and Co(II) onto GCHM. The decrease in Figure 12 is drastic with the increase in temperature.

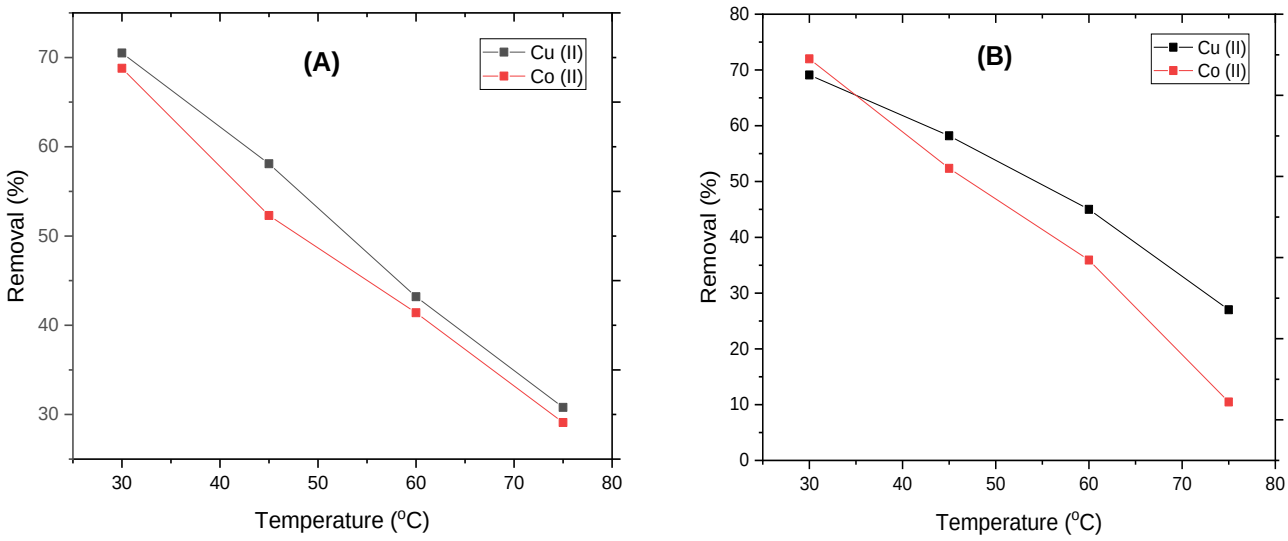

Figure 12: Effect of Temperature on the removal of Cu(II) and Co(II), Ratio 3:1, pH 5 (A) and pH 7 (B)

A decreasing trend in the removal of Cu(II) and Co(II) metals ions was observed while the temperature increased. The percentage removal of Cu(II) and Co(II) ions was decreased from 70.5 to 30.8% and from 63.8 to 24.1 at pH5 for Cu(II) and Co(II), respectively. At pH 7, the percentage removal decreased from 69.1 to 27% and from 74.5 to 32.2% for Cu(II) and Co(II), respectively. This indicates that a high temperature does not favour the adsorption process. Contrary to the study made by Mobasherpour *et al*. (2014), this trend doesn't favour swelling with the increase in temperature.

It was observed that the disintegration of Gelatin-CNCs Hydrogel Membrane while temperature was gradually increased, and the filtration becomes difficult after the adsorption process. This is the reason why it is better to work with lowess temperatures. Therefore, the temperature of 30^{o}C was chosen to run all the experiments.

4.3 Adsorption isotherm models

Adsorption isotherms of Cu(II) and Co(II) ions on GCHM were investigated using three different adsorption isotherm models: Langmuir, Freundlich, and Dubinin-Radushkevich (Shrestha, 2015; El Nemr *et al*., 2010; Blahovec *et al*., 2009; Vieira *et al*., 2007). These models were used to fit the experimental data obtained from this work. The qualities of the isotherm fit to the experimental data were typically evaluated based on the magnitude of the correlation coefficient for the regression. The isotherm giving an R^2 value closest to unity was considered to give the best fit. The adsorption isotherms for Cu(II) and Co(II) ions were studied using different ratios 3:1 at the adsorbent mass of 0.25 g at 303, 318, 333, and 348K and solution pH 7.

The data obtained from linear Langmuir and Freundlich isotherms plot from the adsorption of copper and cobalt ions onto GCHM are presented in Table 2 and plotted in Figures 13 and 14.

From the high values of the correlation coefficient R^2 shown in the Table 2 for both metal ions, the Freundlich isotherm has provided a good fit to the experimental data. The monolayer adsorption capacities of GCHM for Cu(II) and Co(II) are 5.848 and 10.989mg/g, respectively at 303K.

The Freundlich isotherm is based on multilayer adsorption on the heterogeneous surfaces. The data obtained from the linear Freundlich isotherm plot for the adsorption of Cu(II) and Co(II) onto GCHM are presented in Table 2 and plotted in Figures 13 and 14. The value of "*n"* between 1 and 10 shows a good affinity and adsorption which indicated that copper and cobalt ions are favourably adsorbed by GCHM. From Table 2, the Freundlich constant was 0.833 and 1.311, respectively for Cu(II) and Co(II) ion metals at pH 7 (Akpomie *et al*., 2015).

Table 2: Adsorption isotherm parameters of Cu(II) and Co(II) into GCHM

Metal ions		Isotherm model	Parameters	303K	318K	333K	348K
Cu^{2+}	pH 5	D-R	q_m	10.263	2.909	2.909	0.450
			E	5.49	3.32	2.58	1.57
			R^2	0.6779	0.7484	0.8136	0.902
		Langmuir	K_L	0.0333	0.0228	0.0192	0.01464
			q_m	5.848	2.9326	2.2075	0.7734
			R^2	0.877	0.798	0.816	0.850
		Freundlich	n	0.833	0.492	0.383	0.189
			K_F	$1.89x10^3$	$5.39x10^4$	$8.29x10^5$	$7.07x10^{10}$
			R^2	**0.8905**	**0.9068**	**0.9597**	**0.9709**
Co^{2+}		D-R	q_m	8.103	2.755	1.847	5.317
			E	4.26	2.4	2.06	1.3
			R^2	0.7123	0.7957	0.9206	0.7332
		Langmuir	K_L	0.0277	0.0188	0.0172	0.0139
			q_m	4.7169	1.9802	1.8939	0.7559
			R^2	0.861	0.8211	0.9067	0.9186
		Freundlich	n	0.677	0.357	0.305	0.172
			K_F	$5.91x10^3$	$1.51x10^6$	$1.29x10^7$	$8.7x10^{11}$
			R^2	**0.894**	**0.906**	**0.958**	**0.971**
Cu^{2+}	pH 7	D-R	q_m	2.305	2.126	2.091	3.179
			E	5.49	3.25	2.16	1.44
			R^2	0.8351	0.7543	0.8997	0.8918
		Langmuir	K_L	0.0389	0.0229	0.0175	0.0139
			q_m	7.6923	2.7174	1.9084	0.6494
			R^2	0.950	0.796	0.93	0.855
		Freundlich	n	0.932	0.482	0.307	0.168
			K_F	$1.1 x10^3$	$6.3 x10^4$	$1.1 x10^7$	$1.4x10^{12}$
			R^2	**0.954**	**0.887**	**0.971**	**0.936**
Co^{2+}		D-R	q_m	15.341	5.949	4.637	1.089
			E	7.91	3.79	3.07	1.86
			R^2	0.7881	0.7965	0.9113	0.9062
		Langmuir	K_L	0.0519	0.0263	0.0228	0.0157
			q_m	10.989	3.8168	3.7453	1.328
			R^2	0.872	0.844	0.949	0.873
		Freundlich	n	1.311	0.641	0.489	0.248
			K_F	$3.7 x10^2$	$8.1 x10^3$	$6.4x10^4$	$3.4 x10^5$
			R^2	**0.941**	**0.964**	**0.969**	**0.948**

The values of E (Energy) calculated from D-R models (Table 2) were inferior to 8kJ/ mol (E< 8kJ/mol) for all the values of temperature at pH 5 and 7. That means the adsorption mechanism was physical (Garcia-Diaz *et al*., 2018).

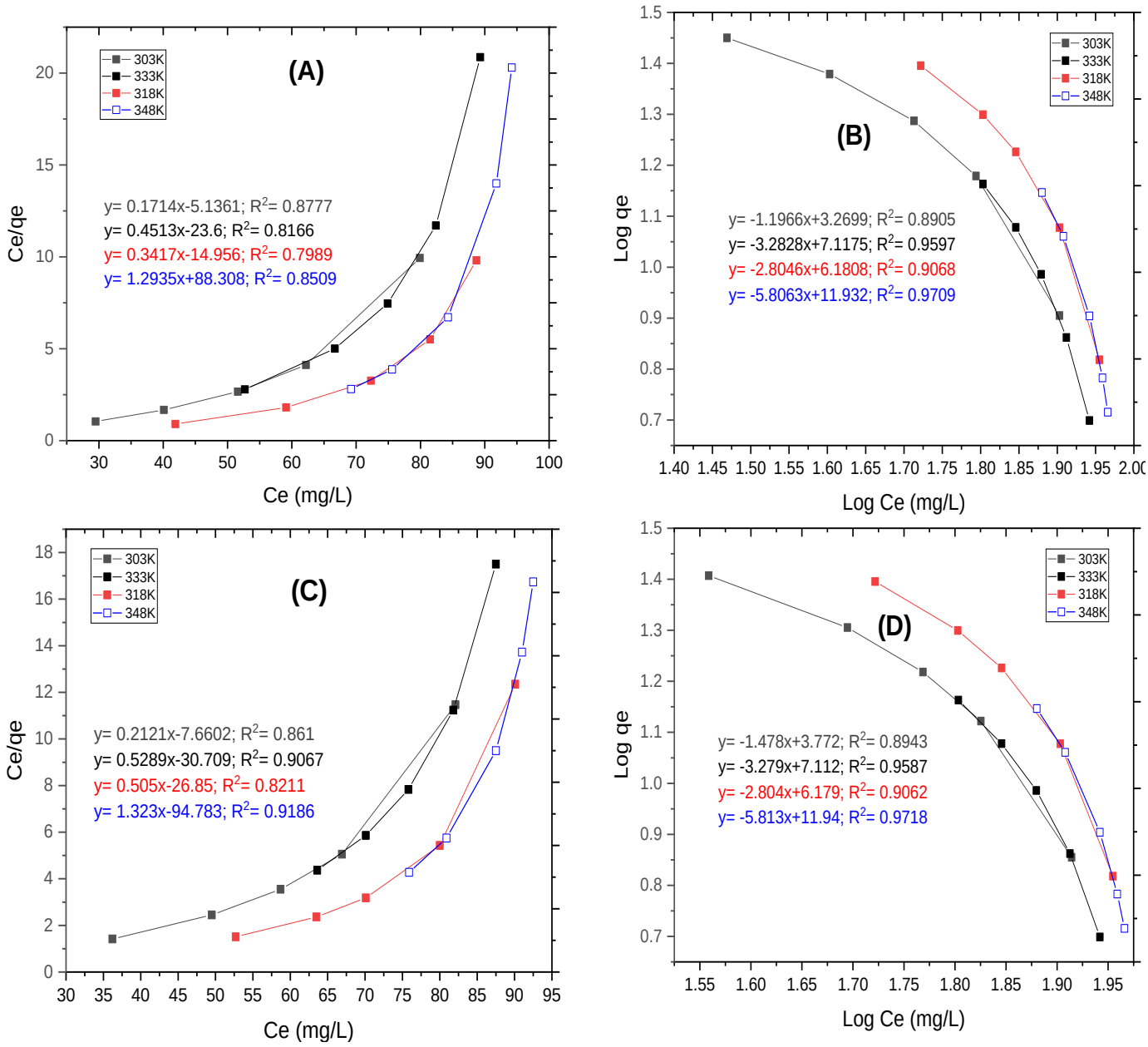

Figure 13: Langmuir Isotherms (A) for Cu(II) and (C) for Co(II) and Freundlich Isotherms (B) for Cu(II) and (D) for Co(II)

where, T is 303; 318; 333 and 348K, Ratio 3:1, dosage is 0.25g, contact time is 120min, and concentration is 100mg/ℓ and pH 5.

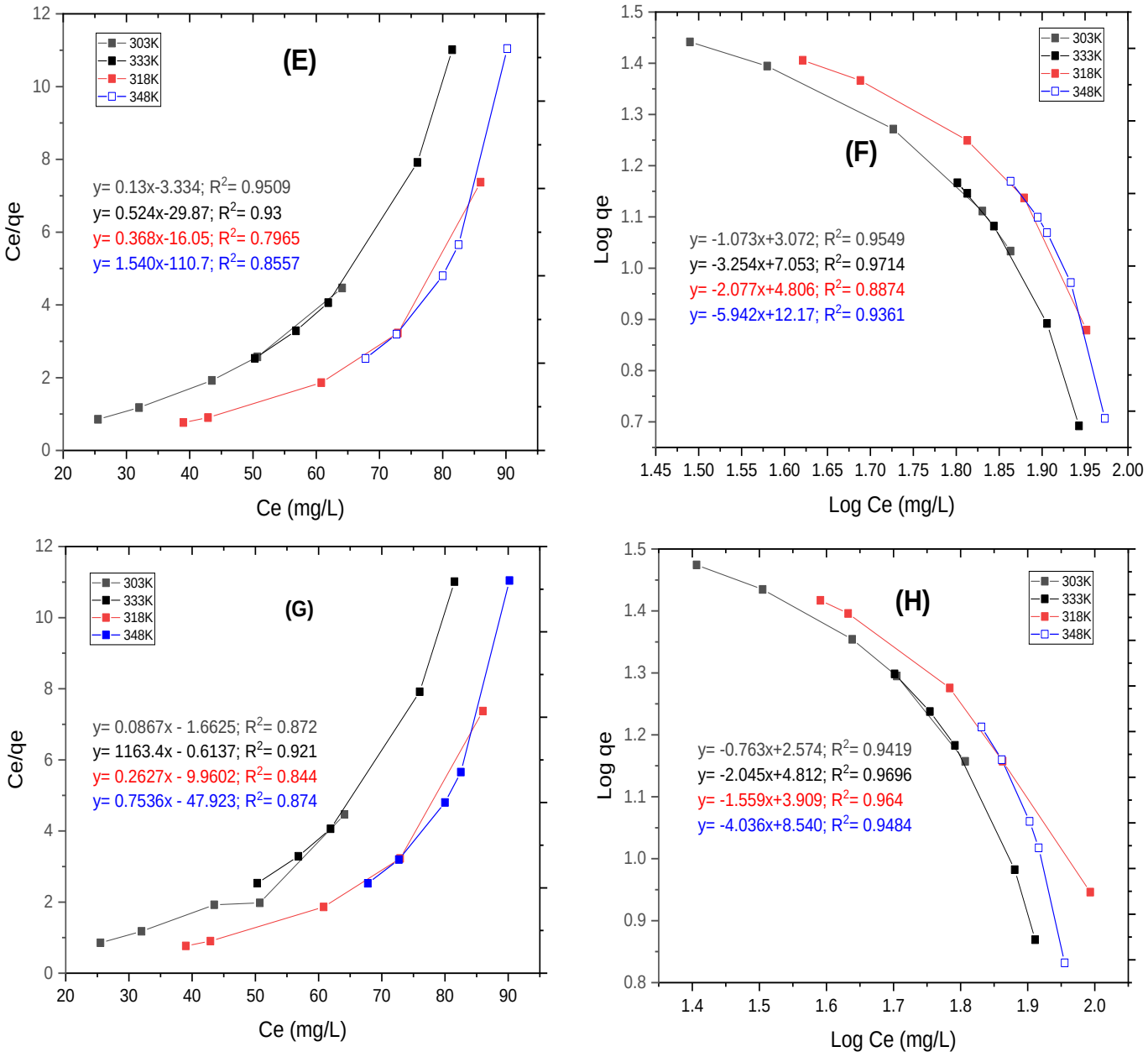

Figure 14: Langmuir isotherms (E) for Cu(II) and (G) for Co(II) and Freundlich isotherms (F) for Cu(II) and (H) for Co(II)

where, T is 303; 318; 333 and 348K, Ratio 3:1, dosage is 0.25g, contact time is 120min, and concentration is 100mg/ℓ and pH 7.

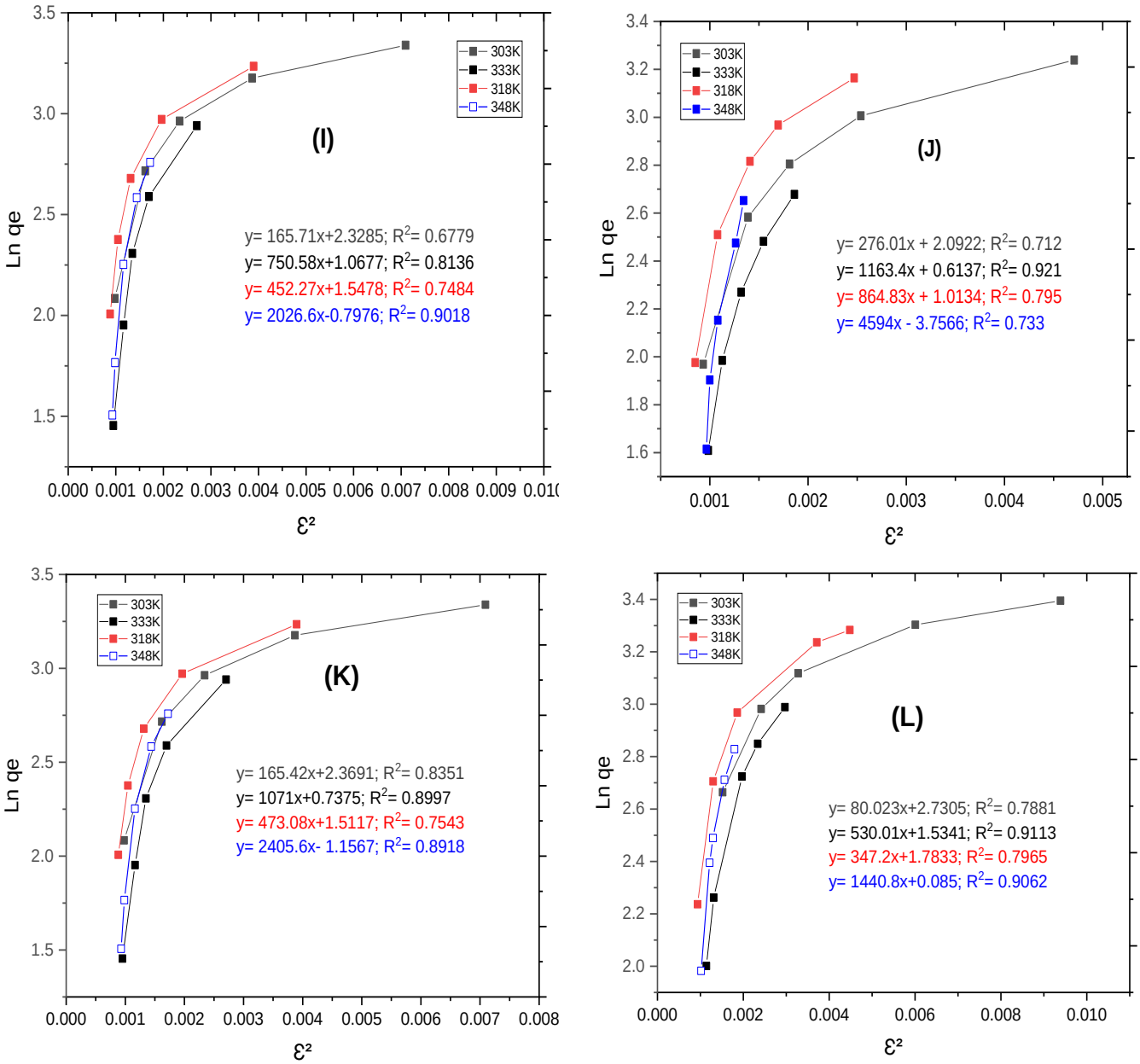

Figure 15: D-R isotherms (I) for Cu(II) and (J) for Co(II) at pH 5 and D-R isotherms (K) for Cu(II) and (L) for Co(II) at pH 7

where, T is 303; 318; 333 and 348K, Ratio 3:1, dosage is 100mL/0.25g, contact time is 120min and concentration is 100mg/ℓ and pH5 and pH7.

4.4 Adsorption kinetic models

Adsorption processes are very attractive and among other advantage the valuable insights into the reaction pathways and the mechanisms of the sorption reaction are very important for effective implementation of the wastewater treatment technology and could be obtained through the study of sorption kinetics (Fosso-Kankeu, 2018).

In this study, the experimental data of the adsorption kinetics were fitted to the pseudo-order and pseudo-second-order models. The kinetic parameters obtained are presented in Table 3. The pseudo-first-order or Lagergren model considers that the rate of adsorption sites occupation is proportional to the number of unoccupied sites. The kinetic parameters for the adsorption process were studied on the batch adsorption at pH 3; 5; 7 and 9 at 303K. The data were fitted to the first-order Lagergren. The linear form of the pseudo-first-order and pseudo-second-order are given by Equations (2.22), (2.23), and (2.24). From Table 3, the values of the regression coefficient, R^2, obtained for both metal ions showed a good fit to the adsorption process.

Table 3: Kinetic model parameters of the adsorption process

Kinetic models		pH			
First order		3	5	7	9
Cu(II)	q_{ecal}(mg/g)	25.235	25.399	29.854	33.729
	k_1 (min^{-1})	2.073	3.224	2.994	3.455
	R^2	**0.846**	**0.977**	**0.966**	**0.906**
Co(II)	q_{ecal}(mg/g)	34.483	66.667	43.478	500
	k_1 (min^{-1})	3.876	1.402	3.809	1.356
	R^2	**0.981**	**0.989**	**0.912**	**0.961**
Second order					
Cu(II)	q_{ecal}(mg/g)	25.351	27.861	32.211	24.889
	k_2 (min^{-1})	2.994	2.533	4.376	2.994
	R^2	0.471	0.968	0.895	0.714
Co(II)	q_{ecal}(mg/g)	58.824	50	38.462	33.333
	k_2 (min^{-1})	1.119	2.296	9.927	1.066
	R^2	0.782	0.971	0.857	0.956

The values of k_2 and *qe* were calculated from the linear plot of *t/qt* versus *t* and are recorded in Table 3. Also, the low R^2 values presented by the Pseudo-second-order equation showed that this model did not provide a good fit to the experimental data for

both metal ions (Figure 16). This suggests that chemisorptions are not the principal mechanism for the sorption of Cu(II) and Co(II) ions onto GCHM. It was observed that both metal ions are fitting the Pseudo-first-order (Figure 16A and 16B) at pH 3 and 7.

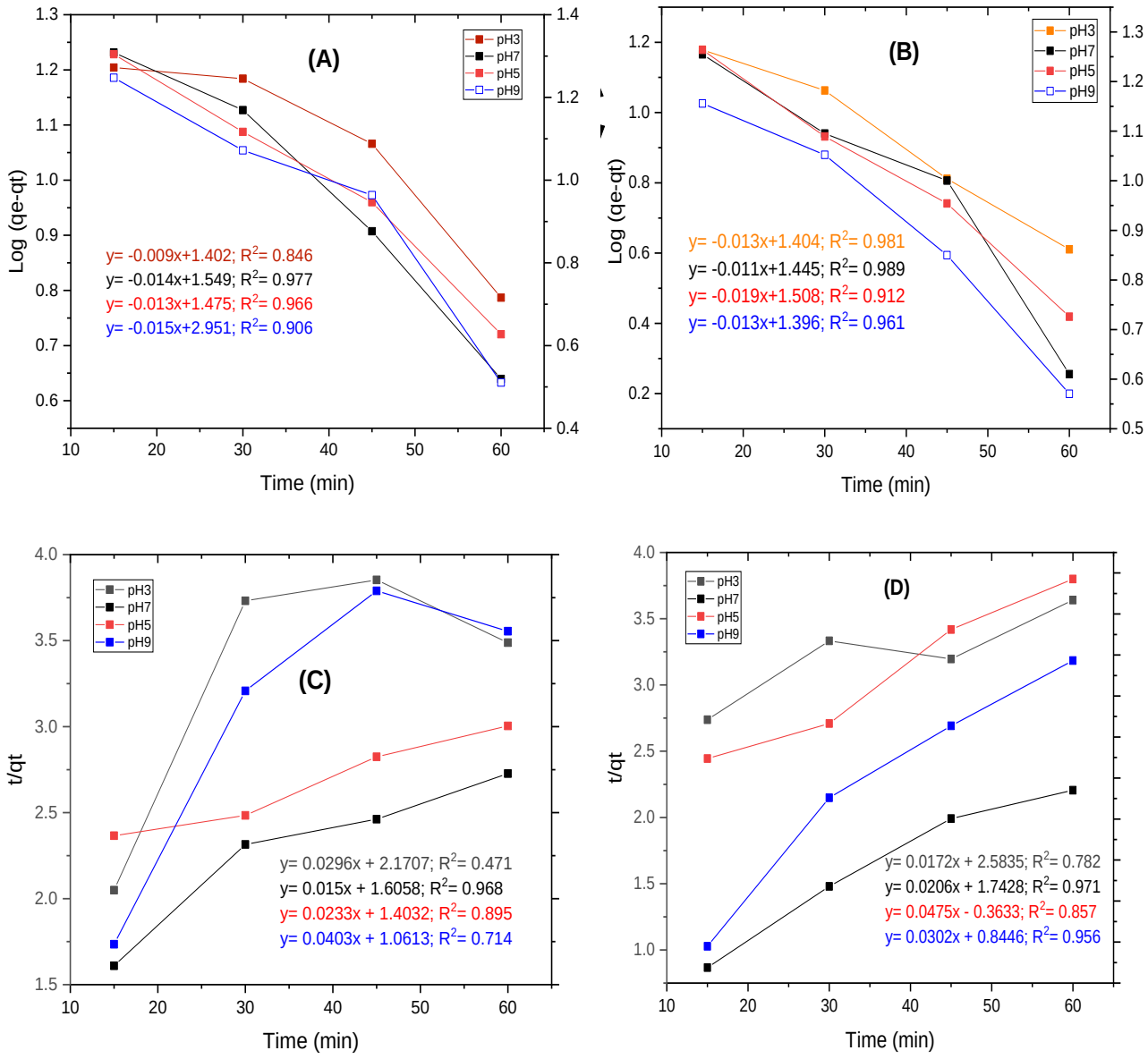

Figure 16: (A) and (B) plots of first-order model for Cu(II) and Co(II); (C) and (D) plots of second-order of Cu(II) and Co(II) adsorption by GCHM. Initial concentration 100 mg/ℓ. GCHM dosage 100 mL /0.25 g; pH 3, 5, 7 and 9, Ratio 3:1.

4.5 Kinetic diffusion models

Kinetic diffusion has been investigated to determine the nature of adsorption of Cu(II), and Co(II) ions to the interface of GCHM. Three transport processes of Cu(II) and

Co(II)ions were investigated as film diffusion, particle diffusion,and moving boundary (Garcia-Diaz *et al*., 2018; Tarawou & Young, 2015; Maiyalagan & Karthikeyan, 2013).

(i) Transport of adsorbates to the external surface of adsorbent (film diffusion);

(ii) Transport of adsorbates within the pores of adsorbent, except for a small amount of adsorption, which occurs on the external surface (particle diffusion);

(iii) Adsorptions of the ingoing ion (adsorbate) on the interior surface of adsorbent (boundary).

Table 4: Kinetic model parameters of the diffusion process

Kinetic models		pH			
Moving boundary		3	5	7	9
Cu(II)	K(min^{-1})	0.0022	0.0165	0.0165	0.0165
	R^2	0.846	0.855	0.951	0.857
Co(II)	K (min^{-1})	0.0164	0.0164	0.0166	0.0166
	R^2	0.921	0.860	0.847	0.961
Particle diffusion					
Cu(II)	K(min^{-1})	0.0131	0.0213	0.0199	0.0222
	R^2	0.885	0.947	0.941	0.852
Co(II)	K(min^{-1})	0.0171	0.0164	0.0353	0.0227
	R^2	0.962	0.97	0.887	0.942
Film diffusion					
Cu(II)	K(min^{-1})	0.0162	0.0316	0.0299	0.0326
	R^2	**0.957**	**0.977**	**0.966**	**0.911**
Co(II)	K(min^{-1})	0.0269	0.0261	0.0463	0.0331
	R^2	**0.981**	**0.989**	**0.912**	**0.962**

The moving boundary, particle diffusion and film diffusion model plots of ln(1-F) versus time were taken for Cu^{2+} and Co^{2+} ions and presented in Figures 17 and 18 at all the values of pH.

The regression coefficient (R^2) values for Cu^{2+} (0.977) and Co^{2+} (0.989) have shown a good fit for film diffusion. The results obtained by kinetic diffusion models show that the Cu^{2+} and Co^{2+} adsorption onto the GCHM could be explained by the film diffusion model where the rate constant model *K*(min^{-1}) is 0.0316 and 0.0463 for Cu^{2+} and Co^{2+} respectively at pH 5 and pH 7.

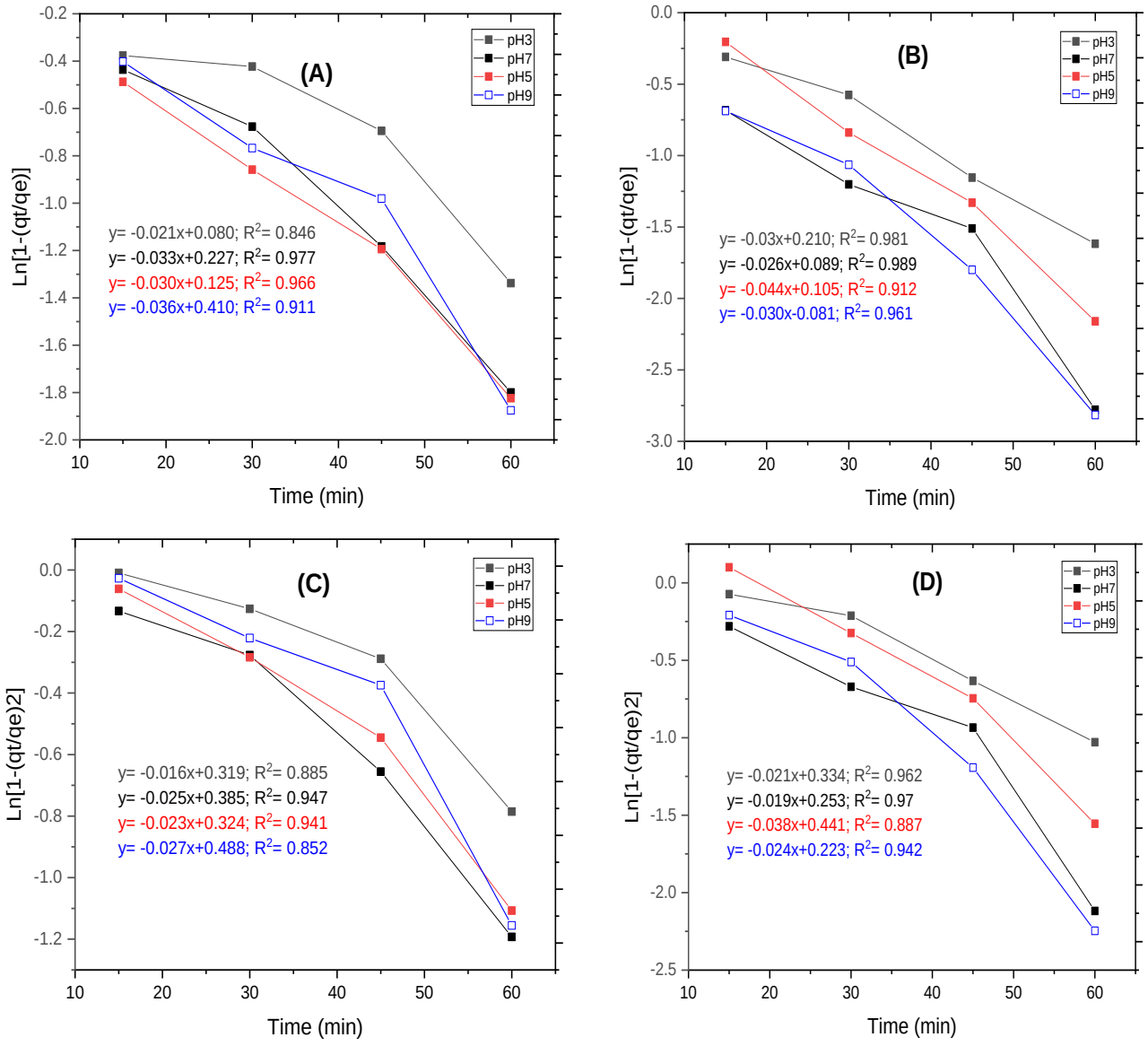

Figure 17: (A) and (B) plots of Film diffusion for Cu(II) and Co(II); (C) and (D) plots of particle diffusion of Cu(II) and Co(II) adsorption by GCHM. Initial concentration 100mg/ℓ; GCHM dosage 100 mL/0.25 g; pH 3, 5, 7 and 9, Ratio 3:1

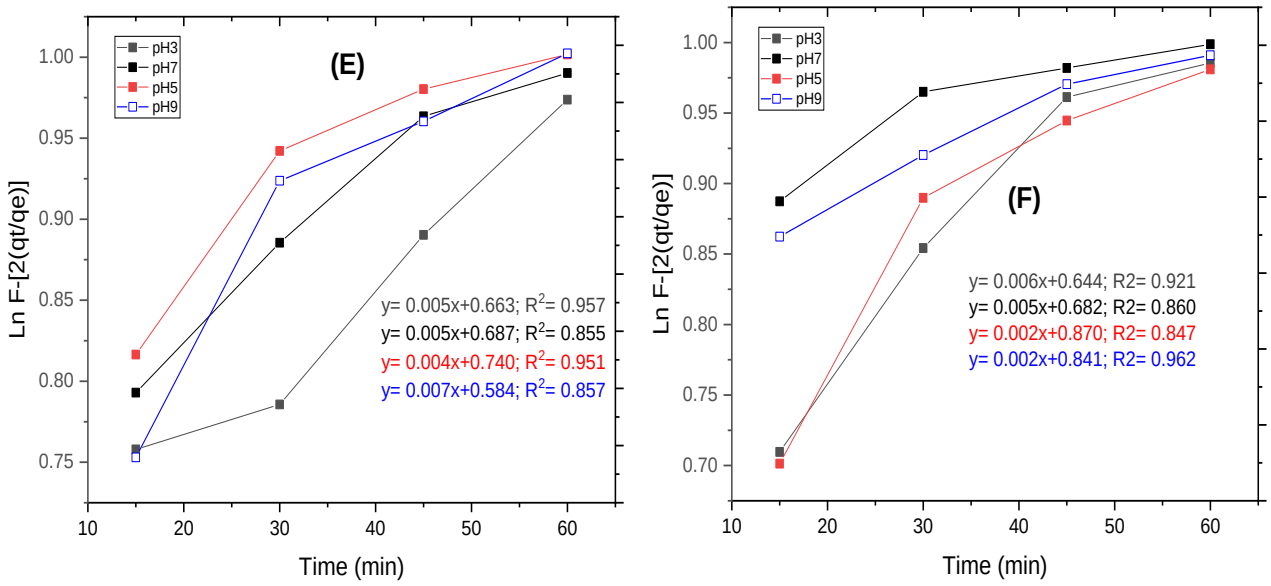

Figure 18: (E) and (F) plots of moving boundary for Cu(II) and Co(II) respectively. Initial concentration 100 mg/ℓ. GCHM dosage 100 mL /0.25 g; pH 3, 5, 7 and 9, Ratio 3:1

4.6 Thermodynamic studies

The effect of temperatures on the removal of Cu(II) and Co(II) was studied at temperature 303, 318, and 333K as shown in Table 4. Thermodynamic parameters such as entropy *(∆S°)*, enthalpy *(∆H°)*, and Gibbs free energy *(∆G°)* for Cu(II) and Co(II) removal ions on GCHM were calculated using the Equations (2.16), (2.17) and (2.20). The values of $\Delta H°$ and $\Delta S°$ from the slope, and intercept of the $ln\ K_D$ versus $1/T$ through the Von't Hoff straight line Equation in Figure 17.

Table 5: Adsorption thermodynamic parameters

Metal ion		Temp (K)	K_D	ΔG° (kJ/mol)	ΔH°(kJ/mol K)	ΔS° (J/mol K)
Cu(II)		303	1.046	-0.114		
		318	1.803	-1.558		
		333	3.287	-3.294	32.732	108.082
		348	5.617	-4.993		
Co(II)	pH 5	303	1.419	-0.881		
		318	2.785	-2.708		
		333	4.368	-4.082	32.499	110.161
		348	7.873	-5.970		
Cu(II)		303	1.118	-0.281		
		318	1.796	-1.547		
		333	3.056	-3.092	34.212	112.987
		348	6.759	-5.529		
Co(II)	pH 7	303	0.856	0.393		
		318	1.598	-1.240		
		333	2.530	-2.570	34.229	111.324
		348	5.264	-4.805		

The negative values of Δ*G*° obtained almost at all temperatures for both metal ions indicate that the adsorption process was spontaneous. It was also observed that the change in free energy increases with an increase in temperature suggesting that higher temperatures are not making the adsorption easier.

The positives values of Δ*H*° indicate an endothermic process. The magnitude of Δ*H*° is very useful in describing the type of adsorption. In the physical adsorption process, the ΔH°<40 kJ/mol K (Abbas *et al*., 2014). From Table 5, the value of Δ*H*° obtained from both metal ions showed a physical adsorption process onto the surface of GCHM. This physical adsorption explains the reason why the kinetic data did not fit the Pseudo-second-order model (chemical sorption model). Also, the positive values of Δ*H*° indicated that the adsorption process of both metal ions was endothermic (Mobasherpour *et al*., 2014). Positive values of Δ*S*° indicate an increase in randomness at the solid/solution interface during adsorption. Also, the magnitude of Δ*S*° reveals whether the adsorption reaction involves an associative or dissociative mechanism. The positive value of Δ*S*° indicated that the reflected the affinity of GCHM for copper and cobalt metals ions and suggested some structural changes in GCHM (Ho, 2003).

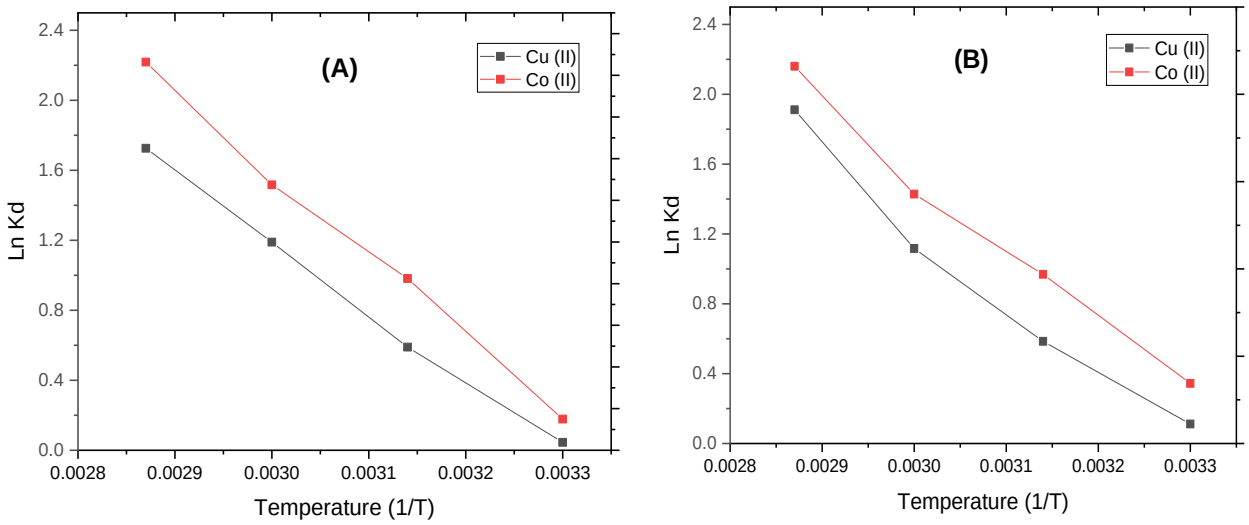

Figure 19: (A) Van't Hoff plot for adsorption of (*ln* K_D versus *1/T*) Cu(II) and Co(II) at pH 5 and (B) at pH 7

4.7 Response Surface Methodology

RSM was employed to evaluate the relations between the response (% removal of copper and cobalt ions) and the four variables. In this study, CCD was selected to evaluate the effect of pH (A), ratio of gelatin (B), temperature (C), and time (D) as independent variables. Copper removal in % (Y_{Cu}) and Cobalt removal in % (Y_{Co}) were taken as response variables. The coded and uncoded independent variables for the adsorption parameter are shown in Table 6.

RSM provides a collection of statistical and mathematical techniques for designing experiments and the interaction for the determination of optimum conditions (Igberase *et al.*, 2017). The experiment was carried out using Design-Expert version 11 software.

Table 6: Range of variables design levels used

Factors	Symbol coded	Low	High
		-1	+1
pH	A	3	9
Ratio gelatin (%)	B	25	75
Temperature (°C)	C	30	75
Time (min)	D	15	120

Equations 4.1 and 4.2 give the final quadratic polynomial equation regarding coded factors that were used to fit the experimental data.

$$Y_{Cu(II)} = +58.45 - 2.20A + 24.29B - 5.29C + 20.79D - 35.68A^2 - 3.08B^2 + 5.00C^2 - 13.87D^2 = 20.64AB + 0.56AC + 23.96AD - 1.91BC - 0.68BD - 0.59CD \quad (4.1)$$

$$Y_{Co(II)} = +60.94 + 1.22A + 23.56B - 3.43C + 21.34D - 38.28A^2 - 3.39B^2 + 5.10C^2 13.38D^2 + 20.00AB - 1.13AC + 22.47AD - 1.13BC + 0.18BD + 0.62CD \quad (4.2)$$

where, A, B, C, and D represent pH, the ratio of gelatin, temperature and time, respectively. The positive sign in front of the terms indicates a synergic effect and, the negative sign indicates an antagonist effect in Equations 4.1 and 4.2.

Table 7: Experimental design and response value

Run	A: pH	B: Ratio of gelatin (%)	C: Temperature (°C)	D: Time (min)	$Y_{Cu(II)}$: Copper removed (%)	$Y_{Co(II)}$: Cobalt removed (%)
1	6.00	25.00	52.50	67.50	29.51	33.11
2	6.00	50.00	52.50	67.50	60.33	62.00
3	3.00	50.00	52.50	67.50	23.41	20.57
4	6.00	50.00	52.50	120.0	63.80	66.02
5	6.00	50.00	52.50	67.50	60.33	62.00
6	6.00	50.00	52.50	67.50	74.81	77.86
7	6.00	50.00	52.50	15.00	22.22	25.34
8	6.00	50.00	52.50	67.50	60.33	62.00
9	6.00	50.00	52.50	67.50	60.33	62.00
10	9.00	25.00	30.00	120.0	11.00	13.00
11	9.00	75.00	75.00	15.00	5.74	8.00
12	6.00	50.00	75.00	67.50	48.95	52.47
13	9.00	25.00	75.00	120.0	7.99	12.00
14	3.00	25.00	75.00	15.00	10.81	8.30
15	3.00	25.00	30.00	15.00	13.70	7.23
16	6.00	75.00	52.50	67.50	78.10	80.23
17	9.00	75.00	30.00	15.00	14.00	16.00
18	9.00	50.00	52.50	67.50	19.00	23.00
19	3.00	75.00	30.00	120.0	19.65	12.11
20	3.00	74.00	75.00	120.0	6.77	5.98
21	6.00	50.00	52.50	67.50	60.33	62.00

Table 8: Experimental and predicted values

Run	Y_{Cu}: Copper actual (%)	Y_{Cu}: Copper predicted (%)	X^2 Chi-square	Y_{Co}: Cobalt actual (%)	Y_{Co}: Cobalt predicted (%)	X^2 Chi-square
1	5.74	3.44	1.5378	8.00	5.46	1.1816
2	14.00	15.52	0.1489	16.00	18.10	0.2436
3	7.99	5.69	0.9297	12.00	9.46	0.6819
4	19.65	21.17	0.1091	13.11	15.21	0.2899
5	11.00	12.52	0.1845	13.00	15.10	0.2921
6	10.81	8.51	0.6216	8.30	5.76	1.1201
7	6.77	4.47	1.1834	12.11	9.57	0.6741
8	13.70	15.22	0.1518	7.23	9.33	0.4727
9	23.41	24.98	0.0986	20.57	21.45	0.0361
10	19.00	20.57	0.1198	23.00	23.88	0.0324
11	29.51	31.08	0.0290	33.11	33.99	0.0228
12	78.10	79.67	0.0309	80.23	81.11	0.0095
13	74.81	68.74	0.5360	77.86	69.48	1.0107
14	48.95	58.16	1.4585	52.47	62.61	1.6422
15	22.22	23.79	0.1036	25.34	26.22	0.0295
16	63.80	65.37	0.0377	68.02	68.90	0.0112
17	60.33	58.45	0.0605	62.00	60.94	0.0184
18	60.33	58.45	0.0605	62.00	60.94	0.0184
19	60.33	58.45	0.0605	62.00	60.94	0.0184
20	60.33	58.45	0.0605	62.00	60.94	0.0184
21	60.33	58.45	0.0605	62.00	60.94	0.0184

ANOVA analyzed the accuracy, or adequacy fitting, of the regression model for Y_{Cu} and Y_{Co} in Equations (4.1) and (4.2) at a 95% significance level and the results are presented in Tables 9 and 10. High F and low P (<0.0500) values of the regression model, as well as each variable term for linear, square and interaction in the model, indicated that they were statistically significant.

F-value of 29.59 and *P*-value <0.0500 for Y_{Cu} and *F*-value of 25.78 and *P*-value <0.0500 for Y_{Co} show that the model was significant in describing the experimental data. The values of Prob > F less than 0.0500 indicate that the model terms are significant. In this study, B, C, D, A^2, D^2, AB, and AD are significant model terms for copper removal (Y_{Cu}) and B, D, A^2, D^2, AB, and AD are significant model terms for cobalt removal (Y_{Co}). Values greater than 0.1000 indicate that the model terms are not significant.

ANOVA was used to show the impact of each factor and results are shown in Tables 9 and 10. Considering that most of the factors are statically significant at 95%, among all factors considered, pH (A^2) and the ratio of gelatin (B) were the most influential in the model with an *F*-value of 105.72 and 38.40 for Y_{Cu} and 98.99 and 29.38 for Y_{Co}. The most ineffective variables were the interactions between pH/temperature (AC) and ratio of gelatin/time (BD) with *F*-value of 0.082 and 0.024, pH (A) and interaction between ratio of gelatin/time (BD) with *F*-value of 0.078 and 1.430E-003 for Y_{Co}. By studying the main effect and the impact of each factor, the process could be characterized. Therefore, the level of a factor to produce the best results could be predicted.

The R^2 values of the models obtained are 0.9857 for Y_{Cu} and 0.9836 for Y_{Co} (Tables 9 and 10). Besides, adjusted R^2 are obtained as 0.9524 and 0.9455 for Y_{Cu} and Y_{Co}, respectively. These values prove remarkable of the fitting model. The high value of R^2 indicates that the quadratic equations can represent the system under the given experimental domain.

Table 9: ANOVA for response surface quadratic model for removal of Cu(II)

Source	Sum of Squares	Df	Mean Square	F-Value	Prob > F	Significance
Model	12735.61	14	909.69	29.59	0.0002	Significant
A	9.72	1	9.72	0.32	0.5942	
B	1180.49	1	1180.49	38.40	0.0008	
C	279.84	1	279.84	9.10	0.0235	
D	864.45	1	864.45	28.12	0.0018	
A^2	3249.67	1	3249.67	105.71	< 0.0001	
B^2	24.19	1	24.19	0.79	0.4092	
C^2	63.73	1	63.73	2.07	0.2000	
D^2	491.36	1	491.36	15.98	0.0071	
AB	681.95	1	681.95	22.18	0.0033	
AC	2.53	1	2.53	0.082	0.7838	
AD	918.72	1	918.72	29.88	0.0016	
BC	29.03	1	29.03	0.94	0.3687	
BD	0.74	1	0.74	0.024	0.8818	
CD	2.81	1	2.81	0.091	0.7727	
Residual	184.45	6	30.74			
Lack of Fit	184.45	2	92.23			
Cor Total	12920.06	20				
R^2	0.986					
Ajusted R^2	0.952					

Table 10: ANOVA for response surface quadratic model for removal of Co(II)

Source	Sum of Squares	Df	Mean Square	F- Value	Prob > F	Significance
Model	13637.92	14	974.14	25.78	0.0003	Significant
A	2.95	1	2.95	0.078	0.7892	
B	1110.15	1	1110.15	29.38	0.0016	
C	117.79	1	117.79	3.12	0.1279	
D	910.79	1	910.79	24.11	0.0027	
A^2	3740.05	1	3740.05	98.99	< 0.0001	
B^2	29.35	1	29.35	0.78	0.4120	
C^2	66.50	1	66.50	1.76	0.2329	
D^2	457.09	1	457.09	12.10	0.0132	
AB	640.24	1	640.24	16.94	0.0062	
AC	10.28	1	10.28	0.27	0.6206	
AD	808.11	1	808.11	21.39	0.0036	
BC	10.28	1	10.28	0.27	0.6206	
BD	0.054	1	0.054	1.430E-003	0.9711	
CD	3.04	1	3.04	0.080	0.7863	
Residual	226.70	6	37.78			
Lack of Fit	226.70	2	113.35			
Cor Total	13864.6	20				
R^2	0.984					
Ajusted R^2	0.946					

The predicted Y_{Cu} and Y_{Co} at a 95% confidence level were compared with experimental results in Figure 20. High values of R^2 show that the quadratic equations are adequate to represent the model under the given experimental area. It was observed that the data points were positioned close together around the line of the best fit. This shows a proper arrangement between predicted and experimental data and means that this model best describes the relationship between reaction variables.

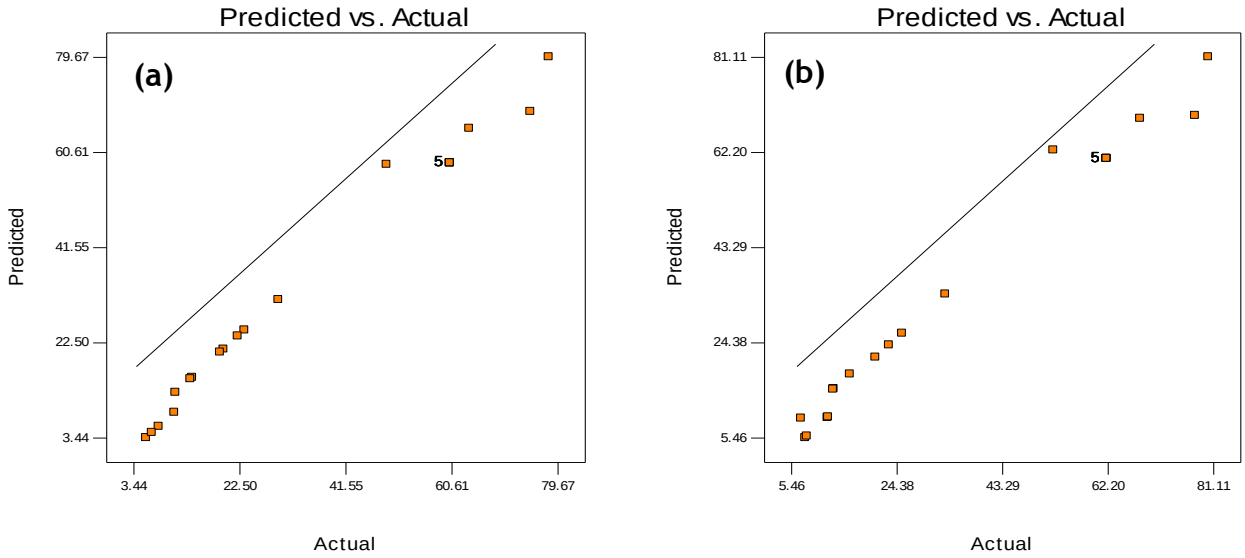

Figure 20: Relationship between predicted and actual values for Y_{Cu} (a) and Y_{Co} (b)

The analysis of variance (ANOVA) was used to evaluate the statistical significance of the quadratic model. It was found that the regression was statistically significant at the F-value of 29.59 and P-value <0.0500 and at the F-value of 27.78 and P-value <0.0500 for copper and cobalt ions, respectively. The determination coefficient (R^2= 0.986 for copper and R^2= 0.984 for cobalt) indicated that the model cannot explain why only 1.4% for copper and 1.6% for cobalt of the total variable. The adjusted determination coefficient (R^2_{adj}= 0.952 for copper and R^2_{adj}= 0.946 for cobalt) is also high, indicating a high significance of the model.

4.7.1 Three dimensional (3D), and two dimensional (2D) RSM Plots

To obtain a better understanding of Cu^{2+} and Co^{2+} removal in aqueous solution onto GCHM, 2D and 3D response plots were analyzed. As each model had four variables that were kept constant at the centre level, therefore, six total response surfaces were produced.

4.7.1.1 Interaction between pH and ratio of gelatin

The RSM indicated that the predicted optimum removal of Cu^{2+} was 81.99% and Co^{2+} was 84.03% with a temperature of 52.50°C and time of 67.50 min. The interaction between pH and ratio gelatin is illustrated in Figures 21 and 22. The circular contour plots revealed that there is a significant interaction between pH and ratio of gelatin on

the removal efficiency. The sharp curvature in pH and ratio of gelatin shows that the response metals adsorption efficiency was very sensitive to this process (Sarkar & Majumdar, 2011). At a lower range of pH and ratio of gelatin, an increase of percentage removal was observed up to a pH 5 and ratio gelatin ratio of 75.00%. The decrease in the response was observed at a pH greater than 5 and gelatin ratio of less than 75.00%. And at higher pH, Co^{2+} precipitate as $Co(OH)_2$.

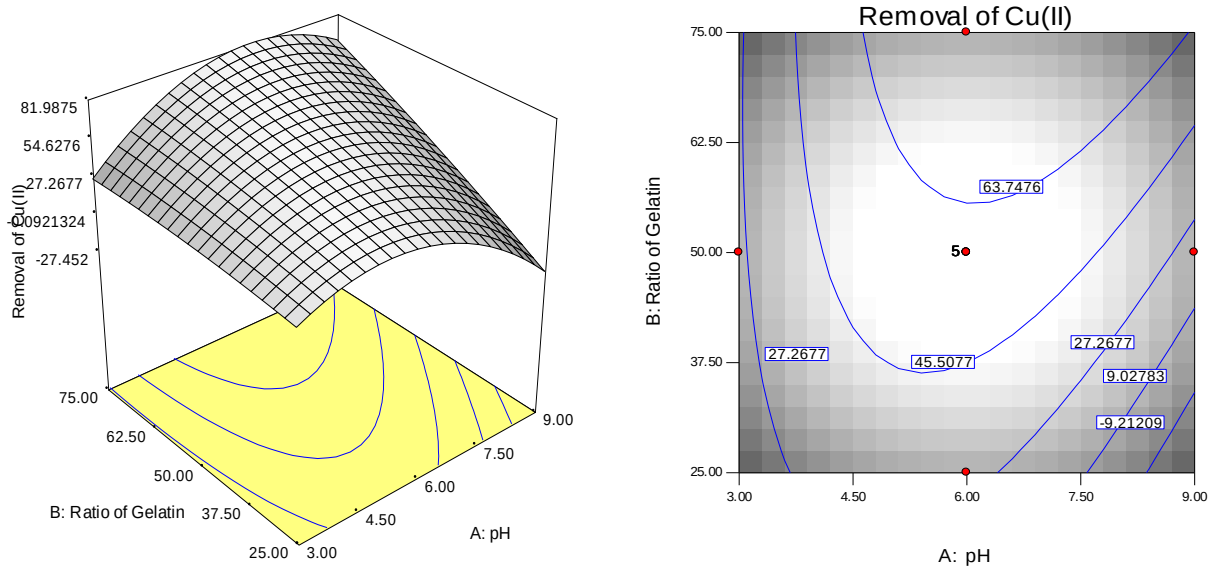

Figure 21: Effect of pH and ratio of gelatin of Cu(II) removal: (a) response surface method and (b) contour surface plots

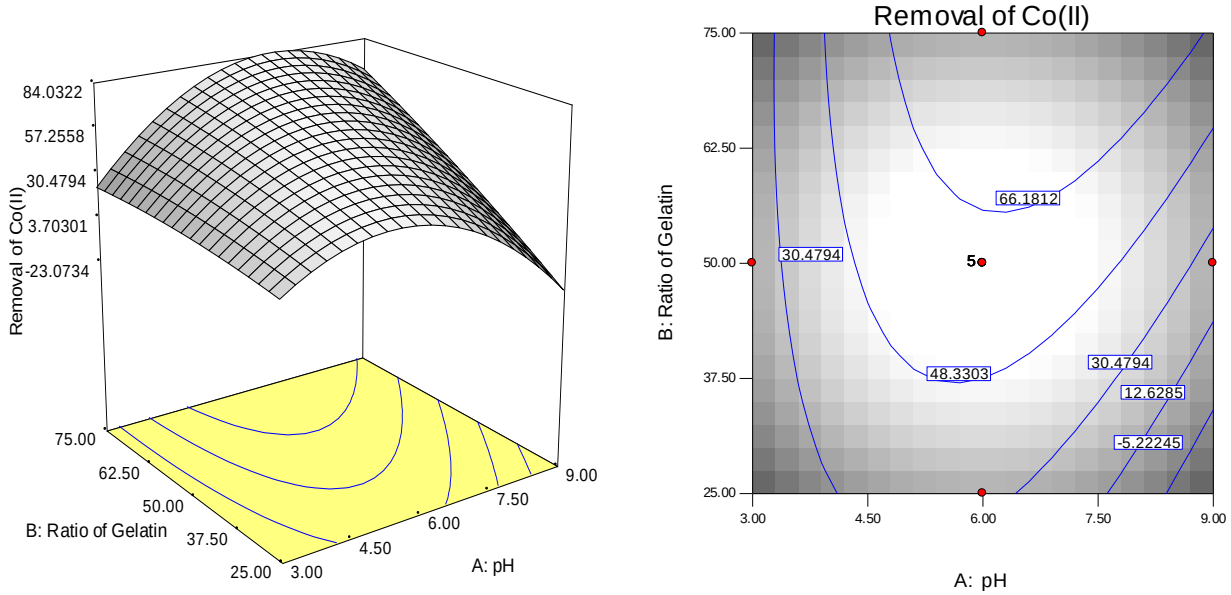

Figure 22: Effect of pH and ratio of gelatin of Co(II) removal: (a) response surface method and (b) contour surface plots

4.7.1.2 Interaction between pH and temperature

Figures 23 and 24 illustrate the interaction between pH and temperature with a ratio of gelatin of 50.00% and a time of 67.50 min. The contour indicated that the two variables are significant to the removal of Cu^{2+} and Co^{2+} and their interaction decrease the removal of both metal ions. The predicted values from ANOVA were found to be 68.74% and 69.49% for Cu^{2+} and Co^{2+}, respectively. Under these conditions, adsorption removal decreases with increase in temperature and pH. As the system is exothermic, a high temperature does not favour the adsorption process (Esfandiar *et al.*, 2014).

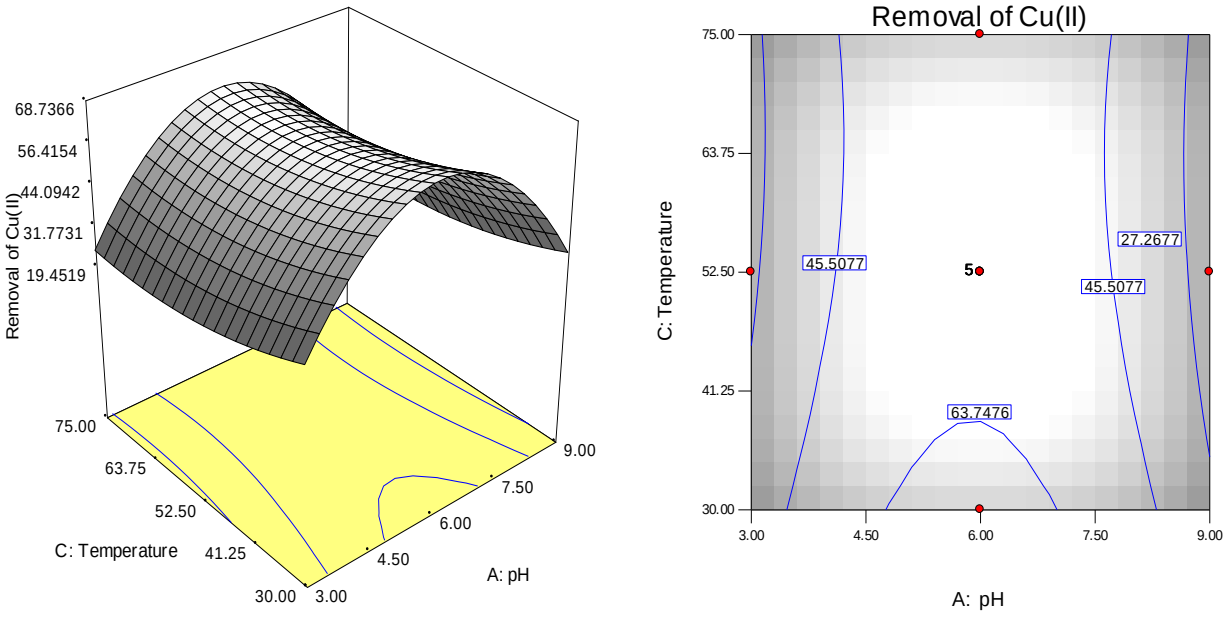

Figure 23: Effect of pH and temperature of Cu(II) removal: (a) response surface method and (b) contour surface plots

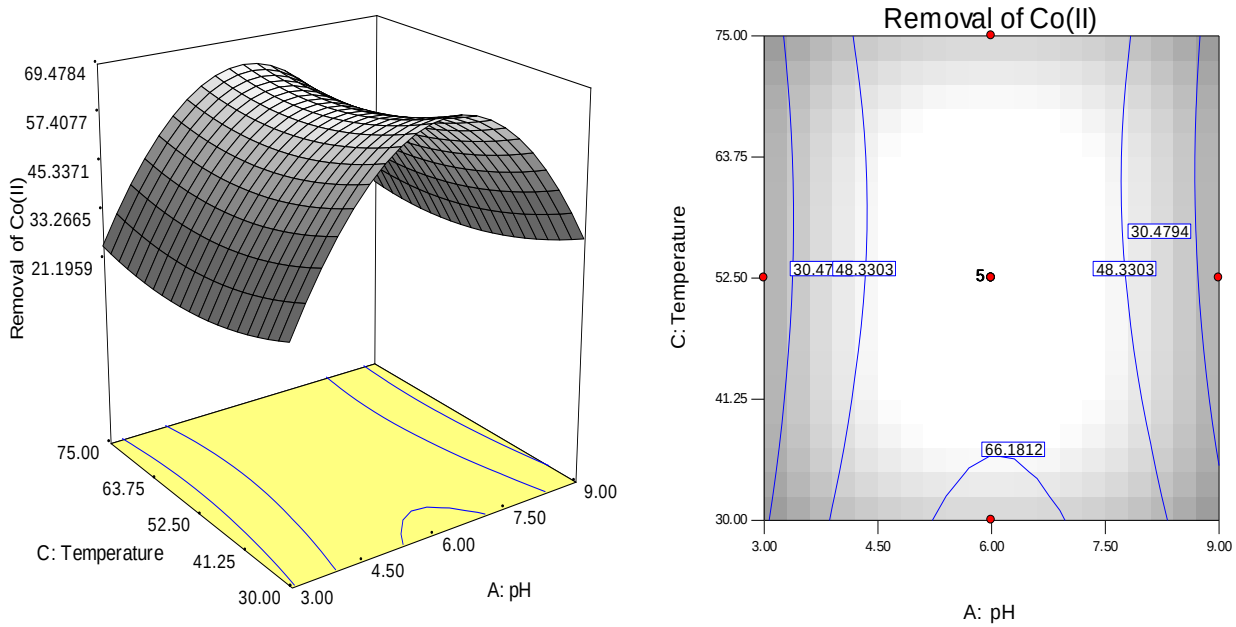

Figure 24: Effect of pH and temperature of Co(II) removal: (a) response surface method and (b) contour surface plots

4.7.1.3 Interaction between pH and time

The RSM plots in Figures 25 and 26 show the interaction between pH and contact time for a gelatin ratio of 50.00% and a temperature of 52.50°C. It can be seen from these figures that initially the percentage removal increases very sharply with increase in time. The predicted values from ANOVA were found to be 68.68% and 72.56% for Cu^{2+} and Co^{2+}, respectively. This trend is expected because as the gelatin ratio increases the number of binding sites increases and thus more Cu^{2+} and Co^{2+} are attached to the surface of GCHM (Kiran & Thanasekaran, 2011; Sahu *et al.*, 2009).

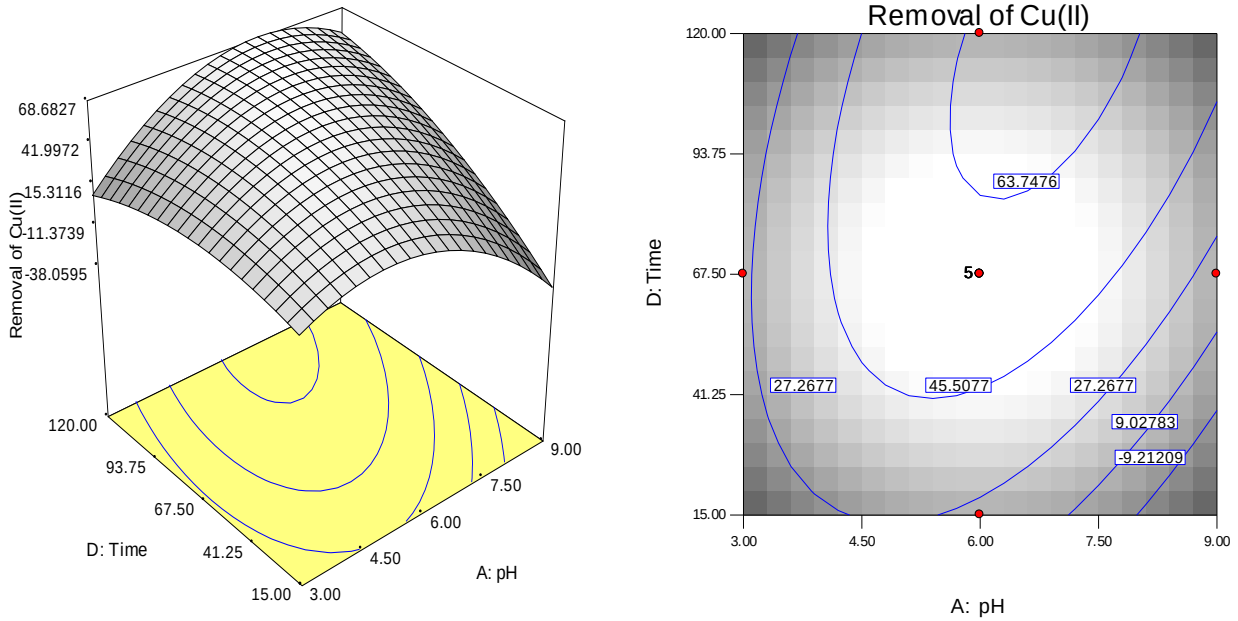

Figure 25: Effect of pH and time of Cu(II) removal: (a) response surface method and (b) contour surface plots

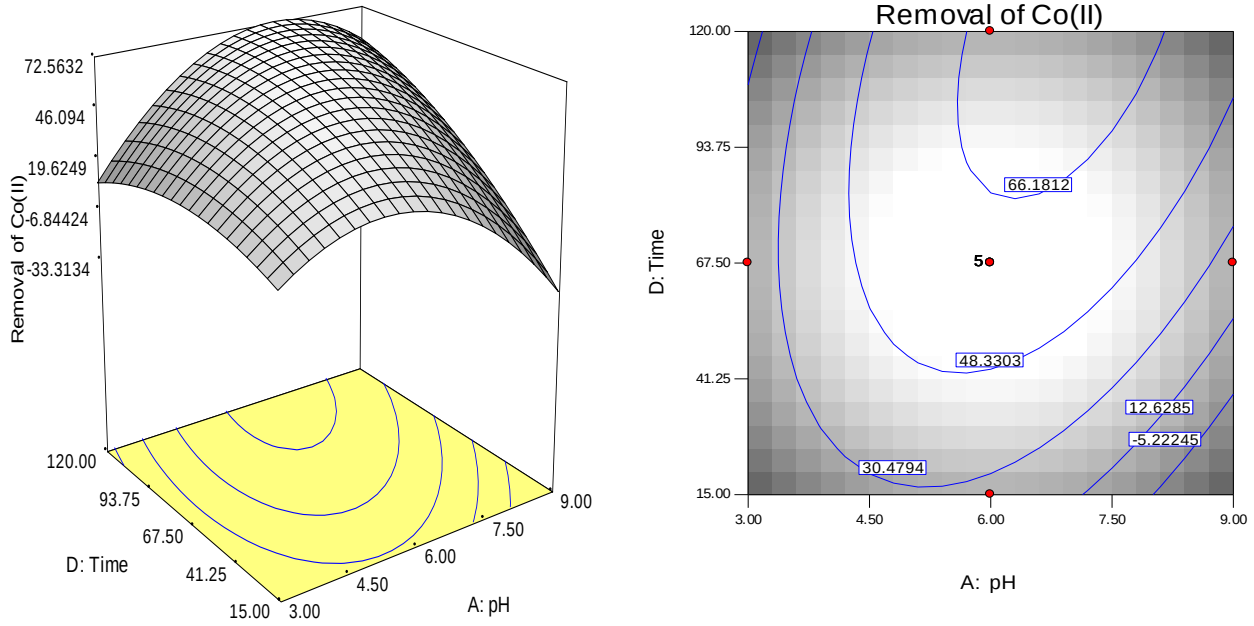

Figure 26: Effect of pH and time of Co(II) removal: (a) response surface method and (b) contour surface plots

4.7.1.4 Interaction ratio of gelatin and temperature

Figures 27 and 28 illustrate the interaction between gelatin and temperature for a pH of 6.00 and a time of 67.50 min. With increasing of gelatin ratio the activity of the functional groups increases which enhances the surface complex formation and reduces the mass

transfer resistance. Therefore, system temperature affects synergistically on the adsorption of Cu^{2+} and Co^{2+}. The highest removal efficiency for the combined effect of temperature and the gelatin ratio was found from the optimization study as 91.86% and 90.78%, respectively for Cu^{2+} and Co^{2+}.

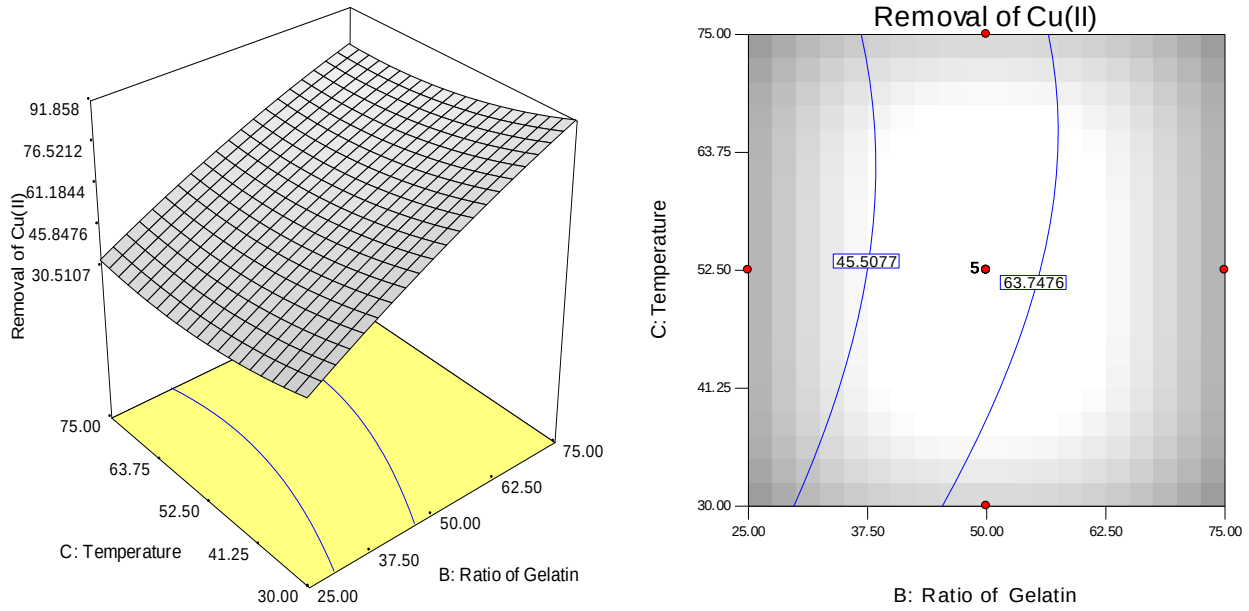

Figure 27: Effect of ratio of gelatin and temperature of Cu(II) removal: (a) response surface method and (b) contour surface plots

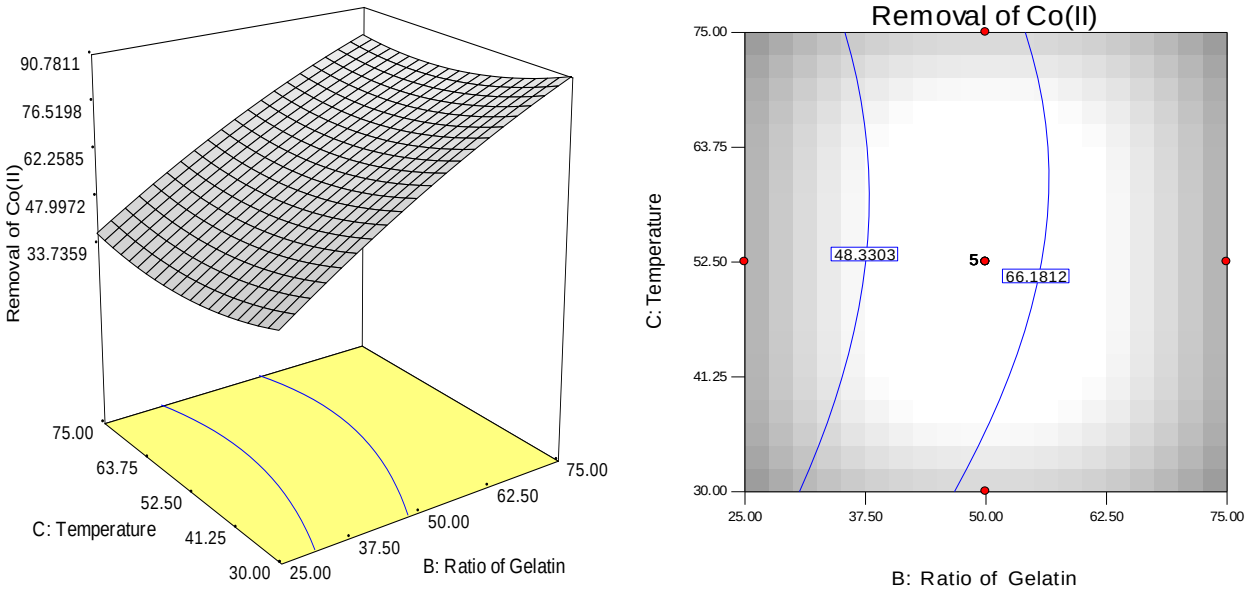

Figure 28: Effect of ratio of gelatin and temperature of Co(II) removal: (a) response surface method and (b) contour surface plots

4.7.1.5 Interaction between ratio of gelatin and time

Figures 29 and 30 illustrate the interaction between of ratio of gelatin and time on the removal of Cu^{2+} and Co^{2+} onto GCHM for a pH of 6.00 and a temperature of 52.50°C. Increasing the gelatin ratio provided more metal binding sites; therefore, the rate of Cu^{2+} and Co^{2+} adsorption increased even when the pH and temperature were kept constant. The predicted values from ANOVA were found to be 86.95% and 89.77% for Cu^{2+} and Co^{2+}, respectively (Esfandiar *et al*., 2014; Kiran & Thanasekaran, 2011).

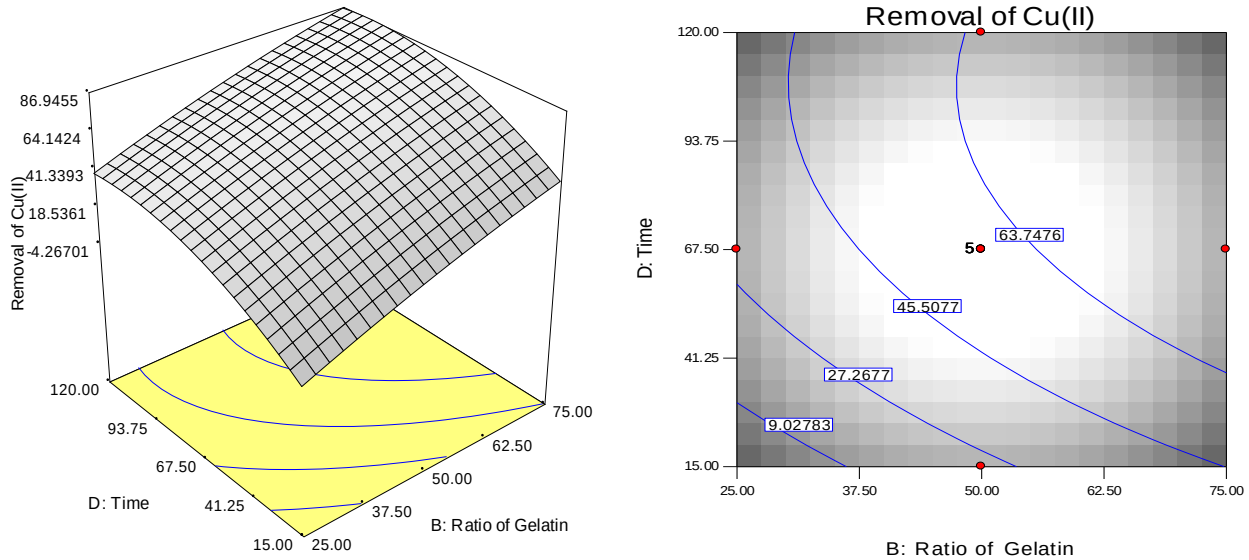

Figure 29: Effect of ratio of gelatin and time of Cu(II) removal: (a) response surface method and (b) contour surface plots

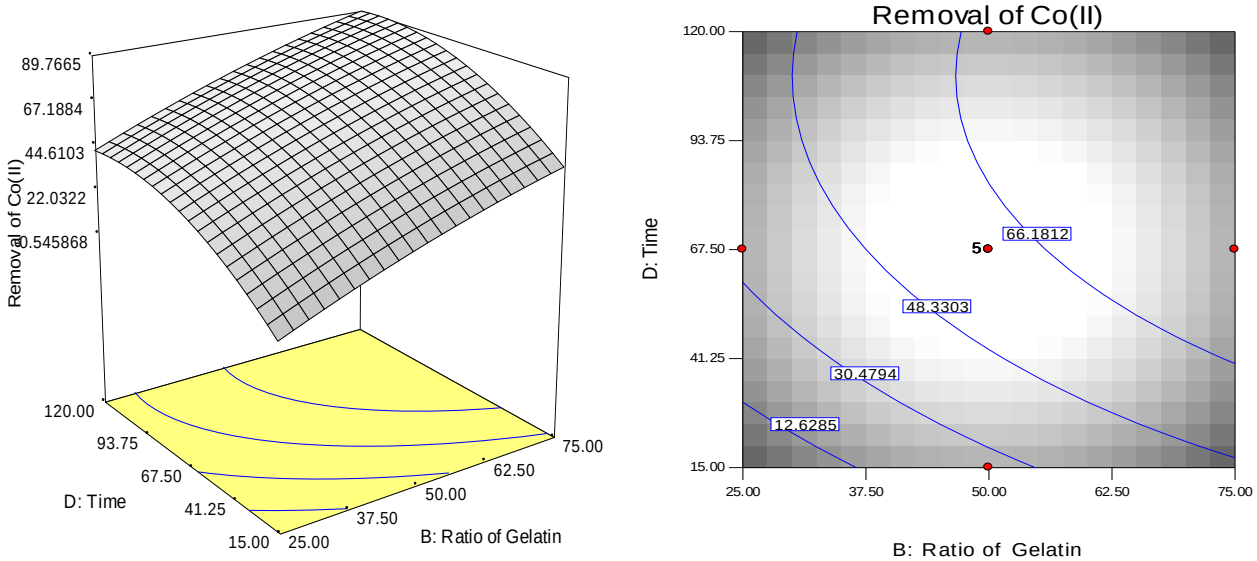

Figure 30: Effect of ratio of gelatin and time of Co(II) removal: (a) response surface method and (b) contour surface plots

4.7.1.6 Interaction between temperature and time

Interaction between temperature and time is shown in Figures 31 and 32 below.

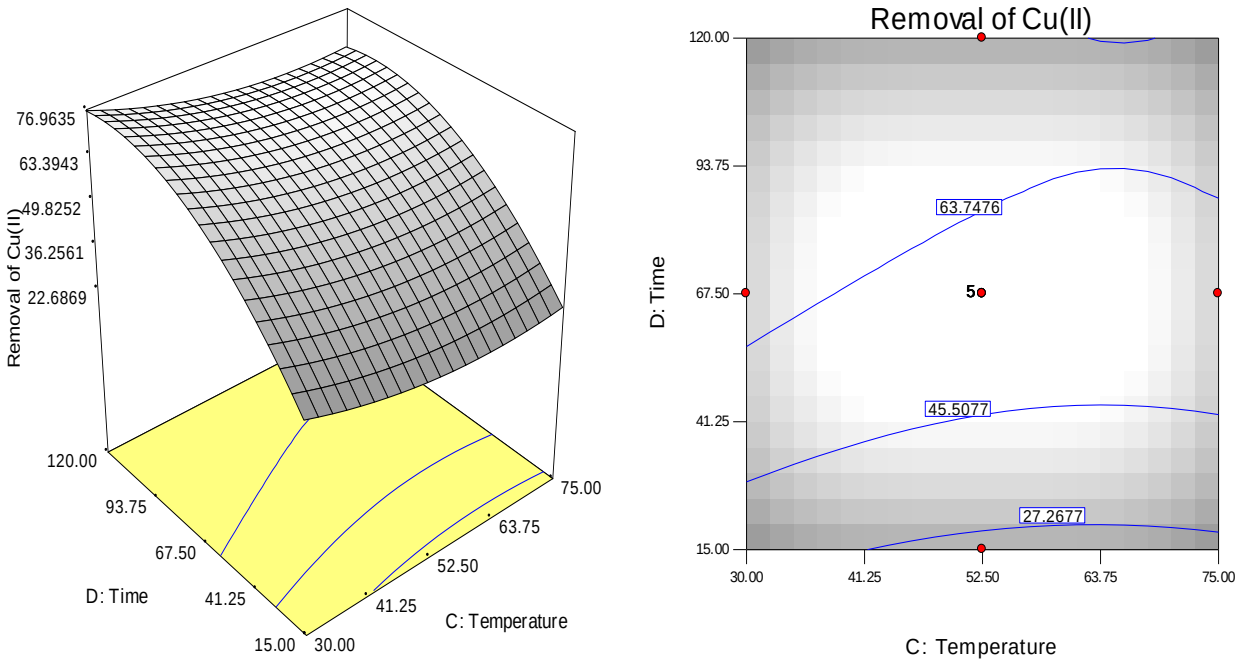

Figure 31: Effect of temperature and time of Cu(II) removal: (a) response surface method and (b) contour surface plots

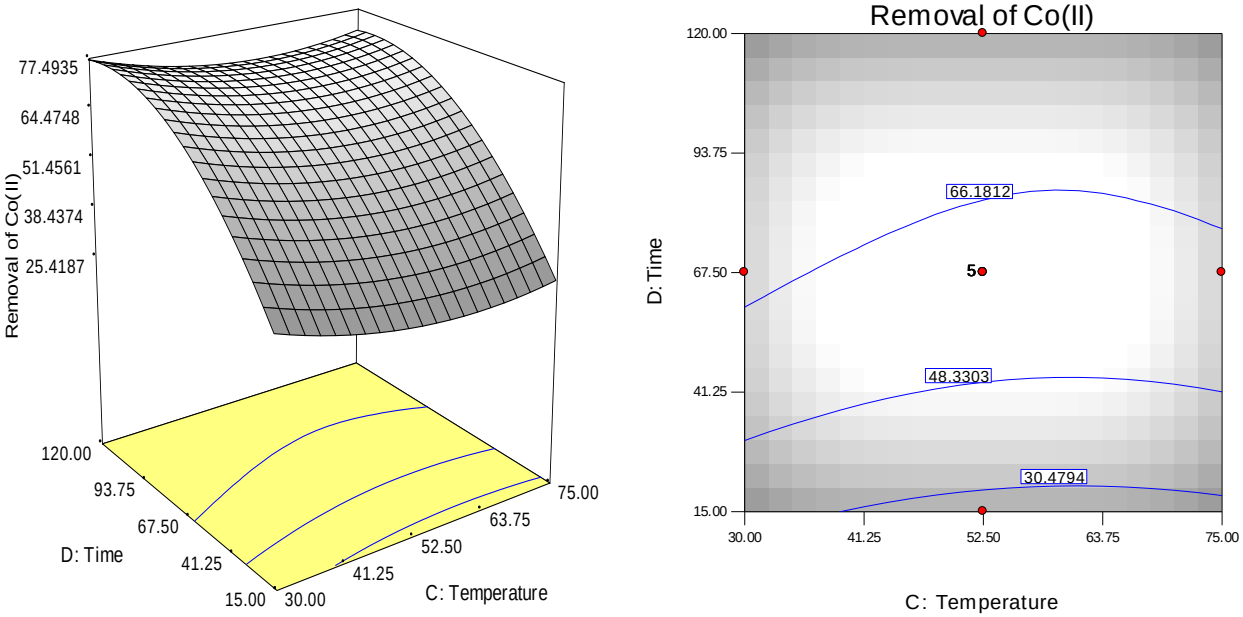

Figure 32: Effect of temperature and time of Co(II) removal: (a) response surface method and (b) contour surface plots

The interaction between temperature and time is shown in Figures 31 and 32 on the removal of Cu^{2+} and Co^{2+} onto GCHM where the pH (6.00) and gelatin ratio (50.00%) have been kept constant. With increasing temperature, the activity of functional groups increases but a decrease is observed in the removal for both metals whilst increasing of the temperature. On the other hand, high temperature does not favour the adsorption process of Cu^{2+} and Co^{2+} onto GCHM. Therefore, system temperature affects synergistically on the adsorption of Cu^{2+} and Co^{2+}. Maximum removal efficiency for a combination of the effect of time and temperature was found to be 76.96% and 77.49% for Cu^{2+} and Co^{2+}, respectively (Yesilyurt *et al.*, 2019; Şahan, 2019; Esfandiar *et al.*, 2014).

4.8. References

Abbas M., Kaddour S. & Trari M.: Kinetic and equilibrium studies of cobalt adsorption on apricot stone activated carbon, *Journal of Industrial and Engineering Chemistry* 20 (2014), 745-751.

Abdelwahab H.E., Hassan Y.S., Mostafa A.M. & El Sadek M.M.: Synthesis and characterization of Glutamic-Chitosan Hydrogel for Copper and Nickel removal from wastewater, *Molecules* 684, 21 (2016), 1-14.

Akpomie K.G., Dawodu F.A. & Adebowale K.O.: Mechanism on the sorption of heavy metals from binary-solution by a low cost montmorillonite and it's desorption potential, *Alexandria Engineering Journal* 54 (2015), 757-767.

Alemdar A. & Sain M.: Isolation and characterization of nanofibres from agricultural residues-wheat straw and soy hulls, *Bioresource Technology* 99, *6* (2008), 1664-1671.

Al-Saidi G.S., Al-Alawi A., Rahman M. S. & Guizani N.: Fourier transform infrared (FTIR) spectroscopic study of extracted gelatin from shaari (Lithrinusmicrodon) skin: effects of extraction conditions, *International Food Research Journal* 19, *3* (2012), 1167-1173.

Al-Shahrani S.S: Treatment of wastewater contaminated with cobalt using Saudi activated bentonite, *Alexandria Engineering Journal* 53 (2014), 205-211.

Blahovec J. & Yanniotis S.: Modified classification of sorption isotherms, *Journal of Food Engineering* 91 (2009), 72-77.

El-Nemr A., El-Sikaily & Khaled A.: Modeling of adsorption isotherms of methylene blue onto rice hush activated carbon, *Egyptian Journal of Aquatic Research* 36, 1 (2010), 403-425.

El-Sheikh R., Hefni H.H., El-Farargy A.F., Bekhit M. & Negm N.A.: Adsorption Efficiency of Chemically modified Chitosan towards copper and cobalt Ions from

Industrial Waste Water, *Egyptian Journal of Chemistry* 55, *3* (2012), 291-305.

Esfandiar N., Nasernejad B. & Ebadi T.: Removal of Mn(II) from groundwater by sugarcane and activated carbon (a comparative study): Application of response surface methodology (RSM), *Journal of Industrial and Engineering Chemistry* 20 (2014), 3726-3736.

Feinsten R.: Guide to spectroscopic identification of organic compound, CRC Press Boca Raton-London-New York (1995), 124.

Fernandes de Almeida P., da Silva Lannes S.D., Araújo Calarge F., de Brito Farias T.M. & Santana J.C.C.: FTIR Characterization of Gelatin from chicken Feet, *Journal of Chemistry and Chemical Engineering* 6 (2012), 1029-1032.

Fosso-Kankeu E.: Synthesized af-PFCl and GG-g-P(AN)/TEOS hydrogel composite used in hybridized technique applied for AMD treatment, *Physics and Chemistry of the Earth* 105 (2018), 170-176.

Garcia-Diaz I., Lopez F.A. & Alguacil F.J.: Carbon Nanofibers: A New Adsorbent for Copper Removal from Wastewater, *Metals* 8, *914* (2018), 1 – 13.

Hashemian S., Saffari H. & Ragabion S.: Adsorption of Cobalt (II) from Aqueous Solution by Fe_3O_4/Bentonite nanocomposite, *Water Air Soil Pollution* (2015).

Hino S., Ichikawa T. & Kojima Y.: Thermodynamic properties of metal amides determined by ammonia pressure-composition isotherms, *Journal of Chemical Thermodynamics* 42 (2010), 140-143.

Ho Y.S.: Removal of copper ions from aqueous solution by tree fern, *Water Resources* 37 (2003), 2323 – 2330.

Hossan M.J., Gafur M.A., Kadir M.R. & Karim M.M.: Preparation and characterization of gelatin-hydroxyapatite composite for bone tissue engineering, *International Journal of Engineering & Technology* 14, *1* (2014), 24-32.

Kabuba J. & Banza M.: Modification of clinoptilolite with dialkylphosphinic acid for the selective removal of cobalt (II) and nickel (II) from hydrometallurgical effluent, *The Canadian Journal of Chemical Engineering*, Accepted, (2020).

Kamaruzaman S., Aris N.I.F., Yahaya N., Hong L.S. & Razak M.R.: Removal of Cu(II) and Cd (II) ions from Environmental Water Samples by using Cellulose Acetate Membrane, *Journal of Environment Analytical Chemistry* 4, *4* (2017), 1-8.

Kiran B. & Thanasekaran K.: Copper biosorption on Lyngbyaputealis: Application of response surface methodology (RSM), *International Biodeterioration & Biodegradation* 65 (2011), 840-845.

Liu P., Borrell P.F., Božič M., Kokol V. & Oksman K.: Nanocelluloses and their phosphorylated derivatives for selective adsorption of Ag^{+}, Cu^{2+} and Fe^{3+} from industrial effluents, *Journal of Hazardous Materials* 294 (2015), 177 – 185.

Maiyalagan T. & Karthikeyan S.: Film pore diffusion modeling for sorption of azo dye to exfoliated graphite nanoplate lets, *Indian Journal of Chemical Technology* 20 (2013), 7-14.

Merina Paul Das, Suguna P.R., Karpuram Prasad, Vijaylakshmi J.V. & Renuka M.: Extraction and characterization of gelatin: a functional biopolymer, 9, International *Journal of Pharmacy and Pharmaceutical Sciences9* (2017), 239-242.

Mobasherpour I., Salahi E. & Ebrahimi M.: Thermodynamic and kinetics of adsorption of Cu (II) from aqueous solutions onto multi-walled carbon nanotubes, *Journal of Saudi Chemical Society* 18 (2014), 792-801.

Münster L., Vicha J., Klofac J., Masar M., Kucharczyk P. & Kuritka I.: Stability and aging of solubilized dialdehyde cellulose, *Cellulose* 24, *7* (2017), 1-14.

Reshetnyak E.A., Ivchenko N.V. & Nikitina N.A.: Photometric determination of aqueous cobalt (II), nickel (II), copper (II) and iron (III) with 1-nitroso-2-naphthol-3,6-disulfonic acid disodium salt in gelatin films, *Central European Journal of Chemistry* 10, *5* (2012), 1617 – 1623.

Şahan T.: Application of RSM for Pb(II) and Cu(II) adsorption by bentonite enriched with -SH groups and a binary system study, *Journal of water Process Engineering* 31 (2019), 100867.

Sahu J.N., Acharya J. & MeikapB.C.: Response surface modeling and optimization of chromium (VI) removal from aqueous solution using Tamarind wood activated carbon in batch process, *Journal of Hazardous Materials* 172 (2009), 818-825.

Sain M. & Panthapulakkal S.: Bioprocess preparation of wheat straw fibers and their characterization, *Industrial Crops and Products* 23, *1* (2006), 1-8.

Sarkar M. & Majumdar P.: Application of response surface methodology for optimization of heavy metal biosorption using surfactant modified chitosan bead, *Chemical Engineering Journal* 175 (2011), 376–387.

Shrestha R.M.: Removal of Cd (II) ions from Aqueous Solution by Adsorption on Activated carbon Prepared from Lapsi (*Choerospondiasaxillaris*) Seed Stone, *Journal of the Institute of Engineering* 11, *1* (2015), 140-150.

Silvestein R.M., Webster F.X., Kiemle DJ. & Bryce DL.: Spectroscometric identification of Organic Compound, 8th edition. Wiley. New York (2007), 81-108.

Singh R., Chadetrik R., Kumar R., Bishnoi K., Bhatia D., Kumar A., Bishnoi N.R. & Singh N.: Biosorption optimization of lead (II), cadmium (II) and copper (II) using response surface methodology and applicability in isotherms and thermodynamics modeling, *Journal of Hazardous Materials* 174 (2010), 623-634.

Tarawou T. & Young E.: Intraparticle and liquid film diffusion studies on the adsorption of Cu^{2+} and Pb^{2+} ions from aqueous solution using Powdered Cacao Pod (*Theobroma cacao*), *International Research Journal of Engineering and Technology* 2 (2015), 236 – 243.

Vieira R.S., Guibal E., Silva E.A. & Beppu M.M.: Adsorption and desorption of binary mixtures of copper and mercury ions on natural and crosslinked chitosan membranes, *Adsorption* 13 (2007), 603-611.

Wang X., Liu P., Liu F.,Wang X., Ji M. & Song L.: Adsorption Pb(II) by a polyvinylidene fluoride membrane bearing chelating poly(amino phosphoric acid) and poly(amino carboxylic acid) groups, *Adsorption Science & Technology* 36, *9-10* (2018), 1571-1594.

Yao Y., Wang H., Wang R., Chai Y. & Ji W.: Fabrication and performance characterization of the membrane from self-dispersed gelatin-coupled cellulose migrogels, *Cellulose* 26 (2019), 3255-3269.

Yesilyurt M.K., Arslan M. & Eryilmaz T.: Application of response surface methodology for the optimization of biodiesel production from yellow mustard (*Sinapis alba L.*) seed oil, *International Journal of Green Energy* 16, 1 (2019), 60-71.

Yin O.S & Amin M.C.I.M.: Synthesis of chemical cross-linked gelatin hydrogel reinforced with cellulose nanocrystals (CNC), *AIP Conference Proceedings* 1614 (2014), 375-380.

CHAPTER 5: CONCLUSION AND RECOMMENDATIONS

The main objective of this study was to prepare the GCHM for the removal of Cu(II) and Co(II) ions from mining processes wastewater. The study was carried out by performing characterization techniques on the GCHM. Adsorption experiments were performed using GCHM at different ratios of CNCs and gelatin using a one factor at a time experimental design to compare the performance of GCHM to determine the effect process variables has on the efficiency of Cu(II) and Co(II) ions from mining processes wastewater. Adsorption isotherms, kinetics, and thermodynamics were studied to determine the mechanism for the adsorption of the removal of Cu(II) and Co(II) ions. Response surface methodology was used to determine the effect of process variables on the adsorption of Cu(II) and Co(II) ions onto GCHM and to optimize the process.

The FTIR shows a bathochromic effect has been observed with an increase in gelatin concentration. A slight constancy of the carboxyl (C=O) band at 1700 cm^{-1} has been observed, that is evidence that new bonds was created and therefore new functions were created. The SEM images showed that there was an important improvement in the surface morphology of GCHM with increasing the gelatin concentration and consequently, several pores have been observed.

Cu(II) and Co(II) removal was favoured by an increase in the pH of the solution (at pH 5 and pH 7 for Cu(II) and Co(II) respectively). High percentage removals of Cu(II) and Co(II) were obtained at ratio of 3:1 (75% gelatin and 25% cellulose) for a maximum time of 120 min and a temperature of 30°C. The equilibrium data at various temperatures fitted well with the Freundlich isotherm. The adsorption process was fast, and the kinetic data showed a great fit to the pseudo-first-order kinetic model. It was also observed that the experimental data fitted well with the film diffusion model for both metal ions. The temperature change has been used to evaluate the parameters such as $\Delta G°$, $\Delta H°$, and $\Delta S°$. The thermodynamic study has shown that the adsorption for both metal ions was spontaneous (negative values of Gibbs free energy) and endothermic (positive values of enthalpy). Randomness was observed at the solid/liquid interface during adsorption because of the positive values of entropy.

Performing adsorption experiments using the RSM-CCD method showed the combined effect of the process variables on the adsorption capacity of the GCHM for Cu(II) and Co(II) ions adsorption. Furthermore, it was possible to determine the optimum operating conditions of the process variables to achieve a maximum adsorption capacity of the GCHM for Cu(II) and Co(II) ions process variables to achieve maximum adsorption capacity of the GCHM for copper and cobalt ions' removal by using a numerical optimization method under CCD and the optimum operating conditions were found to be pH= 6.00, ratio= 3:1 (75% gelatin and 25% cellulose), contact time= 67.50 min and T°= 67.50°C. The optimum operating conditions obtained under RSM were comparable with those obtained under one factor at a time experimental designs were effective in determining the optimum conditions for the adsorption of copper and cobalt ions onto GCHM.

As recommendation, the future studies should focus on the potential regeneration of the GCHM and its biodegradability. A continuation of this study would also explore the adsorption of other heavy metals, such as nickel, cadmium, and lead as well as heavy metal in continuous flow column (dynamic adsorption model).